VARIATION OF SHEAR WAVE VELOCITY WITH SPT-N VALUESIN THE CITY OF SHARJAH

by

Niamatullah Haji Bismillah

A Thesis Presented to the Faculty of the
American University of Sharjah
College of Engineering
in Partial Fulfillment
of the Requirements
for the Degree of

Master of Science in
Civil Engineering

Sharjah, United Arab Emirates

June 2014

Approval Signatures

We, the undersigned, approve the Master's Thesis of Niamatullah Haji Bismillah.

Thesis Title: Variation of shear wave velocity with SPT-N values in the city of Sharjah

Signature **Date of Signature**

_____ _____
Dr. Zahid Khan
Assistant Professor, Department of Civil Engineering
Thesis Advisor

_____ _____
Dr. Mohammad AlHamaydeh
Associate Professor,Department of Civil Engineering
Thesis Committee Member

_____ _____
Dr. Magdi Mohamed El-Emam
Assistant Professor,Department of Civil Engineering
Thesis Committee Member

_____ _____
Dr. Maher Omar
Associate Professor,
Department of Civil & Environmental Engineering,University of Sharjah
Thesis Committee Member

_____ _____
Dr. Aliosman Akan
Head, Department of Civil Engineering

_____ _____
Dr. Hany El-Kadi
Associate Dean, College of Engineering

_____ _____
Dr. Leland Thomas Blank
Dean, College of Engineering

_____ _____
Dr. Khaled Assaleh
Director of Graduate Studies

Acknowledgments

I would like to acknowledge the sincere guidance of Prof. Zahid Khan. His open-hearted cooperationinvigorate me to complete this thesis.

I want to extend my gratitude to Mr. Aqeel Ahmed for his relentless help in conducting the field experiments, in addition to his never-ending support during the completion of this thesis.

This thesis would not have been completed without the continuous support of my family, especially my father whose encouragement and prayers were always with me during the thick and thin of the program advancement.

I am very grateful to Sharjah Municipality and especially to Mr. Adil Al Zaini for his support in providing valuable information for which this work would not have been possible without it.

Many thanks to all of my friends and colleagues, whose partnership I could not have done without.

I am dedicating this effort to my dear father, Allah's prevalent blessing on me, and my major strength and motivation in completion of this thesis

Abstract

Modern building codes require the evaluation of a shear wave velocity profile of the foundation soils for a dynamic analysis of structures and sites to occur. Wave velocities are typically evaluated by conducting laboratory and field tests. Due to the rapid pace of development in the UAE,consultants often rely on shear wave velocity (V_S) obtained from correlations of shear wave velocity (V_S) with N values from Standard Penetration Tests (SPT). Significant variationsin previous studies that predict wave velocities justifythis new study in order to develop correlations specific to the region and applicable to areas of similar geology. These variations can be attributed to factors such as biases in conducting field tests and shortcomings in seismic techniques. This study presents the correlations developed between wave velocity and N values for the city of Sharjah by performing seismic tests in various locations. The velocity profiles are evaluated by using vertical geophones that are traditionally used, as well as, horizontal geophones to evaluate their ability in calculating similar profiles. The analysis of surface waves for velocity evaluation is preferred due to its ability in delineating hidden layers of weaker velocities and for the better characterization of shallow depths from the generation of higher frequency phases. The benefits of using a seismic technique based on surface waves are presented and the results of the regression of V_S-N pairs are compared with the findings of previous studies discussed here. The effect of using horizontal and vertical geophones on the results is evaluated in order to validate the theoretical basis of particle motion during the propagation of surface waves. The results indicate many previous models underestimate the wave velocity as function of N valuesas compared to the proposed model, especially at N values larger than 15. Most recent studies, however, tend to agree with the prediction model of this study;only one model significantly overestimates the shear wave velocity. The velocity profiles computed from horizontal and vertical geophones agree, indicating that the theoretical basis of elliptical particle motion with both horizontal and vertical components in the propagation of surface waves is valid.

Search Terms: SPT-N values; MASW; Shear wave velocity; Correlations

Table of Contents

List of Figures

List of Tables

Chapter 1: Introduction

1.1 General introduction

Modern building codes have provisions in them for the seismic design of the structures that are based on the dynamic properties of subsurface soils. Low-strain dynamic properties, such as wave velocities and material damping ratios, are measured from resonant column [1] and cyclic triaxial[2] tests in the laboratory and in seismic surveys like seismic refraction, seismic reflection, and MASW (Multi-channel Analysis of Surface Waves) in the field. These tests are gaining popularity among many jurisdictions; however, these tests also require specialized equipment and analytical tools to gather, process, and evaluate the data. The rapid pace of development involving schedule-driven projects, especially in developing economies such as of UAE (United Arab Emirates), compels designers to rely on correlations to infer dynamic properties (especially wave velocity) from commonly conducted field tests such as SPT (Standard Penetration Test) and CPT (Cone Penetration Test).

Several relationships correlating SPT resistance (referred to N values in this study) with shear wave velocity (V_S) have been developed[3-7]; however, they exhibit significant variations for many reasons such as site specific stratigraphy, bias in testing methodologies, and differences among the methods of evaluating wave velocities in the field. This study aims at developing prediction relationship that correlates N values with V_S forsoils inSharjah, UAE.

MASW is chosen as the preferred method for the V_S evaluation due its ability to delineate weaker layers inter-layered within stiffer layers (inverse velocity profile). The MASW technique is preferred for high-resolution characterization of soils at shallow depths over other methods due to the generation of higher frequencies (smaller wave lengths) during small energy impacts. The sandy soils of the Quaternary period in the study area become significantly stiffer at shallow depths, and limiting values of N (50 for less than 50 mm of penetration) are encountered within the first five to eight meters on average. The accuracy of SPT tests decreases with the increase in N values all due to various factors, such as a soil's relative density and degree of cementation in sandy soils. The N values of interest (i.e., up to 50) are

contained within the first five to eight meters at most locations of the study area. Similarly, the maximum meaningful depth of exploration with MASW tests is also limited to about 12 meters in this study.

A data acquisition system (GEODE-Geometrics) and 14/4.5 Hz geophones (Geometrics) are used to perform MASW tests in several locations. The field measurements from MASW tests are analyzed by a frequency-wave number (F-K) technique in order to obtain the dispersion curves (variation of phase velocities with frequency). The curves are then inverted by independent software (GEOPSY-geopsy.com and SWAN-Geoastir) for the fitting of theoretical dispersion curves of forward iterative ground profiles. An independent quality check is also carried out in MathCAD (Version 14) to compute phase velocities as a function of frequency (dispersion curve) for a few selected data recordings using the phase unwrapping method.

A simple regression analysis is performed on the data set representing the variation of the shear wave velocity (V_S) as a function of N and N_{60} values. The resulting correlations between N values and V_S are plotted and compared with published correlations from other geographical areas. The correlations (V_S prediction equations) developed in this study agree reasonably well with some other published studies on sandy soils at N values smaller than 15; however, many past studies underestimate the results of this study at larger N values. Some recent studies agree with the shear wave velocities predicted by the proposed model; whereas one model significantly overestimates the present study. The proposed correlations can be used for similar sandy soils where N values are up to 50. Larger values of N are not available for the studied area due to the protocols of not reporting them on borehole logs.

A typical setup of MASW tests involves geophones that measure vertical motion of the particles due to their wide commercial availability and lower price; however, they cannot measure the shear waves directly from surface. Since the particle motion during surface waves is approximate to a retrograde ellipse, both vertical and horizontal motions shall correspond to the same frequency of vibrations[8]. This study also presents the experimental evaluation of a comparison of dispersion curves obtained from the results of MASW tests using horizontal and vertical geophones. Horizontal geophones were used to measure the horizontal

component of the particle motion of the retrograde ellipse; whereas, the vertical geophones were used to measure the vertical component.

The field data is analyzed by commerciallyavailable software of SWAN, which uses the 2DFourier transform and frequency-wave number (F-K) technique to calculate the dispersion curves. The dispersion curves were inverted by computing and iteratively modifying the forward subsurface models to match the experimental dispersion curve as noted above.

The results of the study indicate that dispersion curves as well as the inverted subsurface models, agreed when computed from the horizontal and vertical component of the surface wave propagation from the horizontal and vertical geophones, respectively. The results also validate the theoretical approach of calculating dispersion curves using curve correspondence in the frequency-wave number (F-K) field.

1.2 Objectives of the study

The focus of the research is to develop empirical relationships between the SPT-N values and V_S for the typical soils found in or around the city of Sharjah in the UAE. The relationships (correlations/prediction equations) are developed from the results of regression analyses of data pairs between N values and V_S. The developed relationships are expected to predict V_S as function of N values for regional soils.

Furthermore, this research is an effort to evaluate the ability of horizontal geophones in calculating the dispersion curves and velocity profiles by measuring the horizontal component of the particle motion during the propagation of surface waves. Traditionally vertical geophones are used to analyze the surface waves due to their lower price and use in other commonly conducted seismic tests such as seismic refraction and seismic reflection.

The main objectives of this research are presented below:

1. Evaluate the ability of MASW testing in delineating velocity of weaker layers hidden under the layers of larger velocity.
2. Develop the database representing data pairs of V_S and N values for soils typically encountered in and around city of Sharjah.

3. Propose empirical relationships correlating V_S and N values.
4. Evaluate the ability of horizontal geophones to detect and measure the horizontal component of particle motion during Rayleigh wave propagationand use the results in the measurement of V_S profile.
5. Compare the dispersion curves and the corresponding velocity profiles from measurements of horizontal and vertical geophonesfor companies to use horizontal geophones instead of purchasing vertical geophones.

1.3 Organization of the thesis

The organization of the manuscript is presented in the following chapters:

In Chapter 2, the methods of evaluating dynamic properties from the laboratory and field testing are presented with emphasis on the MASW technique. Correlations of V_S and N values from the past studies are presented towards the end of the chapter.

In Chapter 3, the equipment used in the field tests, software acquired for the analysis, equipment setup, testing methodology, and analysis of the field data is presented.

The first part of Chapter 4 presents the results from field tests involving MASW testing, effect of testing configuration on the inverted velocity profiles, results of regression analysis, and comparison of the proposed prediction model with the models from previous studies. The second part of Chapter 4 presents comparison of the results from MASW testing using horizontal and vertical geophones.

Chapter 5 presents the important conclusion from the study and identifies areas of future research and development on this work.

Chapter 2: Background

2.1 Dynamic Properties

Dynamic properties of geo-materials are required to solve geotechnical or soil-structure interaction problems involving dynamic loadings, such as those from earthquakes, machine foundations, wind loads, and ocean currents. The shear wave velocity and damping ratio are the dynamic properties generally required and measured. These properties are typically functions of shear strain level; therefore, more than onetestis required to evaluate these properties over a range of strain levels.The building codes require that the weighted average shear wave velocity of the first 30 meters should be used for site classification purposes; whereas, the shear wave velocity of individual layers are required for the site response and liquefaction analyses irrespective of the depth of overburden.

Dynamic properties can be measured in the laboratory (low and large strain are possible) and in the field (only low strain is possible). Field tests characterize the soils better than laboratory tests due to scaling effects and sample disturbances. Fields tests, on the other hand, cannot impose large strains and evaluations of damping ratios by field tests. Table 2.1 presents the common laboratory and field tests conducted for the evaluation of dynamic properties.

Table 2.1: Common Field and Laboratory Tests for Dynamic Investigation of Soil

Field Tests		**Laboratory Tests**	
Low Strain (<0.001%)	High Strain (>0.01%)	Low Strain (<0.001%)	High Strain (>0.01%)
Seismic Refraction	Cone Penetration	Resonant Column test	Cyclic triaxial test
Seismic Reflection	Dilatometer test	Ultrasonic Pulse Test	Cyclic direct shear
Multichannel analysis of surface waves (SASW & MASW)	Standard Penetration Test	Piezoelectric bender Element test	Cyclic torsional shear test
Steady-state Vibration	Pressure-meter		

2.2 Laboratory Methods

Many methods have been standardized to evaluate the dynamic properties in the field such as resonant column, cyclic triaxial, and bender elements. Aresonant column test is used to evaluate the dynamic properties at low and mid shear strain levels [9, 10]. Figure 2.1 presents the preparation of soil specimen for testing in a resonant column device.

Figure 2.1: Specimen preparation in a resonant column device

A cyclic triaxial device is used to evaluate the dynamic properties for very large strains. The device is not capable of measuring dynamic properties at low strain levels. The cyclic triaxial device produces axial excitation to the specimen and, therefore, evaluates the Elastic Modulus in compression. The shear modulus is computed from the knowledge of Poisson's ratio and the elastic modulus. The damping ratio in both the triaxial and resonant column device is generally considered frequency independent at the attainable range of frequencies. Most laboratory investigations use both of these devices to characterize the soils for a wide range of shear strain levels.Figure 2.2 presents a picture of cyclic triaxial device.

Figure 2.2: MTS cyclic triaxial device

2.3 Field Methods

For many years now, engineers have used geophysical testing methods for soil and foundation applications. Geophysical investigations are typically used to determine the dynamic properties of geo-materials such as compression and shear wave velocities and attenuation characteristics. In addition, they have also used these methods to detect stratigraphical imaging and elastic module and stiffness of soils. The determined properties from these tests are used to solve many geotechnical and structural analysis problems involving dynamic loadings. The geophysical methods are generally employed in the field and evaluate the in-situ properties of the soils that are more representative of the actual depositional features; i.e., they are not affected by sample disturbances and scaling effects. In brief, the shear wave velocity of soils is an integral element of various seismic analyses, including site classification, hazard analysis, site response analysis, and soil structure interaction. It issignificant that, unlike laboratory testing methods, geophysical tests or methods/techniques do not

require undisturbed sampling, maintain the distribution of in-situ stresses during testing, and measure the properties and characteristics ofa large volume of soil. Irrespective of the geophysical method used, allfield tests try to interpret the profile of the soil by solving an inverse problem.

In geophysical methods, a seismic source, such as a hammer,is used to generate seismic waves, which are then recorded by receivers placed or embedded along a preset geometry (receiver array), and finally they are documented by a digital device called a seismograph. Based on an assumed propagation mechanism used in a seismic survey, seismic waves are grouped primarily into direct, reflected, refracted,and surface waves (Figure 2.3). Each type of seismic survey utilizes a specific type of wave (i.e., reflected waves for reflection survey) and its specific arrival pattern on a multichannel record. Seismic waves can be generated actively by using an impact source like a sledgehammer or passively by natural (i.e., tidal motion) and cultural (i.e., traffic) activities.

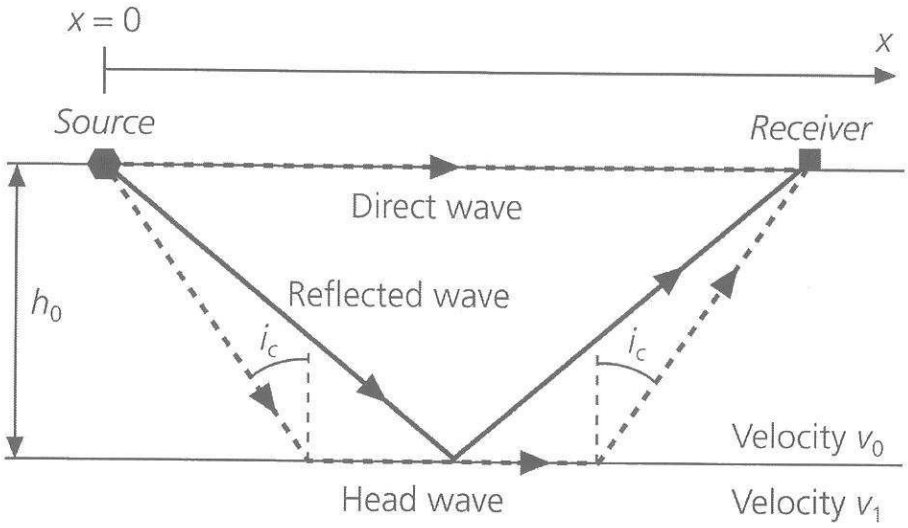

Figure2.3: Generation of Seismic waves

Most seismic surveys utilize active type of seismic wave measurements such as producing the waves by hitting the ground or through the use of explosives.These days, geophysical methods are considered a valid alternative to traditional methods of investigating subsurface materials. Moreover, geophysical tests are helpful inminimizing the number of boreholes advanced during geotechnical studies, which is both economically and environmental friendly. In geophysical methods, the main idea is to use propagation of waves to detect the main characteristics of the studied

medium, which is possible by analyzing the dynamic response of the medium under the propagating wave as a result of excitation of the ground.

2.3.1 Seismic refraction method. The Seismic Refraction method is best in layered soil profile, where wave velocities increase with each successivelower layer. The test measures the arrival-times of the seismic body waves, generated by a seismic source, to a linear array of detectors placed at the ground surface. Generally, compression waves are generatedwhen performing seismic refraction tests [11, 12]due to the fact that compression waves are the fastest among all waves and that they arrive first at the receivers. However,since the shear wave velocities are the required properties of the soils, measured compression wave velocities are converted to shear wave velocities through the Poisson's ratio.Alternatively, shear waves can be generated and shear orhorizontal geophones can be used to measure the shear wave velocities directly [13]. The nature of this type of testing is similar to that described in the Down-hole Seismic Test (DHT)later in this report. Typically, awooden plank peggedunder a large weight (typically a vehicle) is struck, with a hammer, on the sides successively in order to generate thecompression,as well asthe polarized shear waves, i.e.,shear vertical (SV) and shear horizontal (SH) waves.

Although Seismic Refraction is one of the simplest, most common, and non-invasive geophysical methods used for subsurface investigations of soils, this method cannot be applied in particular cases, for instance in residential areas,where it will create a high amount of environmental noise. As such, alternative methods, such as the MASW (Multichannel Analysis of Surface Waves),are consideredas alternatives. The ASTM standard for the Seismic Refraction method for subsurface investigation is designated asD5777 [14]. Refraction testingis time efficient, practical, and also reliable under certain conditions; for example, where velocity inversions are not too important and the purpose of the test is to determine the average shear wave velocity of the subsurface instead of the layer-by-layer velocity[15].

The Seismic Refraction method can be used to map geologic stratigraphy, including depth to bedrock/water table, and lithology. Since the predicted seismic wave velocity, as a result of SR testing, can be related to the mechanical properties of materials, this means that the characterization of material, such as type of rock, degree

of weathering, and rip-ability is decided on the basis of seismic velocity and other complementary geologic information.

A typical experimental setup of SR consists of an array of low frequency vertical or horizontal geophones oriented at right angles to the line of survey[16].The equipment setup for SR tests is similar to MASW testing, as explained in the later section on MASW.

The field data collected from Seismic Refraction test is processed and analyzedby using different available conventional techniques, such as the Generalized Reciprocal Method[17], Delay time inversion [18], and Ray-tracing [19, 20]. The end user result is a plot ofthe velocity with depth of a soil profile as 1D or 2D variations.Recently,a new data processing method has been developed to plot complex 3D velocity models such as the seismic refraction tomography [21, 22].

Both conventional and tomographic methods have advantages specific to them. Although seismic tomography (Figure 2.4) resolves vertical velocity changes better than the conventional method, the conventional method is better placed in determining the depth to bedrock, faster to conduct, and it provides a relatively sharp layer boundary model [24, 25]. Tomography is more applicable to the sub-surfaces in which the velocities increase at a slower rate with depth and where spatially detailed velocity models are required [24].

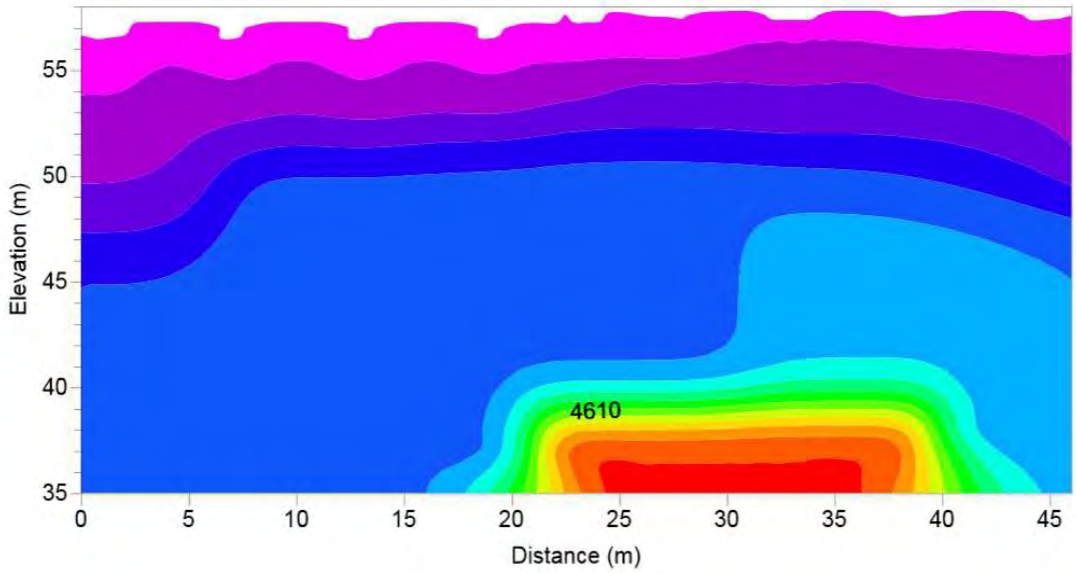

Figure 2.4: Seismic Refraction Tomography[23]

On the other hand, both approaches have their limitations and potential disadvantages. In the conventional method, there are several assumptions made for

simplification about the seismic waves, which makes it less accurate than the seismic tomography. Similarly, the tomography method incorporates velocity gradientsinto the results even if nogradients are present in reality. Moreover, imaging sharp and high contrast boundaries are difficult to resolve in tomography[26].

Although in most applications, seismic tomography is a better choice for data analysis; in general, the conditions of the site where the investigation is being performed, availability of the equipment and expertise, and required end resultsdetermine the appropriate method to be used [26].The list presented belowcontains several computer applications that have been developed to perform data processing of seismic refraction based on both types of techniques discussed above:

1. SIPQC - Rimrock Geophysics® [27, 28]
2. MacRay –[29,30]
3. Interpex IXSEG2SEGY[29]
4. Vista 7.0 (Seismic Image Software Ltd.)
5. ‘SeisOpt22D’ from Optim software® [27]
6. Seismic transmission tomographic algorithm [31]
7. SeisImagerPickWin data analysis (OYO Corporation 2001)
8. ATOM-3D code[32]

As with any other surface tests, the Refraction Test has the benefit in that no boreholes are required to be excavated. Therefore, the most attractive advantage of the RefractionTest is the cost which can bethree to four times less than an invasive test such as Down-hole Test [33, 34]). Refraction Tests are very effective in determining the depth of bedrock since bedrocks typically have a much higher wave propagation velocity thanthe overburden layers [35].

The biggest shortcoming of a Refraction Test is the inability of the test to detect blind zones, i.e., a thin layer between two larger layers [36]. Therefore, a Refraction Test can't be performed independently for site characterization especially if the soil is known to be highly non-homogenous. Another drawback of this test method is that the presence of the water table in the overburden layers will result in false interpretation of bedrock depth because saturated soils have a higher velocity than unsaturated soils [37, 38].

Similarly keeping in view the strengths and weaknesses of the Refraction Test, it is not effective in detecting the changes in soil formation such as testing the soils before and after compaction [39]. Reliable results in seismic refraction can be achieved for depths of 30-40meters in areas reasonably free from background noise[28] and the watertable.

In a nutshell, a refraction test should not be substituted for an invasive seismic investigation such as the Cross-hole or Down-hole tests or better methods such as MASW. This is especiallytrue in studies that require detailed shear wave velocity models of the soil profile[40, 41], even with use of modern equipment and computer applications. However, if the requirement is only to estimate the average shear wave velocity then refraction test is enough[34].

In addition to the shortcomings noted above, seismic refraction is applicable to ground profileswhere the seismic velocities increase as function of depth. In sites where low-velocity (i.e., clay) layers are sandwiched or hidden between layers of higher velocities (i.e., sand or gravel) layers, seismic refraction will yield inaccurateinterpretations.

In seismic refraction testing,the length of geophone arrays should befour to five times the depth of interest; therefore,seismic refraction is typically constrained to evaluating the soil profileswith depths less than 40 meters to space available at typical sites. Although larger depths can be explored, the length of arrayswould exceed available space, and as a result explosive charges might be needed to transmit the energy to deeper layers for refractions to take place.

2.3.2 Seismic reflection method. Seismic Reflection is a method of geophysical exploration that uses the principles of seismology to predict the properties ofthe subsurface from reflected seismic waves.Seismic waves are mechanical disturbances that travel in the earth at a speed governed by the seismic impedance of the medium in which they travel. While travelling through the earth, some energy will reflect off the interface between two materials, having different impedances (i.e.,where significant changes in the material density and conductive velocity of the seismic waves areobserved), and some energy will refract. In simple terms, the seismic reflection technique consists of generating seismic waves and measuring the time taken for the waves to travel from the source, after reflecting off an interface, and being detected by

an array of receivers (or geophones) at the surface. By knowing the travel times from the source to various receivers,hence the velocities of the seismic waves (since receivers spacing is known), the image of subsurface can be built up by reconstructing the pathways of the waves.

In common with other geophysical methods, reflection seismology may be seen as a type of inverse problem ofhaving a set of data collected by experimentation and knowing the physical laws that apply to the experiment, which then allows for a model of the physical system being studiedto be developed. In case of a reflection test, the experimental data is seismograms and the required result is a model of the structure and physical properties of the subsurface soil. As withany other type of inverse problems, the results obtained from the reflection seismology is usually not one of akind (more than one model can fit the data) and as such may be sensitive to relatively small errors in data collection, processing, or analysis. For these reasons, great care must be taken when interpreting the results of a reflection seismic survey.

Typically, the recorded signals are subjected to considerable amounts of signal processing before they are ready to be used; this is an area of active research within industry and academia. In general, the more complex the geology of the area under study, the more complicated are the techniques required to remove noise and increase resolution of the data.Important applications of the Seismic ReflectionMethod are not limited to understanding geology at depths of up to approximately 1 km, but also usedfor engineering and environmental surveys.A more recently developed application for seismic reflection is for geothermal energysurveys, although the depth of investigation can be up to 2 km deep in this case.Seismic reflection profiling is the principal method the petroleum industry uses to explore for oil and gas-trapping structures in sedimentary rocks.The suitability of seismic reflection in marine applications (i.e., lakes, rivers, and oceans) is very high. In marine environments,shear waves cannot transmit through water and the use of compression wavesenables the possibility of collection of reflection data of high quality.

The field equipment used in seismic reflection is similar to the equipment used in seismic refraction tests. With the seismic reflection method, the reflected energy from deeper contrasting layers is maximized by employingdiffering data generation and analyses techniques. The processing of reflection data is complex due to the fact that reflections are not the first arrivals and must be identified by overlapping shots at

different geophone locations, as well as by employing signal processing techniques such as stacking and filtering techniques to remove unnecessary data. This indicates that a much larger testing and processing time is required in comparison to the refraction and MASW techniques.

On the other hand, seismic reflection is capable of detecting blind zones and the length of geophone array required is much shorter than the refraction for the required depth of investigations. However, the seismic reflectionworks well when contrasting layers are high and targets that are deeper.The seismic reflection surveysare costlier to conduct than the seismic refraction tests and they are not capable of resolving structures shallower than about 15 meters. At shallower depths, reflections from shallow contrasts and higher energy surface waves arrive at geophones and the shot sound simultaneouslythus masking these reflections. Reflections from greater depths are easier to detect and isolate as the above noted perturbations have already passed the geophones.

2.3.3 Comparison of seismic refraction and reflection methods. The difference between seismic refraction and seismic reflection is generally seen as an area of interest for non-geophysicists. In sites where both refraction and reflection can be appliedthen the choice is based on economics and resolution. Seismic reflection provides much higher resolution of layers; however it is more expensive than refraction to conduct. In some cases, such as very deep and small targets,seismic reflection is the method of choice.Table 2.2 summarizes the comparison between the two techniques of refraction and reflection.

Table 2.2: Comparison of Seismic Refraction and Seismic Reflection

	Refraction	**Reflection**
Typical Targets	Horizontal layers at depths less than 100 feet	Horizontal to slightly dipping contrast at depths greater than 50 feet
Required Site Conditions	Spatial dimensions larger than 5x the depth of target.	None
Vertical Resolution	10 to 20 percent of depth	5 to 10 percent of depth
Lateral Resolution	~1/2 the geophone spacing	~1/2 the geophone spacing
Effective Practical Survey Depth	1/5 to 1/4 the maximum shot-geophone separation	>50 feet
Relative Cost	$	$x3 to $x5

2.3.4 Cross-hole method. This method is one of the oldest methods used to evaluate theshear wave velocity of site with depth. In this test, at leasttwo boreholes are needed. A typical test method includes the generation of shear waves in one borehole designated as the trigger, while the other borehole is designated as the receiver. By knowing the boreholes spacing and wave travel time, the velocity of the seismic wave can be easily calculated. The cross-hole test can be used to measure the compression wave and shear wave velocity directly depending upon the orientation of the trigger[11, 42]. The measurement of theshear wave velocity and compression wave velocity are then used to calculate the shear and elastic module.

For enhancing the results of the test, three or more boreholes are utilized to increase precision of the data and eliminate any random obstacles.In order to get purer arrivals of shear waves, the trigger shall be oriented to ensure generation of shear waves with much higher energy levels than the compression waves, if generated as a by-product.The accuracy of the wave velocities depend on the measurement of arrival times and its accuracy. The arrival times can be measured either by direct methods or indirect methods. In direct time measurements,digital oscilloscopes of sufficiently large resolutions in time will be used. In direct methods, the time signals are first converted into frequency domain and then cross correlations and cross- spectral density functions are used to estimate the arrival times at different receiver boreholes[11, 42, 43].

The accuracy of the measurements in cross-hole method also depends on the frequency response of the geophones, which should be sufficiently broad. The orientation of the geophones to the particle motion also affects the measurements. Similarly, the contact of the geophones with the soil in the borehole is important and should have direct contact with soils in the case of cohesive deposits.Low velocity layers can also be detected when they are sandwiched between high velocity layers and if the spacing between the boreholes is sufficiently closed enough. The seismic sources are similar for all types of borehole based tests. In the cross-hole tests, the arrival of shear waves can also be resolved by changing the direction of the trigger, which changes the polarity of shear waves for easy identification in the time signals. The compression waves are unaffected by change in the direction of the trigger, and hence, the polarity of the compression waves remains unchanged.

2.3.5 Down-hole method. Down-hole test (DHT) is another invasive methods that providescomprehensive, site specific shear wave velocity profiles. This method used to determine soil stiffness properties by analyzing shear waves along the depth of a borehole. Hence, a borehole must be excavated to carry out this test.

However, contrastingwith a Cross-hole Test,and since only one borehole is required, DHTs are more practical and economical if performed on boreholes that are made for normal geotechnical investigations, thereby avoiding the extra cost of doing separate boreholes specifically for the DHTs.

Figure 2.5 shows a schematic of the Down-hole testing equipment arrangement [44]. A seismic energy source is located near the borehole, on the ground surface. Impulse signals are either received by using a single receiver with changing the height or use an array of receivers placed on preset heights. With one triggering receiver at the impulse source, other receiver(s) are fixed against the wall of borehole.

In DHT, the seismic source is mainly a horizontal rod [44]. The rod is loaded on top with a vehicle to apply normal load (Figure 2.6);this provides good resistance/contact between the rod and the ground surface. To generate the shear waves, the horizontal rod is stroked in the length direction. Shear waves are polarized and directional, geophones used in the borehole must be oriented parallel to the surface rod [44].

As a best practice for clearly noting down the shear waves' arrival times, striking the source in both directions and hence reversing the shear wave polarity is highly recommended [45-47].

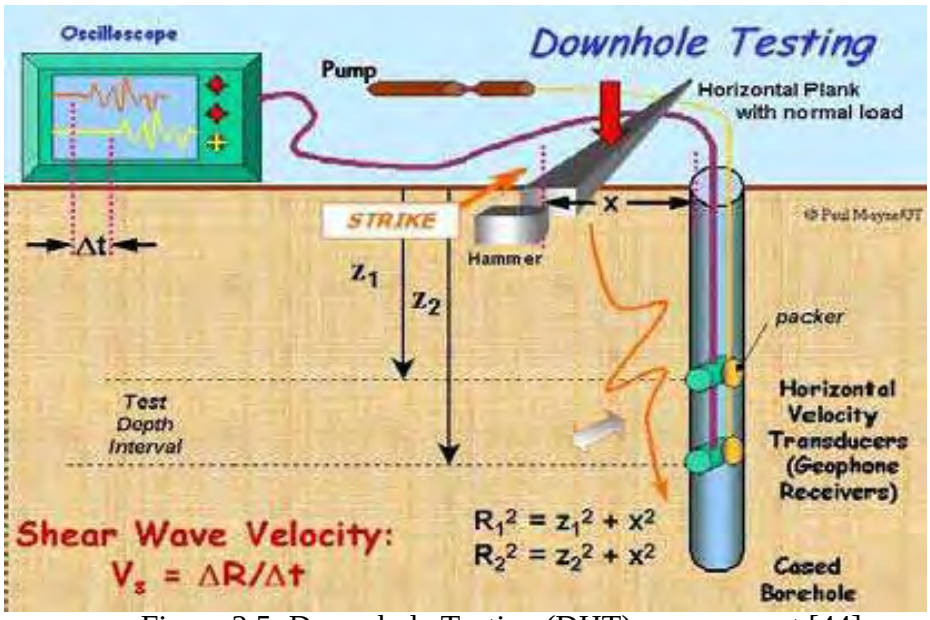

Figure 2.5: Down-hole Testing (DHT) arrangement [44]

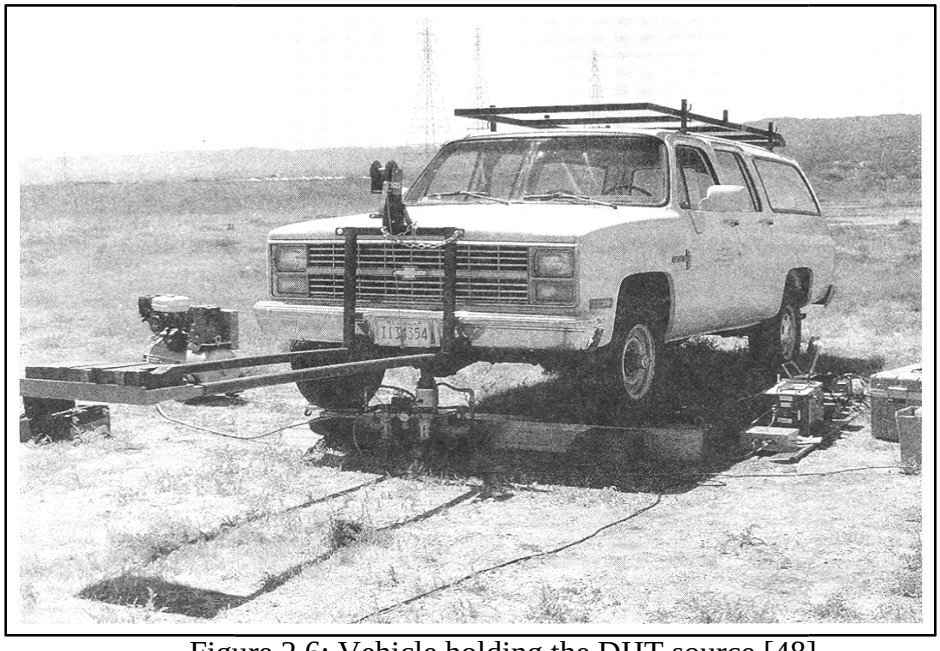
Figure 2.6: Vehicle holding the DHT source [48]

DHT is very similar to a Cross-hole Test (CHT) in terms of the depth of information of soil profile. However, unlike the CHT, DHT requires only one borehole to obtain the shear wave velocity data making it comparatively cost effective. Similarly, another attraction of DHT is that, unlike CHT, the source is

placed on the ground surface; hence, generating the shear waves and reversing the polarity of shear waves are easier in a DHT as compared to the CHT.

It should be noted that DHT results are as accurate as the non-invasive methods such as the Single-channel Analysis of Surface Waves (SASW) and Multi-channel Analysis of Surface Waves [49]. This is because shear waves generated in Down-hole Tests are similar to the waves generated in an earthquake event, in addition to, shear waves are vertically propagated asin Shear Horizontal (SH) waves. While in a Cross-hole Test, the waves propagate in the horizontal direction and are vertically polarized (Shear Vertical-SV); note,this would not resemble the real earthquake scenario in an anisotropic medium[50].The seismic waves on an earthquake event are generally horizontally polarized and propagated through bedrocks that change their orientation and ray paths.

2.3.6 Up-hole Test (UHT). As the name reflects, the Up-hole test (UHT) is the reverseof the Down-hole Test (DHT), i.e., locations of the energy source and receiver(s) are interchanged. Although results interpretation is similar in both the UHT and DHT the difference is that application of UHT is uncommon because of the difficulty in generating shear waves from inside the borehole. However, the advantage of UHT is it can be combined with a commonly used Standard Penetration Test (SPT) to obtain static and dynamic soil properties simultaneously.

Bang and Kim [51] introduced the modified form of Up-hole seismic test to obtain the shear wave velocity profile of a site. This method is called SPT based up-hole method. The impact energy of the split spoon sampler of the SPT was used to work as a source of shear waves (Figure 2.7).

Two data reduction/interpretation methods were recommended by Bang and Kim [51] to process the results of this modified UHT Test setup. The ‘Delay time between serial receivers’ (DTR), which involves the use of the travel time difference between two receivers at the same testing depth, and the ‘Delay time between serial sources’ (DTS), which involves using the travel time difference between different testing depths at the same receiver.

To use this method, the authors [51] have presented a few suggestions for an easier interpretation of the results. These suggestions can also be applicable to traditional DHTs and UHTs.Since reversing of polarity to differentiate shear waves

cannot be used in this method, the two component geophones (horizontal and vertical) should be used to obtain the first peak of shear waves (DTS method).

In a UHT, the frequency content of the propagating waves influence the speed, and hence, a separate set of sensors, usually accelerometers, are deployed to study the frequency content of the generated waves. In addition to the frequency content, the strain levels also are sometimes affected due to the energy that is transmitted during waves generation at the bottom of the borehole. The types of waves generated at the bottom of the boreholes are complex enough to resolve from the time signals as multiple reflections can occur during the course of the journey of the superimposed waves.

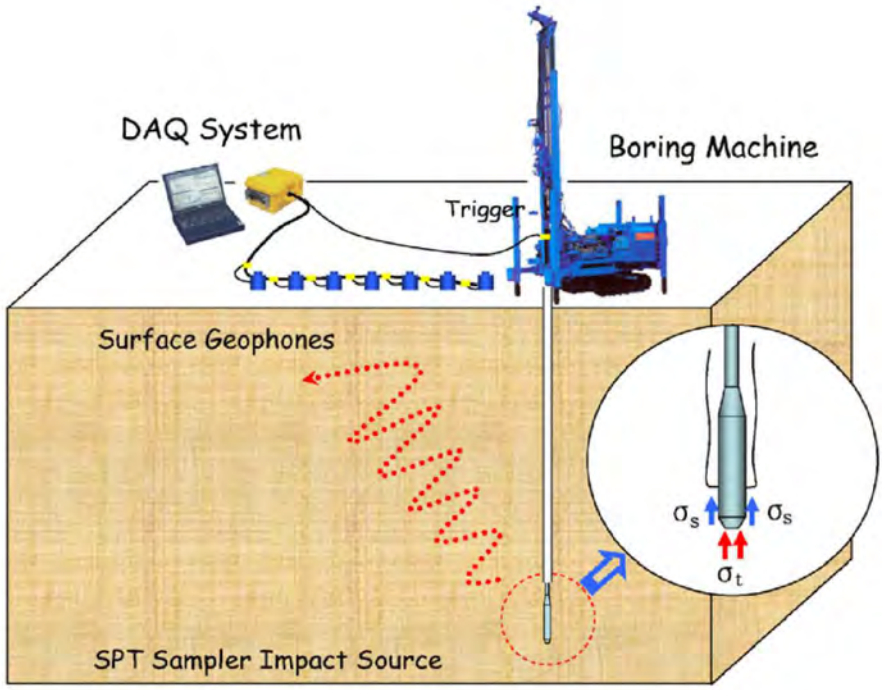

Figure 2.7: SPT based up-hole test [51]

2.3.7 Spectral analysis of surface waves (SASW). Surface waves such as Love Waves and Rayleigh Waves are formed at the surface and are due to interaction of the shear and compression waves. SASW Tests are conducted from the surface and without the use of boreholes and provide detailed profile of shear wave velocities for shallow depths. In this method, two or more receivers are involved in capturing the waves generated at the surface by a trigger such as a hammer. The length of the array is varied to capture a range of wave lengths. Due to the strike of hammer or weight

dropped on to the ground surface, transient Rayleigh Waves are generated[43, 52]. The verified signals are digitized after they are recorded by a dynamic signal analyzer. The time domain recordings are then transformed to the frequency domain using a fast Fourier transformsfor analysis and computation of Rayleigh phase velocities as a function of frequency. This method is explained in further details in the later sections.

The evaluation of Rayleigh phase velocity (V_R) and the corresponding Rayleigh wavelength (λ_R) is performed at each frequency present in the spectrum, and is plotted as a variation of velocity with a frequency known as a dispersion curve (Figure 2.8). Several dispersion curves are evaluated for different geophone spacings to characterize the site being studied.

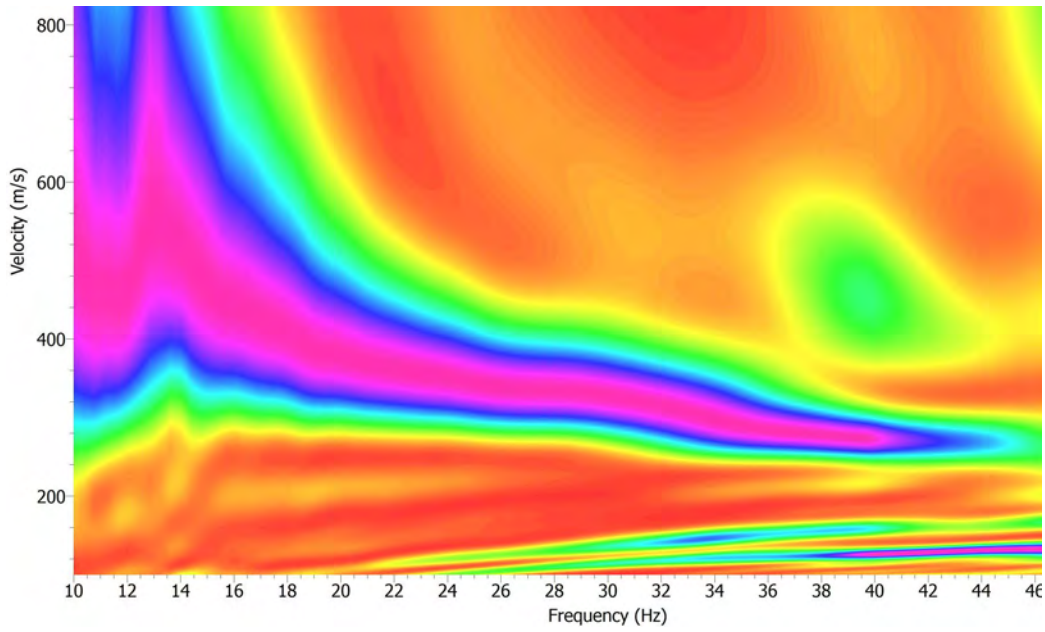

Figure 2.8: Spectral amplitudes in frequency domain between velocity and frequency.

The velocity profiles of the site under consideration (i.e., Figure 2.9) are estimated by the use of forward ground models and inversion techniques. Forward modeling involves the generation of a ground profile and the computation of the theoretical dispersion curve. The velocity profile and the depths of each layer of the ground model are iteratively varied to change the theoretical dispersion curve. The iterative process is repeated several times until a good match between the theoretical and experimental (measured) dispersion curves is achieved. The velocity profile representing the best fit dispersion is adopted as the representative velocity profile of

the site. The velocity profile can be then converted to either shear module or compression wave velocity profile [52].

Figure 2.9: Preparation for a MASW test setup on a site under consideration.

2.3.8 Multichannel analysis of surface waves (MASW). Seismic provisions in building codes are based on the dynamic properties such as the wave velocity of subsurface soils. These properties are usually measured in a laboratory by resonant column, cyclic triaxial and torsional shear devices, and in field by seismic surveys such as refraction, reflection, and SASW (Spectral Analysis of Surface Waves). The resulting dynamic properties are usually represented as a function of shear strain level and frequency [10, 53]. If an accurate value of the material damping ratio is not desired then low strain seismic surveys are usually performed in the field. Although borehole based seismic tests such as cross-hole, down-hole, seismic CPT, and suspension logger testing is typically performed, seismic methods performed from the surface can provide similar results. Seismic methods performed from the surface such as seismic refraction, seismic reflection, and MASW are especially useful where boreholes have already been advanced (such as in cases of retrofitting), the spacing of

the boreholes are large enough to constraint the use of in-hole tests, and when considering the environmental and monetary needs.

Many government organizations and clients from public and private sectors are exploring the use of geophysical techniques, in addition to,the advancing of boreholes to save costs and considerations to environment. Although still in infancy, for such use geophysical methods have been widely used and have been developed for their capability in estimating wave velocities and stratigraphical profiles reliably and repeatedly. Wave velocities are determined by employing field seismic methods for life-line projects; however, many projects in the UAE use correlations between wave velocities and other easily obtainable properties such as from SPT and CPT tests.

MASW was used in this study to evaluate the shear wave velocity profile of the sites and develop correlations with N values for the soils found in Sharjah, UAE. The MASW technique, which is based on the analysis of Rayleigh waves [8], is preferred due to its ability to delineate layers of weaker velocities underlying layers of higher velocities. This property is especially useful as neither wave velocity and/or N values always increase with depth.

The MASW Test methodology uses similar equipment and layouts as the seismic refraction method; however, shot points are located outside the spread of geophone array (Figure 2.10). The exploration depth in MASW is a function of the wave lengths that are typically produced by using high energy shots; however, the resolution at shallower depths is compromised. The accuracy of the MASW to resolve the velocity decreases with depth due to decreases in the amplitude of particle motion; therefore, the reliable wave lengths should typically exceed the depths of intended exploration.

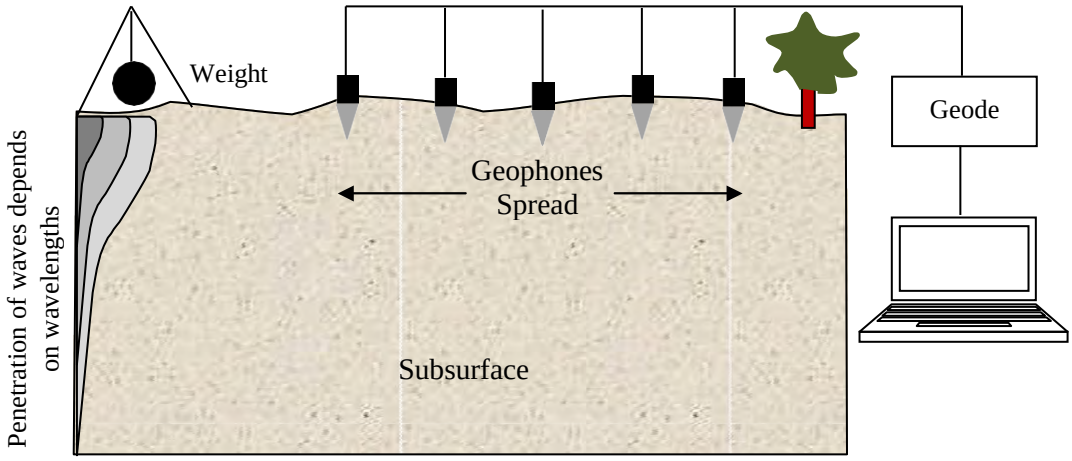

Figure 2.10:Typical schematic test setup during seismic testing in the field

The MASW method captures the propagation of elastic stress waves in the subsurface for evaluating the stiffness (through velocity of seismic waves) of the ground for analysis of problems involving dynamic loads. MASW is a development over the Spectral Analysis of Surface Waves (SASW) technique that uses two receivers (geophones); whereas, the MASW takes advantage of the multichannel (12 or more channels) test configuration as shown in Figure 2.11. The advantage and effectiveness of analyzing several channels at the same time provides significant in time savings when conducting the tests, in addition to, a better characterization of the strata [54].

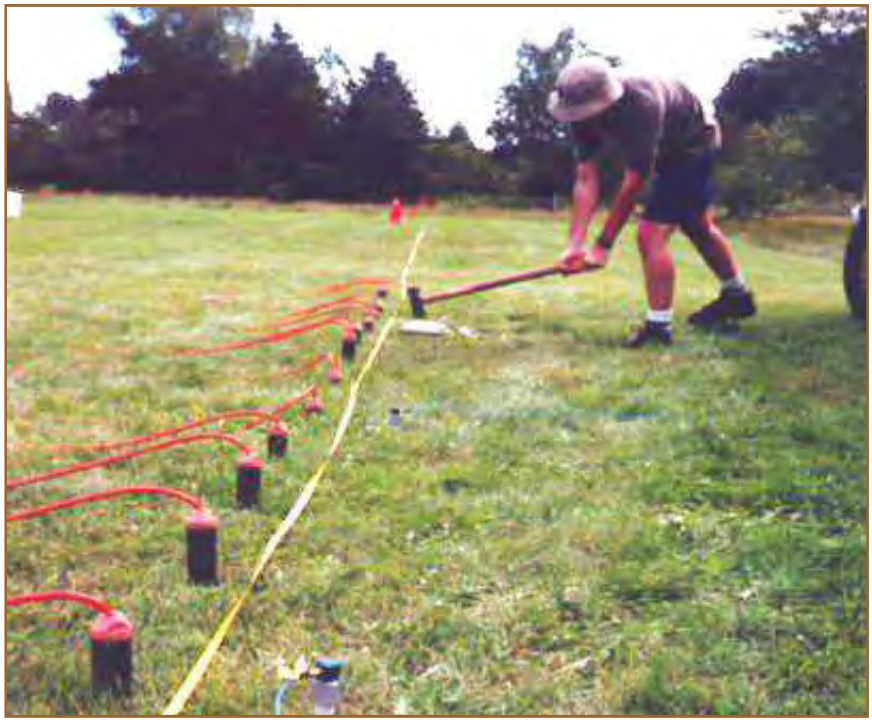

Figure 2.11: Typical test setup and wave generation during seismic testing in the field

A typical MASW Test configuration uses a seismic source located at different distances from an array of geophones where the source offset is measured from the first geophone [54, 55]. The phase difference, as function of spatial distribution for different frequencies of Rayleigh waves, is measured and used to calculate phase velocities (Raleigh Wave Velocity, C_R,). The variation of wave velocity, as a function of either frequency (f) or wavelength (λ), is developed as a dispersion curve that is used in the inversion process. The phase velocity (Equation 1) is obtained from measuring the phase difference ($\Delta\phi(f)$) at each frequency in the spectrum as

$$C_R(f) = 2\pi\ f \cdot \frac{\Delta x}{\Delta\phi(f)} \tag{1}$$

where,Δx is the distance between two successive receivers. A test configuration in the MASW method can only resolve and analyze a certain range of wavelengths reliably [56,57] depending upon the test setup and energy of the impact (shot). The Rayleigh wavelength (λ_R) is related to Rayleigh wave velocity (C_R), and frequency (f) as:

$$\lambda_R = \frac{C_R}{f} \tag{2}$$

Phase function at some ranges of frequency is sensitive to contamination from other seismic sources such as traffic or industries; therefore, a range of wavelengths where the phase function is governed by only the Rayleigh waves shall be determined. Many empirical relationships have been proposed to test the effectiveness of a MASW test setup [58-60].

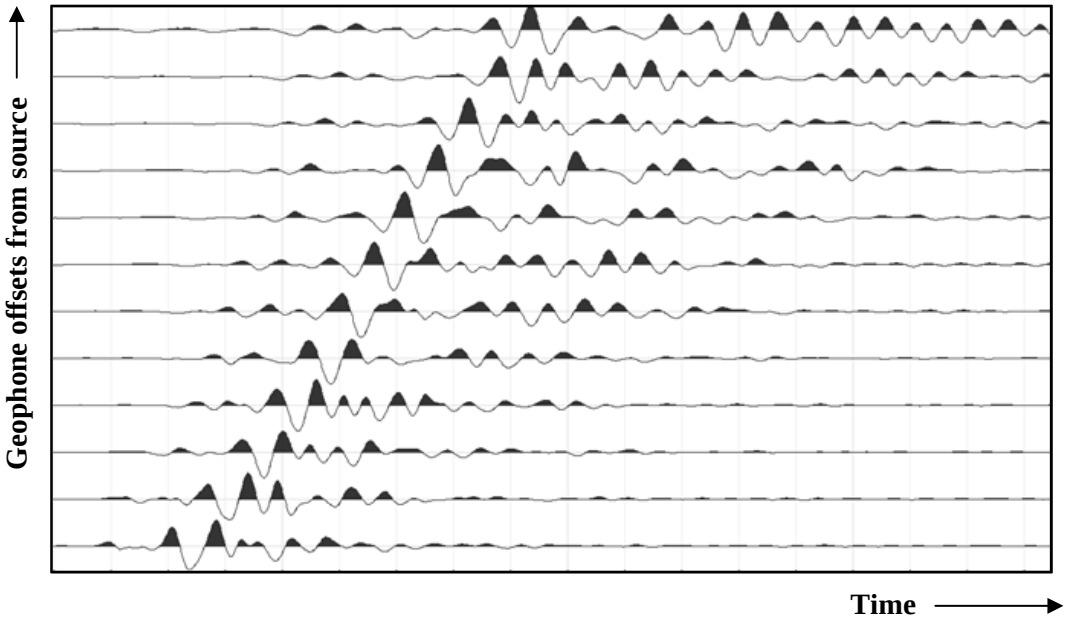

Figure 2.12: Typical velocity time histories recorded at different geophone locations.

The criterion (Equation 3) proposed by Heisey et al.[58] considers the distance of the source to the first receiver as equal to the receiver spacing, Δx. In a typical MASW test, receiver spacing and shot distances are varied to determine and analyze a range of wavelengths corresponding to different depths of exploration.

$$\frac{\lambda}{3} \le \Delta x \le 2\lambda \tag{3}$$

Three different techniques of the one-third rule, the phase unwrapping method [61], and the frequency wave number (F-K) analysis or 2D Fourier transform are used to compute the experimental dispersion curves. Irrespective of the method used, the experimental dispersion curve is computed by conversion of the data from the time-offset domain (Figure 2.12) into frequency-phase velocity (F-V) or frequency-slowness [62], or frequency-wavenumber (F-K) domains (Figure 2.13). These domains are interchangeable due to the inherent relationships between the velocity, frequency, wavelength, wave number, and period.

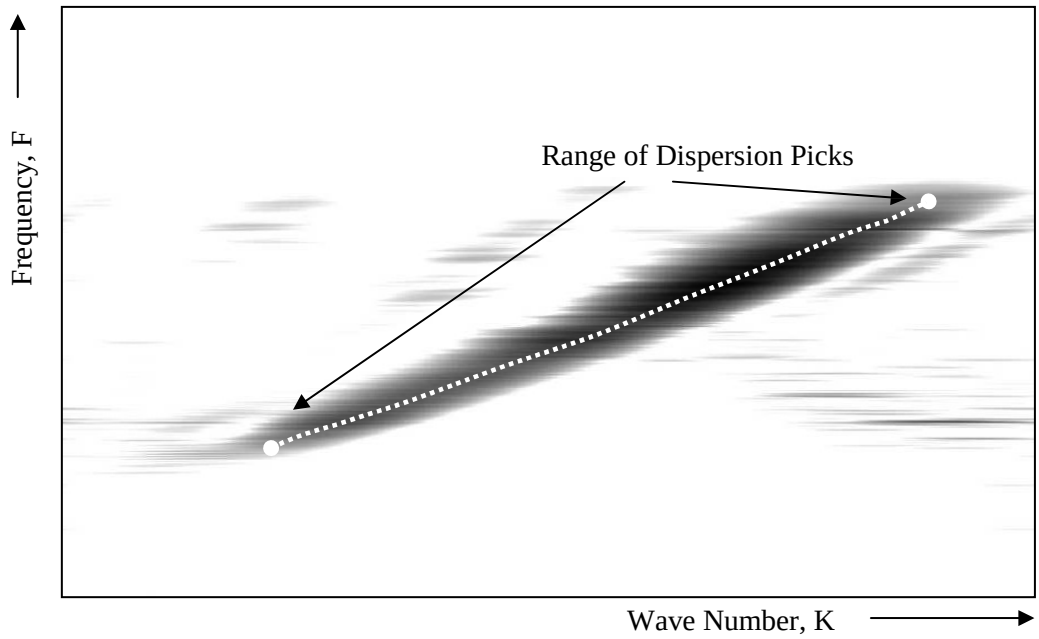

Figure 2.13: Spectral amplitudes of frequency-wave number (F-K) domain and dispersion picks.

The dispersion curve is obtained by selecting the region within the frequency-wave number (F-K) plot with an acceptable correspondence and the highest spectral magnitudes (Figure 2.8 or Figure 2.13). Forward iterative models of velocity profiles are used to calculate theoretical dispersion curves (Equation 4) and are fitted to experimental dispersion curve to identify the velocity profile of the tested site [63-66].

The computation of theoretical dispersion curve finds its basis in Knopoff'sMethod [67]. The non-linear implicit form of the function for calculating of phase velocities is given by

$$Q(f_j, c_{Rj}, V_S, V_P, \rho, h) = 0 \qquad (j = 1, 2, \ldots\ldots\ldots\ldots, m) \quad (4)$$

where f_j is the frequency, c_{Rj} is the Rayleigh-wave phase velocity at frequency f_j, V_S is the shear wave velocity vector of i layers in the ground model, V_P is the

compression(P-wave) velocity vector of the i layers, ρ is the density vector of the i layers, and h is the thickness vector of the i layers. If a set of V_S, V_P, ρ, and h of different layers in the ground model are given for specific frequency (f_j), then the roots of Equation 4 will yield the phase velocities.

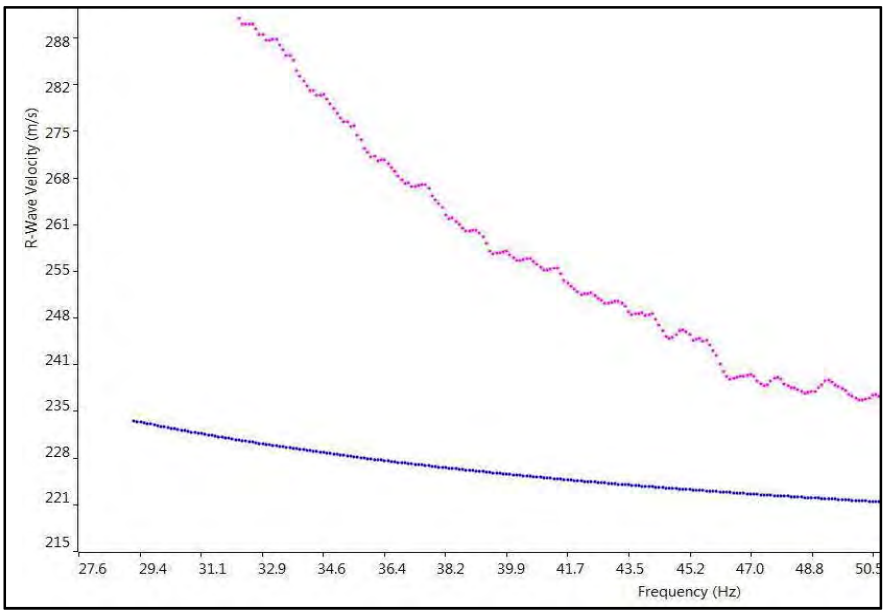

Figure 2.14: Theoretical dispersion curve of initial guess (blue line).

An initial guess of the ground profile is selected as the input and theoretical dispersion curve is calculated (Figure 2.14). The ground profile is iteratively varied until an acceptable fit (Figure 2.15) is achieved between the theoretical dispersion curve and the experiment dispersion curve typically usedthe bisection method [68].

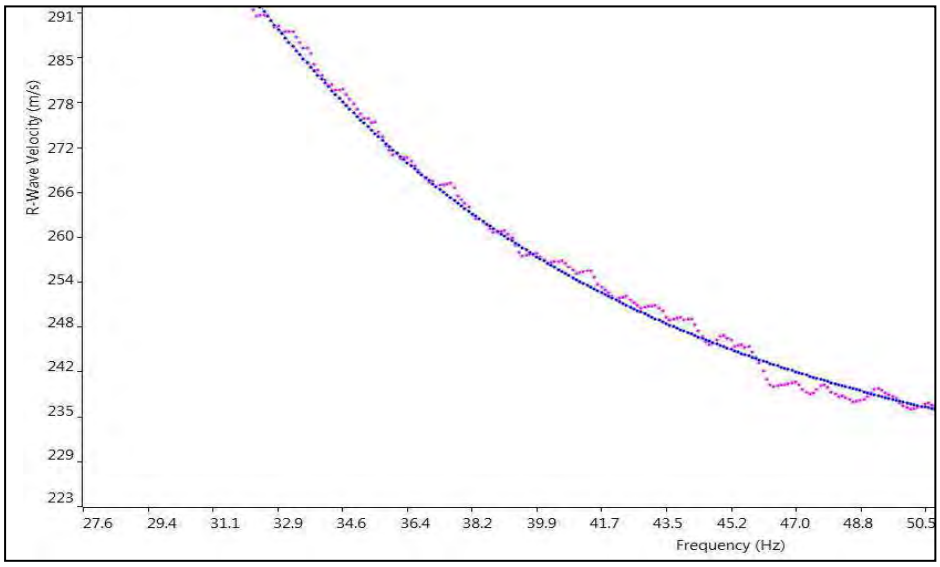

Figure 2.15: A theoretical dispersion curve fitted to experimental dispersion curve (current study).

Figure 2.16presents the effect of shot distance on the estimated velocity profile. Increase in the distance of shot/trigger from the geophone array allows the development of surface waves with longer wave lengths. A shorter distance allows for better characterization of shallow deposits due to predominant shorter wave lengths especially in near geophones. Figure 2.16illustrates the effect by evidence of increasing variation at larger depths.

Figure 2.17 presents the effect of geophone spacing on the estimated velocity profile. The discrepancy in the measurement of shear wave velocity at shallower depth is possibly due to inadequate spatial frequency. The smaller wave lengths are better resolved by smaller geophone spacing; whereas, longer wave lengths are better characterized by geophones having larger separation. The agreement of velocities from 6 m to 9 m corresponds to wavelengths agreeing with the criterion presented by Equation 3.

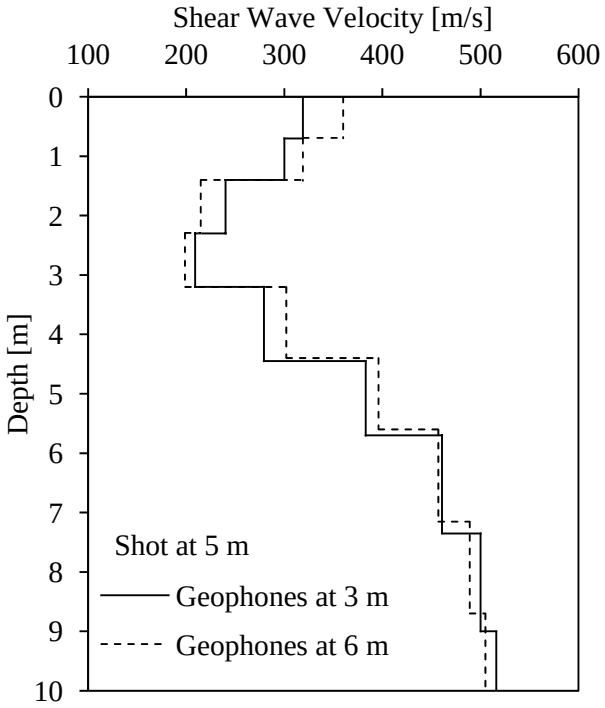

Figure 2.16:Effect of geophone spacing on the inverted velocity profile (current study).

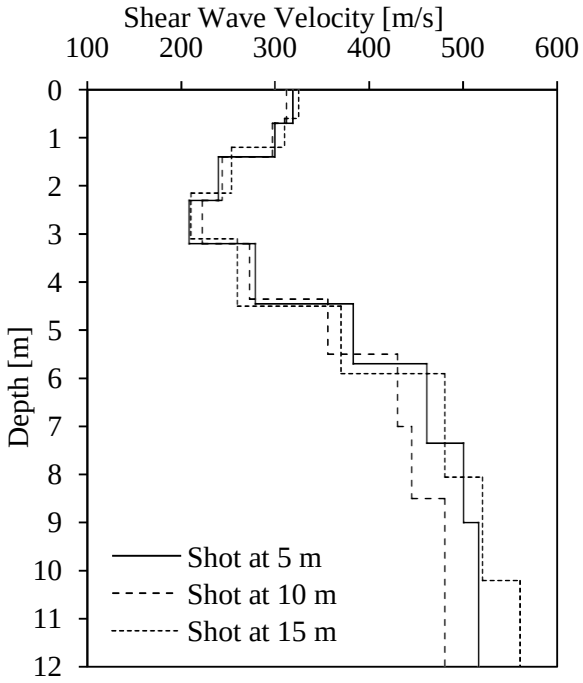

Figure 2.17:Effect of shot distance on the inverted velocity profile (current study)

2.4 Cone Penetration Test (CPT)

The Cone Penetration Test (CPT) is another type of soil exploration method that measures the strength of soils. CPT is being used more frequently in geotechnical engineering study because of its pace, economical costs, and the ease of results presentation. This test is also favored because there is no soil sampling or boreholes required as in the Standard Penetration Test (SPT).

The CPT was first employed by the Dutch engineer Barentsen in 1932 where he used a field cone to measure the tip resistance with depth in a four meters thick fill[69]. A mechanical penetro-meter was used to measure the resistance in this field cone. In 1948, the electric friction penetro-meter was introduced as a substitute for the mechanical one.In 1965, the sleeve friction measurement was added to the cone rod to collect data for identification of soil type. Since then several new technologies have been added to the CPT such as a piezocone, resistivity cone, seismic cone, and acoustic cones [69].

The CPT system consists of several components such as an electrical penetro-meter, hydraulic pushing system with rods, a wired cable or transmission device, depth recorder, and a computer for recording the data. There are two sizes of penetro-

meters normally used in the industry, a 35.7 mm diameter and a 44 mm diameter with individual sleeve and cross-sectional areas. Modern CPTpenetro-meters are also equipped with transducers to measure the pore water pressure, temperature sensors to detect the zones of saturation, and inclinometers to measure the inclination while the probe is advancing under the ground.

The CPT procedure was standardized by ASTM [70] as Test Designation D 3441 for mechanical cone penetration testsand the testing procedures are outlined in detail in ASTM (14) D 5778which uses electronic friction cone penetration and a peizocone apparatus. CPT is typically used in very soft clays and dense sand along with other liquefiable materials such as silt, sands and granule gravel. Although the CPT is particularly effective in gravel and rocky terrains, there are instances where tertiary age rocks can be penetrated by the penetro-meters [71].The two basic measurements of CPT are the tip (q_C) and sleeve (f_S) resistances. These resistances are measured as the penetro-meter is pushed into the ground at a rate of two cm/s. The wired cable, which connects the penetro-meter to the computer, is used to transfer the data continuously as the penetro-meter penetrates. As a result, a computerized log of both the measures is produced. The inclinometer provides a view of the inclination of the penetro-meter,ensuring that the penetro-meter is taking a straight path. Figure 2.18shows a schematic of a typical CPT setting.

Tip resistance of the soil is measured by the load cell behind the tapered cone and the sleeve friction is measured by the tension load cells attached to the friction sleeve at a distance of around 10 cm from the 10 cm^2 cone tip. The tip resistance is related to the un-drained shear strength of saturated and cohesive soils [72].

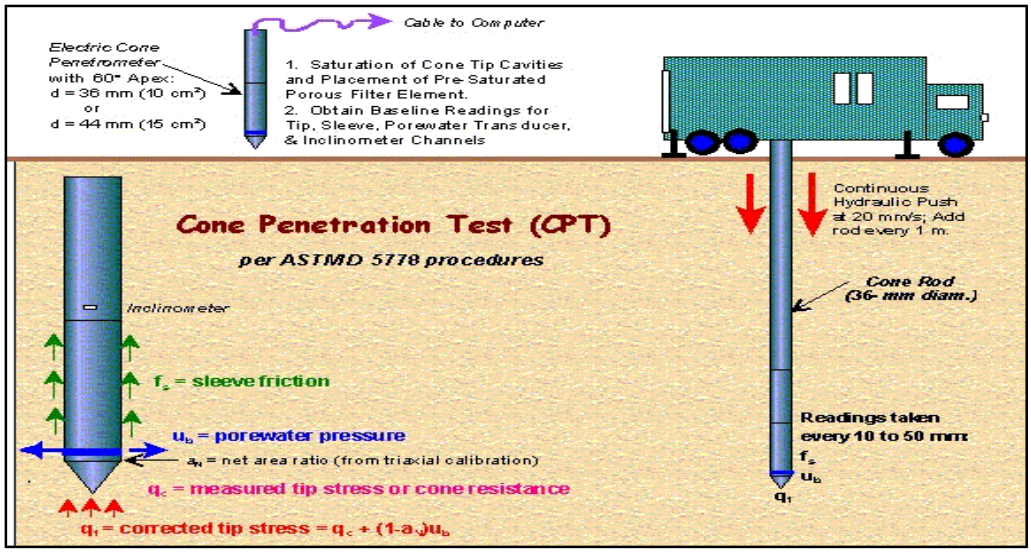

Figure 2.18: CPT procedure and components [44]

2.5 Standard Penetration Test (SPT)

The Standard Penetration Test (SPT) has been used extensively in the in-situ characterization of soils. Terzaghifirst presented the term SPT in a conference on Soil Mechanics in 1947. The primary objective of the test is to provide an indication of the relative density (Table 2.3) of the granular deposits, such as sands and gravels, due to difficulties faced in getting undisturbed samples. The advantage of the tests, and hence its wide use, lies in its comparatively easier deployment and inexpensive operation. The strength parameters, which are either correlated as in Table 2.3 or approximated from the results of SPT, are practically useful when the borehole samples are difficult to obtain.The accuracy of SPT depends on the soil deposits being tested. SPT results provide a good representation of fine granular soils such as fine to medium sands. The accuracy of the results decrease with the increase in coarseness of the cohesionless soils and cohesive and very fine soils yield the most inaccurate representation of soils. The ASTM standard for a SPT test has its designation provided by the test standardD1586−11 [73].

Table 2.3: Correlation of N to Relative Density, and Friction Angle [74]

SPT (Blows/0.3m)	Soil Packing	Relative Density (%)	Friction Angle (º)
<4	Very Loose	<20	<30
4-10	Loose	20-40	30-35
10-30	Compact	40-60	35-40
30-50	Dense	60-80	40-45
>50	Very Dense	>80	>45

In a typical SPT, a sample tube of a thick wall is used, having an outside diameter of 50 mm, an inside diameter of 35 mm, and a length of approximately 650 mm (Figure 2.19). The sample tube is driven into the ground for seating at the bottom of a borehole using a hammer with a weight of 63.5 kg (140 lbs). The slide hammer falls through a distance of 760 mm (30 in) in each strike. The number of strikes for the sample tube driven for the first 150 mm into the ground is not recorded. The number of strikes/blows needed for the tube to penetrate next 300 mm (12 in) is

recorded. The total strikes required to achieve a penetration of 300 mm after the initial seating of 150 mm is called the “standard penetration resistance” or the “N-values” (Figure 2.20). However,in some case where the ground is very dense and required penetration is not possible, the penetration after 50 blows is recorded. The N values provide information about the denseness of the ground that is used to correlate many other engineering properties such as angle of internal friction and shear wave velocities.

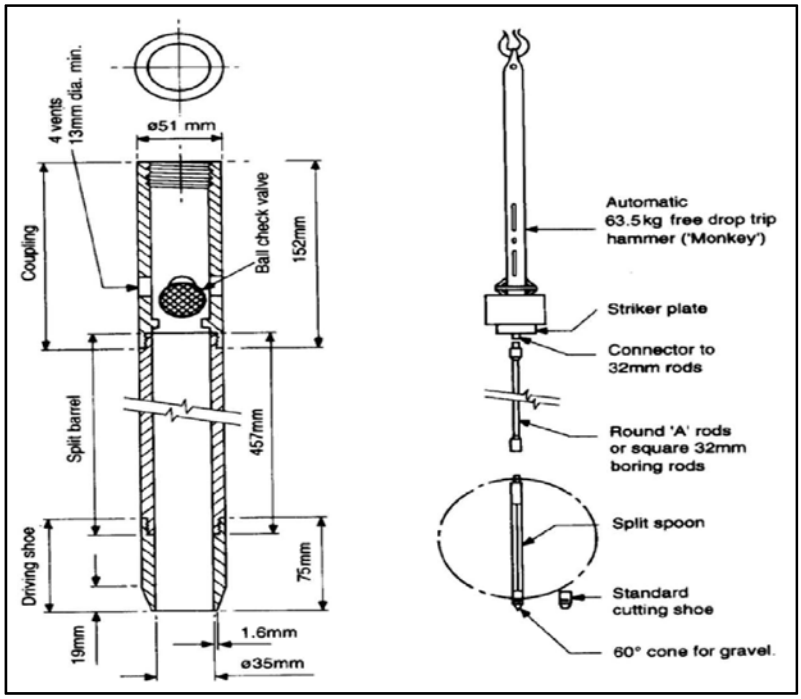

Figure 2.19: Equipment used in SPT (ASTM).

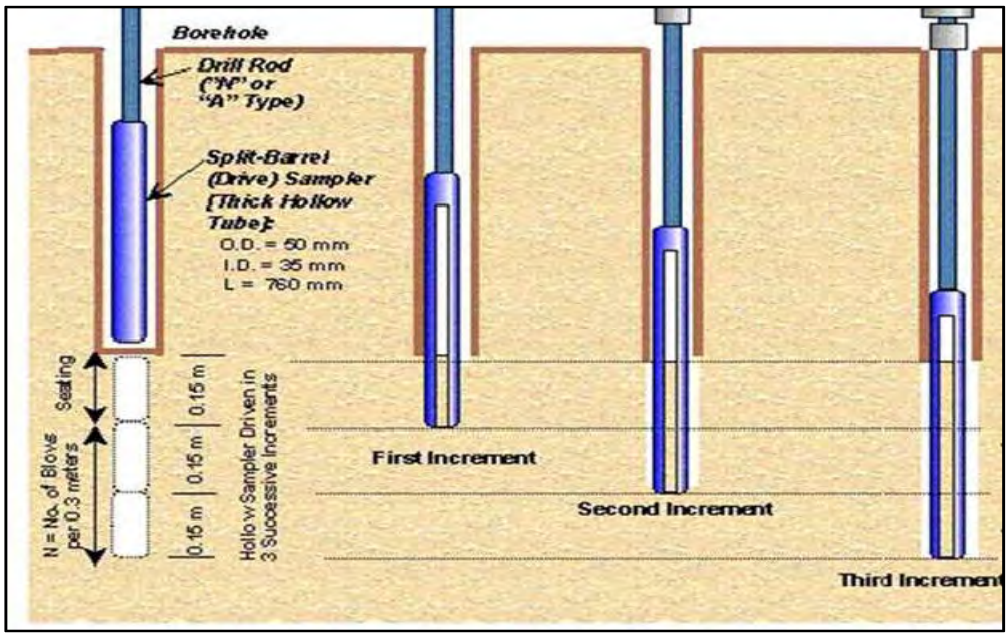

Figure 2.20: Schematic of barrel penetrations in SPT[44]

N values are often corrected for hammer efficiencies, borehole diameters, rod lengths, sampler types, and over burden stresses. The corrected values of N are referred to N_{60} or $(N_1)_{60CS}$ depending upon whether the overburden stress correction is applied. Equation 5 is used to correct the N values, whereas Figure 2.21 contains some correction factors for the parameters used in Equation 5.

$$N_{60} = \frac{N \eta_H \eta_B \eta_S \eta_R}{60} \tag{5}$$

whereη_H is the correction for hammer efficiency, η_B is the correction for borehole diameter, η_S is the correction for sampler type, and η_R is the correction for rod length.

1. Variation of η_H

Country	Hammer type	Hammer release	η_H (%)
Japan	Donut	Free fall	78
	Donut	Rope and pulley	67
United States	Safety	Rope and pulley	60
	Donut	Rope and pulley	45
Argentina	Donut	Rope and pulley	45
China	Donut	Free fall	60
	Donut	Rope and pulley	50

2. Variation of η_B

Diameter		
mm	in.	η_B
60–120	2.4–4.7	1
150	6	1.05
200	8	1.15

3. Variation of η_S

Variable	η_S
Standard sampler	1.0
With liner for dense sand and clay	0.8
With liner for loose sand	0.9

4. Variation of η_R

Rod length		
m	ft	η_R
>10	>30	1.0
6–10	20–30	0.95
4–6	12–20	0.85
0–4	0–12	0.75

Figure 2.21: Correction tables for N values[74]

The correction of N values for overburden stress values and groundwater levels is also applied especially when the N values are used for liquefaction analysis. In some situations, the difference between N values and corrected values are small, especially at shallow depths. In such situations the corrections are not applied.

2.6 Correlating SPT-N values and Shear Wave Velocity (V_S)

Many studies provide the correlations between SPT-N values and V_S based on SPT tests and some other form of a past seismic survey. These correlations have a typical power functional form of $V = aN^b$. The N values, as well as V_S

values,typically are not corrected for overburden pressure in most of the relationships. Table 2.4presents a summary of correlations found in the literature for sandy soils only.

The significant variations in the predictions are mainly due to the applicability of these relationships to particular geological deposits and the variability in the properties of similar soils due to variations in inter-particle states and petro-graphical differences. Testing bias from SPTs, as well as seismic surveys, can also contribute to variations. The N values are typically corrected for factors such as machine efficiencies, borehole diameter, rod length, sampler type for N_{60}, and sometimes for overburden stress correctionsin obtaining $(N_1)_{60CS}$. The choice of using the type of the N values depend on the correlation strength of the data set with N, $N_{60,}$ or $(N_1)_{60CS}$.

Table 2.4: Correlations for the prediction of V_S from N values for sands

Reference	Correlations	Identifier
[75]	$Vs = 80.6\ N^{0.331}$	A
[76]	$Vs = 100.5\ N^{0.29}$	B
[77]	$Vs = 57.4\ N^{0.49}$	C
[78]	$Vs = 145\ (N_{60})^{0.178}$	D
[79]	$Vs = 87.8\ [(N_1)_{60CS}]^{0.253}$	E
[80]	$Vs = 90.8\ N^{0.319}$	F
[80]	$Vs=131\ (N_{60})^{0.205}$	G
[3]	$Vs = 79\ N^{0.434}$	H
[4]	$Vs = 73\ N^{0.33}$	I
[5]	$Vs = 100.53\ N^{0.265}$	J
[5]	$Vs = 96.29\ (N_{60})^{0.266}$	K
[6]	$Vs = 79.7\ N^{0.365}$	L
[7]	$Vs = 60.17\ N^{0.56}$	M

Sykora and Stokoe[76]indicated that the geology and type of soil are not good predictive indicators of V_S, andin contrast that the uncorrected SPT-N valuesare most important factor in the V_S measurements. The authors [76] evaluated V_S as a variable

in relationship with $(N_1)_{60}$ and found a poor correlation. They recommended the useof a correlation with N or N_{60} instead for the prediction of V_S.

Hasançebi and Ulusay[80]developedtheir theory along the same linesregression correlations on97 data pairs collected from a small area in the northwestern part of Turkey. They produced empirical relationships for sands, clays, and for all soils and used both corrected and uncorrected SPT-N values.

Dikmen[4]suggested many correlations for sand, clay and silty soils, in addition to developing correlations that are applicable to all types of soils. The study area where the shear wave velocity measurements and borehole logs were compared was Eskisehir,which is located in west of Turkey. Most sites were deposited with alluvial soils. SPT-N values were obtained at 264 locations. For the determination of the blow counts, CPTs and SCPTswere done at 45 locations. Additionally, seismic tests such as MASW and refraction wereconducted at nine sites. A total of 700 soil samples (disturbed and undisturbed) were collected for further laboratory testing and their physical properties were measured by conducting standard laboratory tests of sieve analysis, consolidation, water content analysis, Waterberg limit analysis, and a triaxial shear test. A total of 193 data pairs were produced and the pairs consisted of uncorrected SPT-N and $V_S$in the database. A non-linear regression analysis, based on theLevenberg-Marquardt algorithm approach, was performed to obtain the correlations.

Another study was performed by Anbazhagan[7], which was slightly different from some of the other studies because they derived a correlation between the SPT-N and low strain shear modulus G_{max} in addition to deriving equations for V_S. This study used the MASW test to estimate the V_S values, and to obtain a total of 215 data pairs of uncorrected SPT- N and V_S. The G_{max} was calculated using the measured V_S and density. While other studies assumed the values of density of soil, this study actually measured the density of in-situ samples from undisturbed samples.

Uma Maheswari et al.[5] reported that the corrected and uncorrected N values predicted V_S with equal accuracy. They used suspension logging and other seismic tests, such as cross hole, to measure the shear wave velocity profile. The developed data set was based on pairs of corrected N values with V_S and uncorrected N values with V_S.

Tsiambaos et al.[6] performed a regression analysis on the data that was collected for the last 10 years on projects in Greece. They looked at the data from the

SPTs and CPTs performed on many soil types in Greece. They also collected data from cross-hole tests to measure shear wave velocity profiles. The developed correlation equations between N values and V_S for all soil types, which is considered as the best method if performed properly for the measurement of shear wave velocity profile.

Hanumantharaoand Ramana[3]performed dynamic testing of soils in a laboratory using the torsional shear device. They proposed the correlations based on the V_S obtained in the laboratory and N values from field tests. Although the tests were performed on remolded cohesionless soils, they do not appear to exhibit a loss of inter-particle structure as evident by the high rate of increase in the power of N values.

Chapter 3: Experimental Program and Setup

3.1 Experimental Program for V_S-N correlations

The MASW tests were performed by using the equipment supplied by Geometrics. A 12-channel geode (Figure 3.1), 12 geophones of 14 Hz (Figure 3.2) and 12 geophones of 4.5 Hz, was used to conduct the field tests. A 10-kg hammer fitted with a triggering sensor was used to generate the stress waves and activate the recordings of channels with relatively small pre-trigger recordings of the time histories.

The equipment was tested on a test site for proper functioning of the electronics and sensors for accuracy of the results. The equipment was purchased as new with factory calibrations from the supplier.Some test recordings were also performed and the data was analyzed by both MASW and seismic refraction approaches. The results were also used to estimate the anticipated range of probable frequencies, wave lengths, and depths of investigations.

Figure 3.1: A 12-channel Geode supplied by Geometrics USA

Signals in time domain (e.g. Figure 3.4) and their Fourier transforms (e.g. Figure 2.13) are used to evaluate the range of frequencies and wave numbers for

estimation of wave lengths.Determining geophones distances, shot distances, sampling rates to prevent aliasing (loss of data due under sampling) of the signals, and evaluation of the Nyquist criterion,which is used to prevent aliasing, is also crucial [81]. Shot media and contact plates of different materials and stiffness are tested and frequencies of interest are determined on test sites. Several geophones spacing, hammer padding and energy of fall, and shot distance combinations are considered to adequately address the issues with wavelengths, depths of penetrations, and temporal and spatial aliasing of the signals.

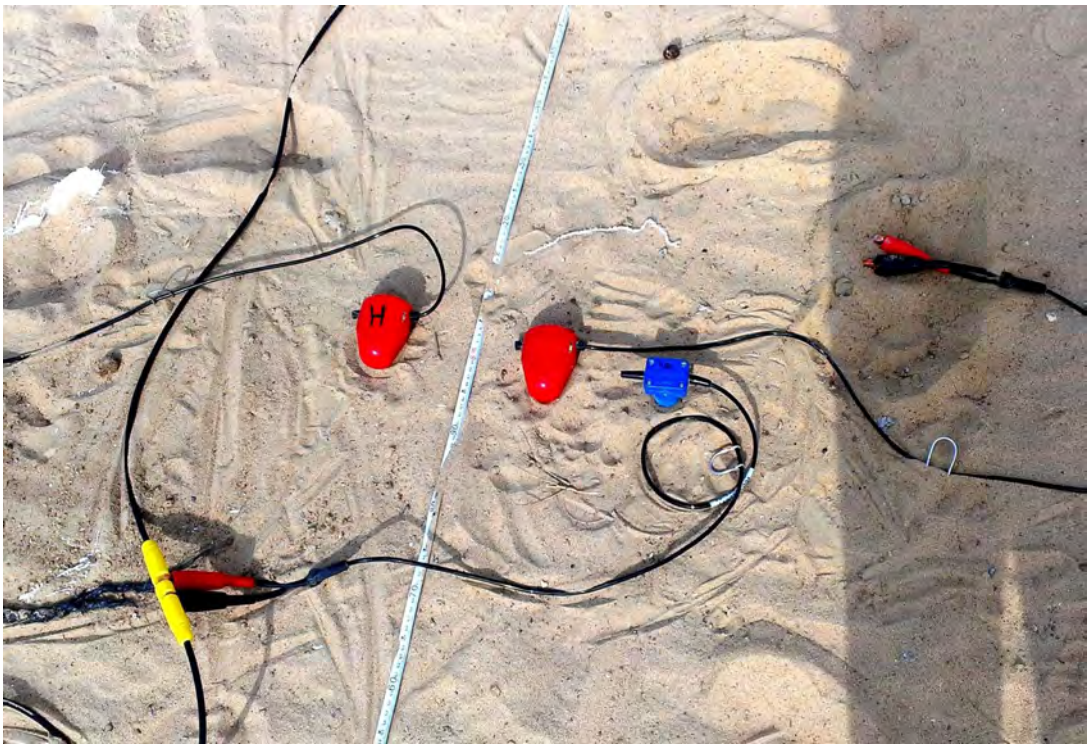

Figure 3.2: 14 Hz vertical geophones (Blue) and 4.5 Hz horizontal geophones (Red)

A total of fifteen (15) locations are identified and surveyed to collect the data (shown in Figure 3.3). The selection of sites is based on soil types representative of the region and the availability of boreholes (SPT results) recently advanced. Sites on reclaimed land are neglected in an attempt to focus on the natural deposits of soils. Similarly, sites with a ground water table within the first few meters are also neglected due to possibility of shallow reflections and possible effects on SPT values. The boreholes logs prepared within the authorized jurisdiction are collected after approval from competent authorities. The boreholes logs presented N values smaller than 50 and N values larger than 50 are reported as 50+, which are subsequently not used in this study.

Figure 3.3: Site locations of field testing indicated by solid circles

Depending upon the number and proximity of boreholes at each site, up to three lines are surveyed. The testing is performed on weekends during the early mornings to reduce noise contamination from traffic. The geophone type (frequency response and sensitivity) and spacing are varied in order to obtain detailed velocity profiles of near surface and the deeper strata. The shots (hammer drops) are located at 5, 10, and 15 m from the first geophone.

The connections, signal saturation, noise levels are checked before each test (i.e., Figure 3.4) by making test shots and previewing them in the GEOPSY software. A preliminary dispersion curve analysis is also performed on test shots to validate the equipment setup. Data files are also backed up on removal storage media for additional copies.

The data files are analyzed by commercial software “SWAN” provided by Geoastier (Version 1.4). The results are also independently validated for some measurements by performing the analysis in GEOPSY (Version 2.8.0), a freeware with public license. GEOPSY uses the neighborhood algorithm for inversion of the dispersion curves [82].

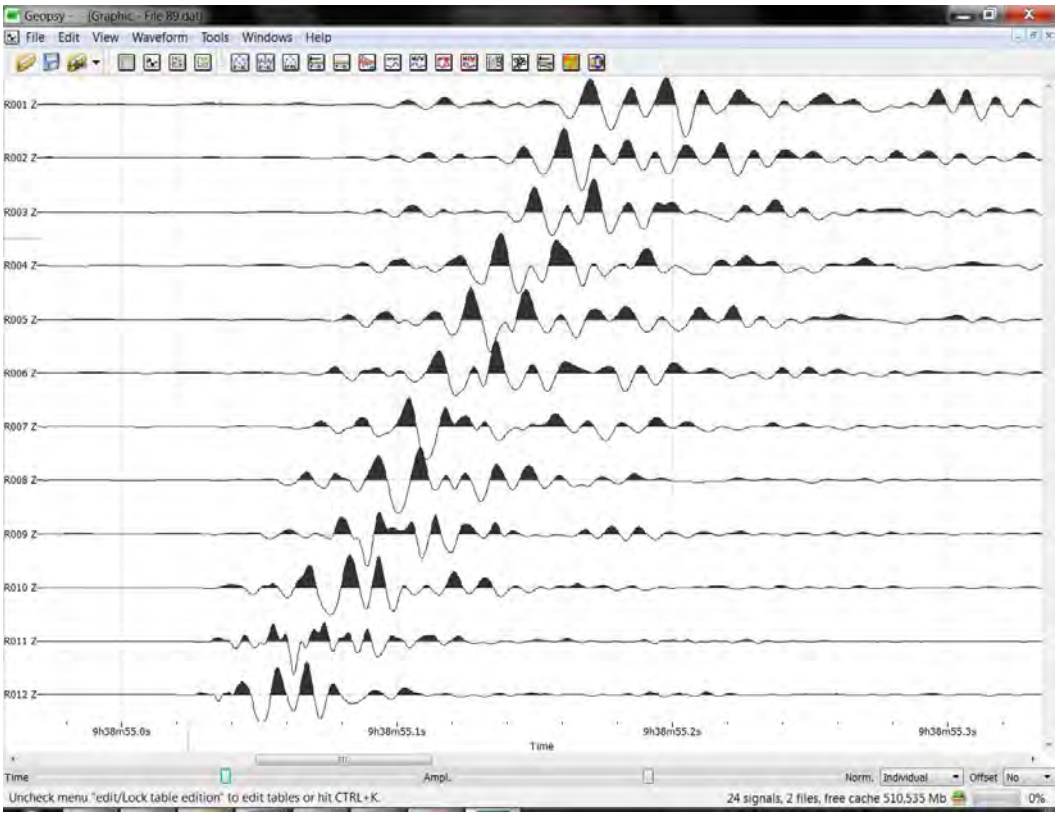

Figure 3.4: Typical signal visualization and verification in GEOPSY at site.

For additional validation and verification of the results from the software ,SWAN,the phase unwrapping method is also used to compute dispersion curves for few data files in MathCAD (Version 14). Figure 3.5 presents the comparison of dispersion curve obtained from SWAN and GEOPSY.

The dispersion curves from a survey line with different combinations are loaded in SWAN for inversion. The subsurface velocity profiles are calculated by matching of the experimental dispersion curves by theoretical dispersion curves of forward iterative models.

A database of shear wave velocities and corresponding N values (as well as N_{60} values) is developed. The database contains pairs of V_S-N values for N values of up to 50. N values greater than 50 are ignored due to local protocols of not reporting N values larger than 50 on borehole logs. The data set is then analyzed by performing a regression analysis and developing models with power functional form. The functional forms of the models predicting V_S values as function of N values and the comparison with previous studies are presented and discussed in the following chapter.

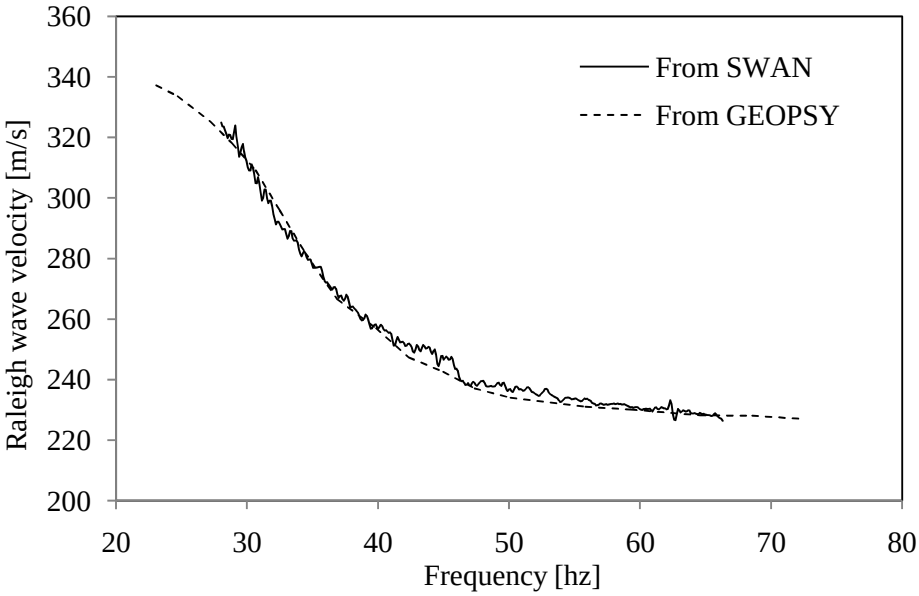

Figure 3.5: Comparison of experimental dispersion curves computed by SWAN and GEOPSYusing vertical geophones

3.2 Experimental Program for Horizontal and Vertical Geophones

The testing program consists of conductingMASW tests on two (2) sites to evaluate and compare the results of using geophones capable of measuring horizontal and vertical components of particle motion. The testing equipment deployed in the field consists of 12 channels geode supplied by geometrics, twelve geophones (4.5 Hz) capable of measuring horizontal motion, twelve geophones (14Hz) capable of measuring vertical motion, spread cable of 12 connectors, a 10 kilo hammer, and a triggering cable with sensor.

The MASW tests are conducted by first using the vertical geophones in the array marked by configuration for vertical geophones as shown in Figure 3.6. The shots at five meters, 10 meters, and 15 meters are recorded. The vertical geophones are disconnected from the spread cable, and horizontal geophones are connected to the spread cable as the configuration for horizontal component shown in Figure 3.6. The shots are repeated at the shot offset distances used for vertical geophones. In the third round of testing, both vertical and horizontal geophones are connected simultaneously at double the spacing due to the limitation in the number of channels

in the geode. In this configuration, a pair of vertical and horizontal geophones is at the same place (also, see Figure 3.2).

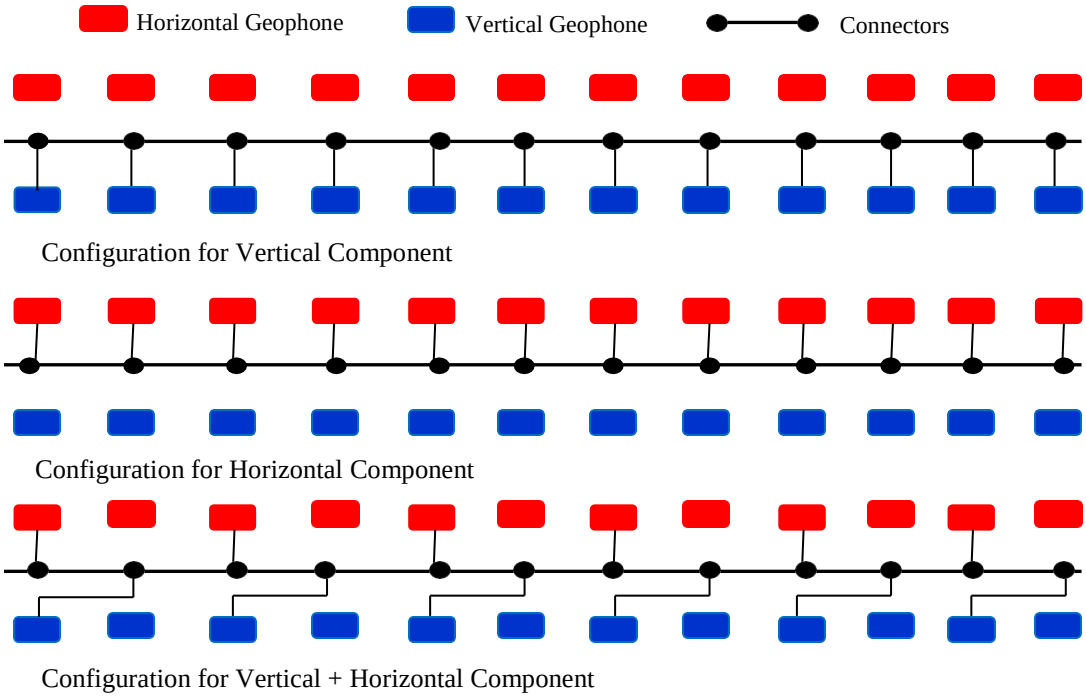

Figure 3.6:Schematic layout for connecting different geophone arrays

Each recording was verified on site by GEOPSY (e.g. Figure 3.4) before performing another test. Also each shot was verified by quick analysis by generation of dispersion curves.The data was backed up on USB drives from the computer hard drive before leaving the site. All tests were performed on weekends during the early hours of the morning soon after sunrise to avoid signal contamination from traffic vibrations.

The analysis was performed by using the commercially-available licensed software of SWAN by Geoastir, which usesa 2DFourier transform and frequency-wave number analysis to determine the dispersion curves. The performance of the software is independently verified by using freely available software of GEOPSY as discussed in section 3.1.Figure 3.7 presents the comparison of dispersion curves from SWAN and GEOPSY for the data measured by horizontal geophones.

The experimental data of several data files are also analyzed in MathCAD using the phase unwrapping method. During a typical analysis F-K plots, dispersion

curves, inverted models, and theoretical dispersion curves were saved for presentation and discussions.

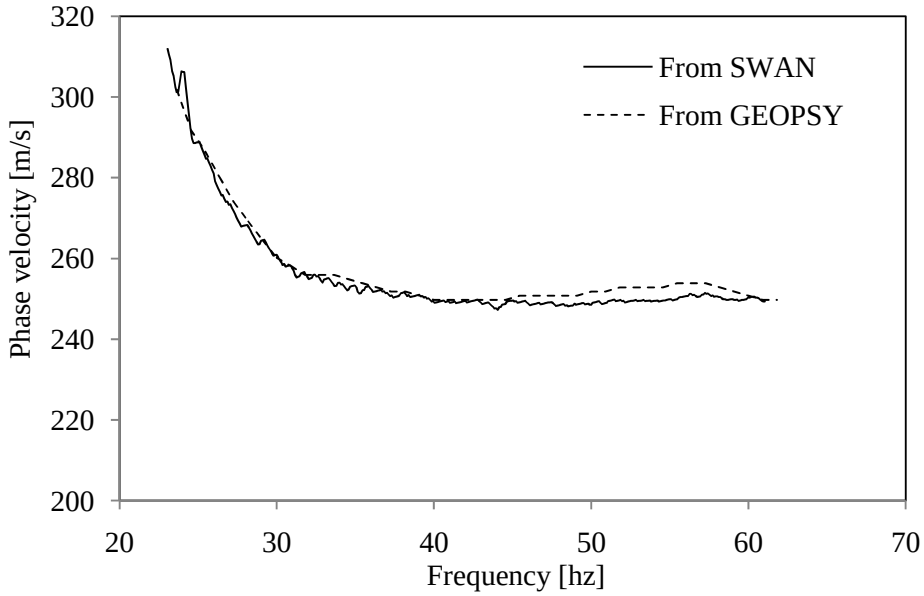

Figure 3.7:Comparison of dispersion curve from SWAN and GEOPSY for horizontal geophone (current study)

Figure3.8presentsthe typical frequency-Velocity (F-V) plot (Dispersion curve)for data measured by vertical geophones. The plot presents amplitudes of spectral power to be distributed over the first Raleigh mode. The mode is clearly visible in the data from the vertical geophone. Similarly Figure 3.9presents the F-V plot or dispersion curve from the horizontal geophone at the same location. The first Rayleigh mode of vibration is clearly visible in the Figure 3.9, thereby illustrating the ability of horizontal geophones to measure the horizontal component of particle motion during the Rayleigh wave propagation.

Additional dispersion curves and F-K plots are presented in the Appendix. During the testing, the shot offset distances were varied to analyze the effects of different wavelengths on the dispersion curves and inverted velocity profiles. The effects of the shot offset distance on the inverted velocity profiles for the horizontal, as well the vertical geophones were also studied.

The experimental dispersion curves were inverted in SWAN, which uses the theoretical dispersion curves of ground profiles iteratively fitted to the experimental dispersion curve. During the inversion process some properties of the soil layers were

introduced such as the Poisson's ratio and densities whereas other properties such as thickness and shear wave velocities were iteratively varied by the software SWAN in an attempt to achieve the best fit with experimental dispersion curves.

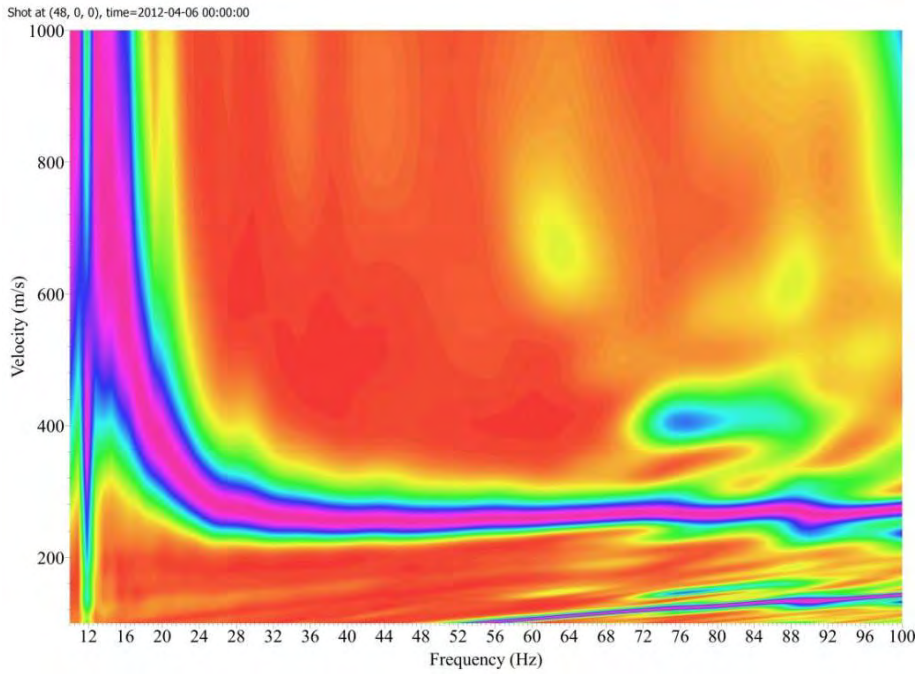

Figure 3.8:Dispersion from the data measured by vertical geophone configurations.

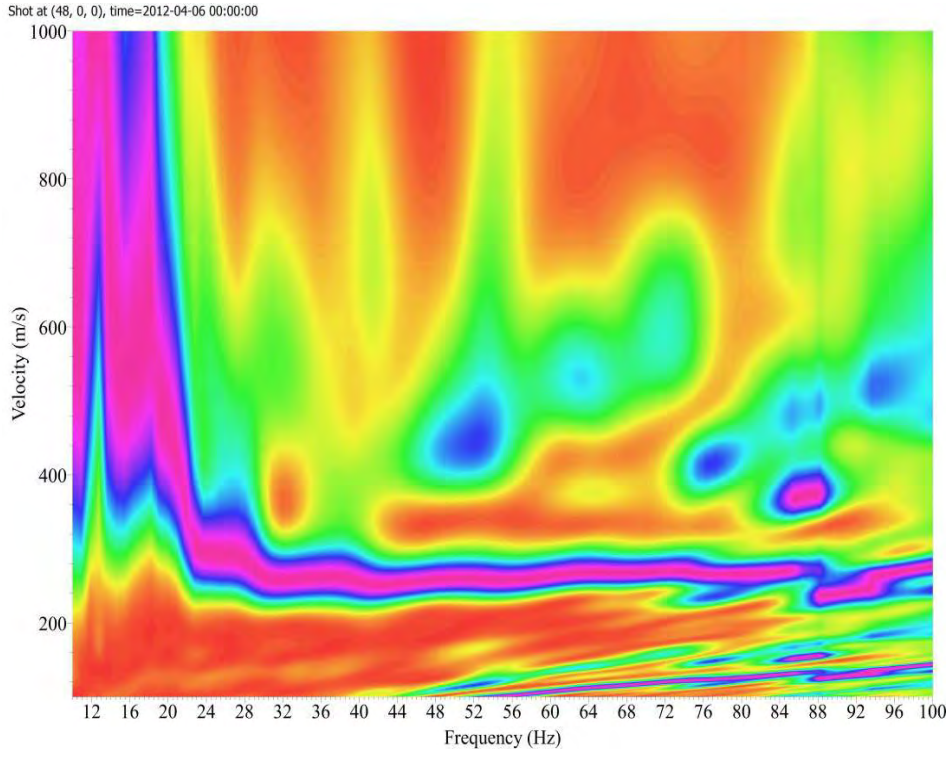

Figure 3.9:Dispersion from the data measured by horizontal geophone configurations.

3.3 Challenges faced during the field testing

The seismic testing requires the recording of ground response with as little contamination from the ambient sources such as traffic and industry. The field surveys and the data collection had to be stopped and sometimes repeated due to the passing of heavy traffic on nearby roads or airplanes.

The sampling rate required to prevent the aliasing of the signals was a challenge as it was a compromise between large number of data and data loss. Determination of appropriate sampling rate that would neither create aliasing nor very large data files required great amount of initial testing on sites.

The insertion of geophones itself, as well as creating a proper contact with the natural surface, was challenging due to loose material at the surface. A proper insertion would therefore require readjustment of the geophones several times before the actual shot. Similarly, the connection of the geophones to the spread cable, as well as battery terminals, would require readjustment occasionally to get a good signal free of noise.

Some sites were retested at slightly different locations due to unusual signals possibly caused by reflection from buried anomalies.

There were no significant challenges faced during the data analysis from the software. Since more than 200 data files were processed, and more than 600 figures of F-K plots, dispersion curves, and velocity profiles were produced, the time required to organize them into respective folders was challenging.

Chapter 4: Results and Discussions

4.1 Results for V_S-N correlations

The results of the MASW tests for evaluation of velocity profiles, regression analysis on the data sets, and development of V_S-N correlations are presented in this section. The MASW tests were performed at sites in Sharjah where, SPT-N values were measured recently and pairs of V_S with known N values were developed.

Figure 4.1 presents the set of some dispersion curves for some locations to illustrate the range of phase velocities as function of frequency. Not all curves are presented for clarity. The original F-K plots of the dispersion curves (i.e., Figure2.13 or Figure 3.7) indicate strong spectral amplitudes representing fundamental mode of vibration in all results with some locations having a faint glow of higher mode(s). The dispersions indicate all locations as dispersive in nature with wave velocities increasing steadily with depth. Most locations indicate a significant increase in velocity at shallow depths (low frequencies corresponding to higher velocities results in longer wavelengths).

The dispersion curves are also plotted at two different axes for clarity and to avoid overcrowding of the figure. Some other selected dispersion curves are presented in the Appendices. The dispersion curves in Figure 4.1 indicate dispersive media with wave velocity increasing with depth.

The geology of Sharjah area consists predominantly of sands, and the stiffness (which is measure of the wave velocities) increases with depth due to densification, cementation, and increase in overburden pressure. The stiffness of sands at most sites is denser at shallow depths (5 to 8 m) with N values typically exceeding 50. The local jurisdiction therefore does not report N values larger than 50 and indicates 50+ instead.

The velocity profiles at most sites indicate high rate of velocity increase with depth and becomes significantly larger at shallow depths corresponding with the significant increase of N values.

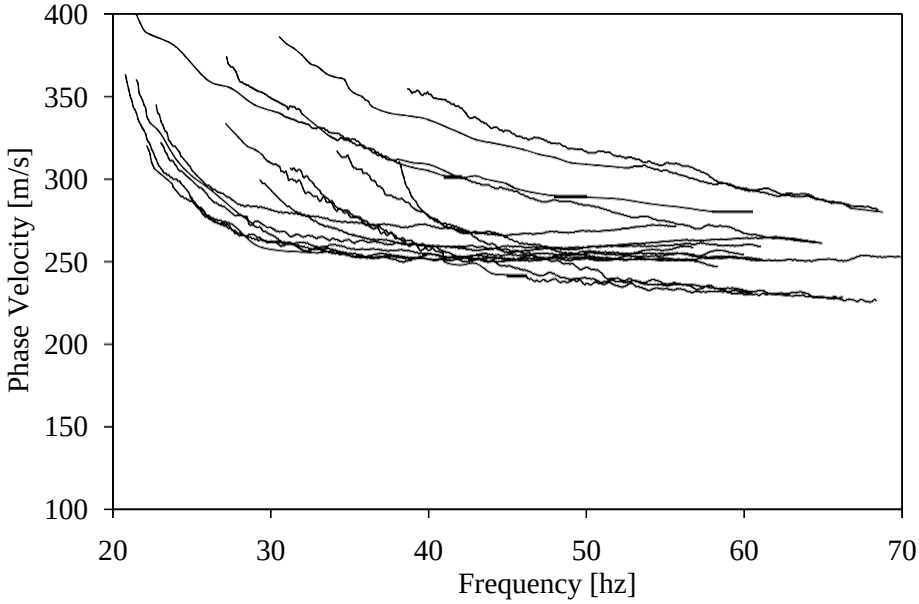

Figure 4.1: Typical dispersion curves representing tested sites (current study)

Figure 4.2 presents the velocity profiles of survey lines corresponding to Figure 4.1. The distribution of velocity with depth indicates a range of 200 m/s to about 580 m/s up to depths of nine meters. The maximum velocity remains below 580 m/s for depths less than six meters. The computed velocity profiles represent the best fit of dispersion curves obtained from different combinations of shot distances and geophone spacing. The range of measured velocities at a given depth presented in Figure 4.2 will change slightly with the inclusion velocity profiles from additional survey lines.

At some locations, the variation of velocity with depth indicates increasing velocity with depth; whereas, at other locations velocity variation is indicative of a slightly stiffer layer overlying the weaker layer. The trend in velocity variation at these locations is also replicated by a variation in SPT-N values. Almost all velocity profiles tend to saturate at depths larger than nine meters (i.e., velocity remains constant with depth) due to limitations with generation of higher wavelengths.

The ability to generate larger wave lengths is also dependent on the stiffness of subsurface soils. The stiffness of the soils at tested locations increases significantly within shallow depths and requires significant energy in the shots to produce large wave lengths. Since deeper explorations in this study are not of concern due to the range ofSPT-N values of interest availablewithin shallow depths, a characterization of soils at shallow depths is considered sufficient.

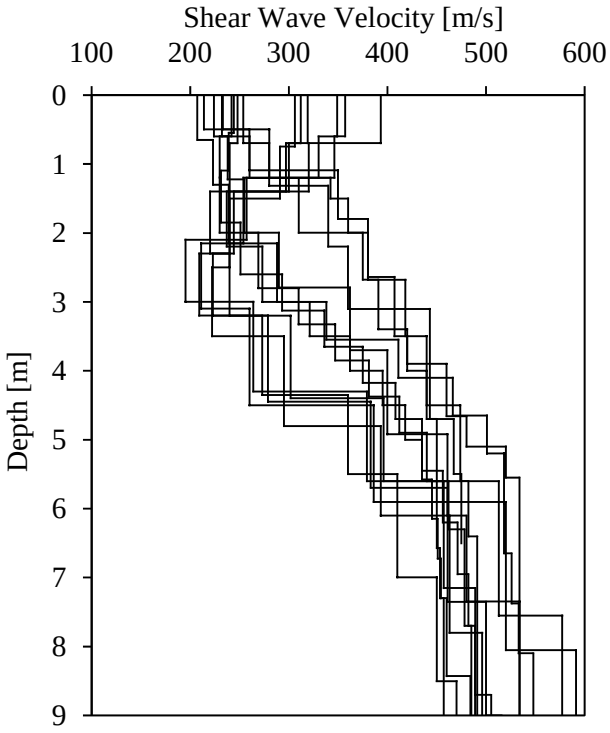

Figure 4.2: Inverted velocity profiles representing tested locations

4.1.1 Development of Dataset and Correlations. Figure 4.3 presents the pairs of shear wave velocity and N values. The data set contains almost 200 pairs for predominantly sandy soils with occasional cemented sand pockets. Figure 4.3 also presents the fitted model with a functional form given by Equations 5. The upper and lower bound limits representing 80% probability of occurrence are also shown in the figure. The data set represents smaller scatter at lower N values than at larger N values; this is possibly due to a much smaller number of available data points. The slope of the data set at lower N values also appears to be steeper than that for the data set at higher N values (>20).

This change can be attributed to the presence of cemented pockets that affect the propagation of wider wave fronts, but could also be missed by a discrete sampler of SPTor could be encountered by SPT and give inaccurate N values. However, the slope tends to flatten again towards the upper limits (40<N<50) possibly due to limiting values of stiffness at larger depths.The regression analysis on the data set is performed by using the power functional form of a non-linear model presented in Equation 5.

$$Vs = 84.868\ N^{0.373} + 14.63 \quad (5)$$

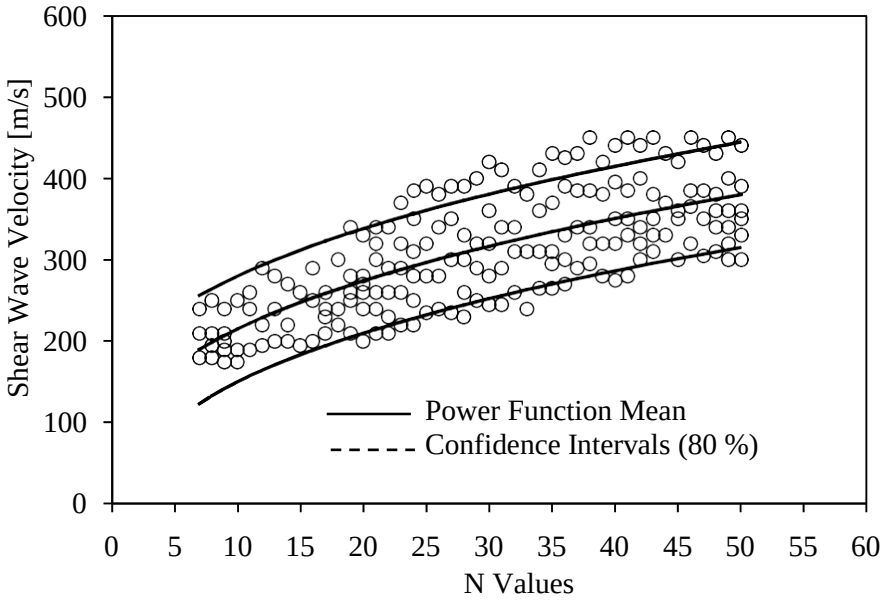

Figure 4.3: Dataset of V_S-N pairs and fitted model with confidence intervals (current study)

The goodness of fit is computed by first calculating the Mean Square Error (MSE) and Mean Square Regression (MSR),these also being used for the analysis of the variance. A rough estimate of the fit obtained by Equation 6 is found to be 0.526.

$$Goodness \quad = 1 - \frac{SSE}{\sum (Vs \ - \ mean\ (Vs\ ))^2} \quad (6)$$

where*SSE* is the summation of square of errors computed from the residuals. The confidence intervals for any value of V_S predicted by given N value are computed in the form of a range or asymptotic error bars. Similarly confidence intervals with different levels of probabilities are computed. The confidence interval with 80% probability that the parameters will be in a certain range is plotted on Figure 4.3.

The data is fitted with a power function of an intercept value forced to origin. The resulting expression is presented and plotted in Figure 4.4. The V_S values predicted by this model (Equation 7) are under estimated compared to the prediction of Equation 5. The results, however, are practically similar. The predictions of the two models are expected to deviate further at N_{60} values larger than 50.

$$Vs = 94.655 \quad N^{0.3512} \tag{7}$$

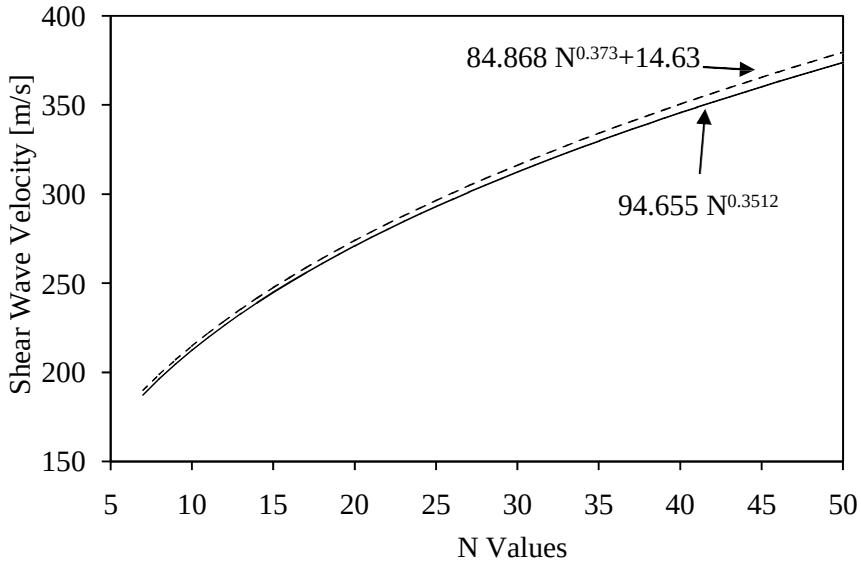

Figure 4.4: Comparison of models (power functions) with and without intercept constraints

Few researchers [79, 83] noted the influence of overburden stress on the regression of the data sets between wave velocity and N values. They also observed a better correlation and goodness of fit; however, other researchers observed no or a negative effect when considering the overburden correction of N values on the goodness of fitted models. Figure 4.5 presents the comparison of V_S predicted by other models in the literature with the range of V_S determined in this study for sandy soils.

The models (I, J, K, Table 2.4) given in the literature strongly underestimate the mean V_S predicted by this study. Model G agrees with the proposed model (mean) at N values smaller than 15, but then underestimates the velocities at higher N values. However, some models (E, L, B), predict V_S within the lower bounds of this study. Some models (M and H) overestimate the mean of the proposed model, but remain within the upper bound for most of the N values. In spite of the underestimation, 80% confidence intervals of most models might overlap the 80% confidence intervals determined in this study.

All models are plotted against their respective definition of N values such as N, N_{60}, and $(N_1)_{60CS}$. The prediction among most models is practically similar at N values smaller than 15.

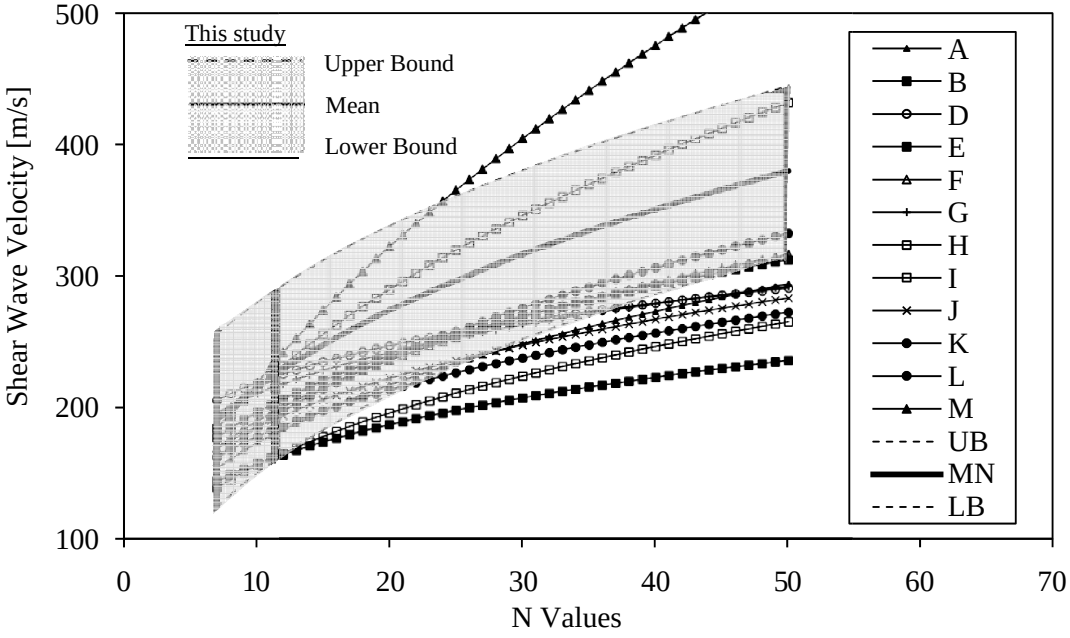

Figure 4.5: Comparison of the proposed V_S predictions with previous studies

The higher rate of prediction in this study is possibly due to a better characterization of shallow depths due to the generation of shorter wavelengths. In addition to better characterization with the MASW by resolving layers of lower velocity hidden between higher velocity layers, most of the N values of interest (<50) were reported within the first five to seven meters of depth at most locations. Shear wave velocities measured in other regions [40] using the MASW technique, or even refraction technique, indicate wave velocities higher than those predicted by many correlations presented in the literature for the range of N values presented in this study.

Figure 4.6 presents the comparison of a proposed model with some recent studies that tend to agree with the findings of this study. Models proposed by [3] and [6] presenta similar agreement with the predicted shear wave velocity; whereas, a study by [7] significantly overestimates the proposed model at higher N values.

On the other hand, the prediction model proposed by [78]agrees at N values smaller than 30, but the model tends to underestimate the wave velocities at higher N values. As stated in the preceding section, the disagreement between various studies presented in the literature can be attributed to many reasons. A comprehensive assessment and comparison of the previous methods,which is not the objective of present study, would provide greater insight into the discrepancies.

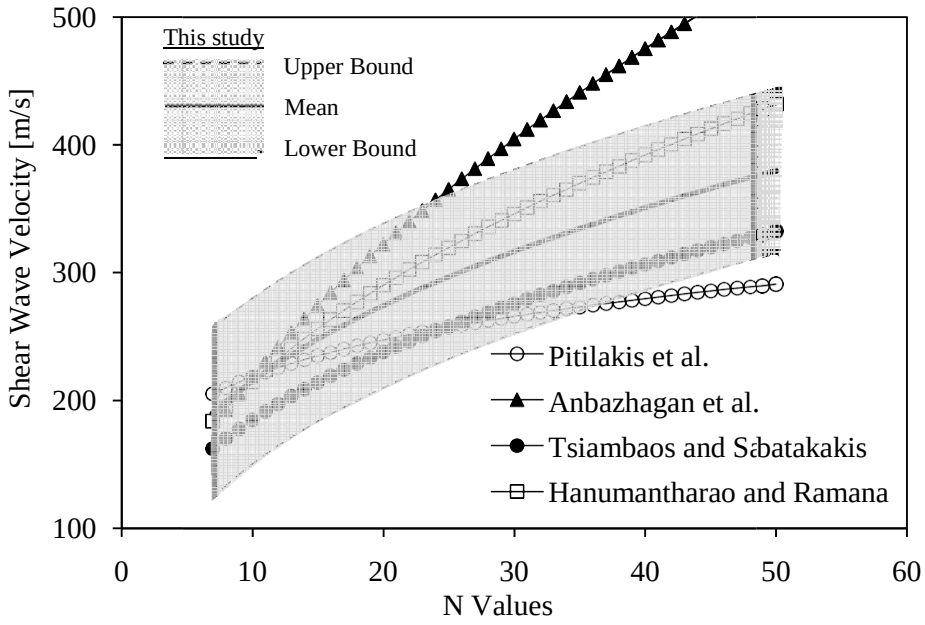

Figure 4.6: Comparison of the proposed V_S predictions with selected studies

Figure 4.7 presents the comparison between the prediction of the proposed model and the measured shear wave velocity profile at a site. The upper bound (UB) and lower bound (LB) values are also indicated on the graph that corresponds to 80% confidence intervals. The comparison indicates that the measured values of V_S lie within the bounds of the predictions.

The mean values of the predictions approximate the measured values at depths smaller than four meters but then deviate at larger depths. The deviations at larger depths are possibly due to the decreasing accuracy of N values as they reach 50. The values of N also can be affected by the presence of occasional cemented sand pieces that are encountered by the SPT sampler.

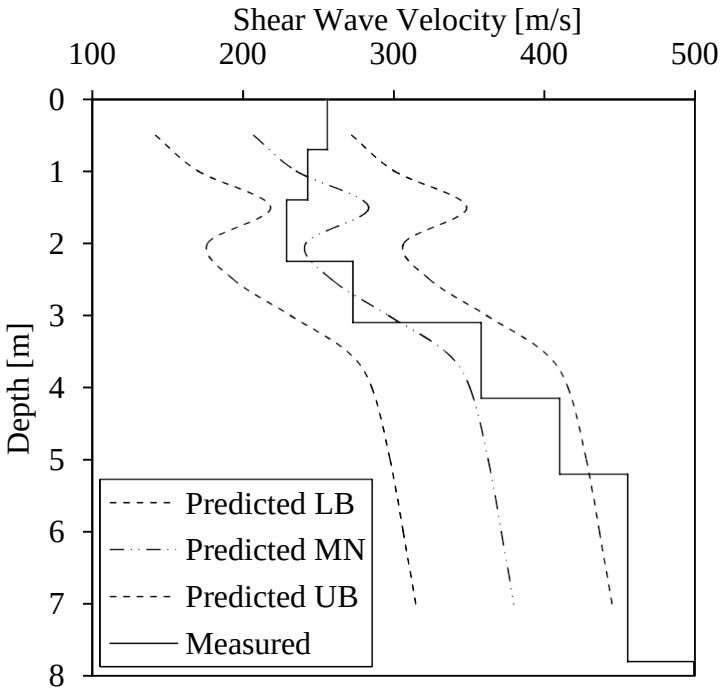

Figure 4.7: Comparison of the measured and predicted VS profile at site S13

4.2 Results for comparison of Horizontal and Vertical Geophones

The MASW tests were performed to evaluate the ability of shear (horizontal) geophones to measure the horizontal component of particle motion during the propagation of surface waves. The data was analyzed to evaluate the shear wave velocity profile and compare them with profiles computed from MASW tests usingthe vertical component of particle motion. These results are presented below.

Figure 4.8shows the comparison of dispersion curves obtained from the particle motion recorded in horizontal and vertical direction during the propagation of Raleigh waves. The curves agree at all frequencies. This agreement indicates that the dispersion curves can be obtained reliably independent of the recording axis of geophones. The founding principle of converting the time domain data into the frequency domain data relies on the frequency content of the signals. The Rayleigh waves create a particle motion that resembles a retrograde ellipse. The horizontal or vertical component of the motion is therefore expected to oscillate harmonically at the same frequency.

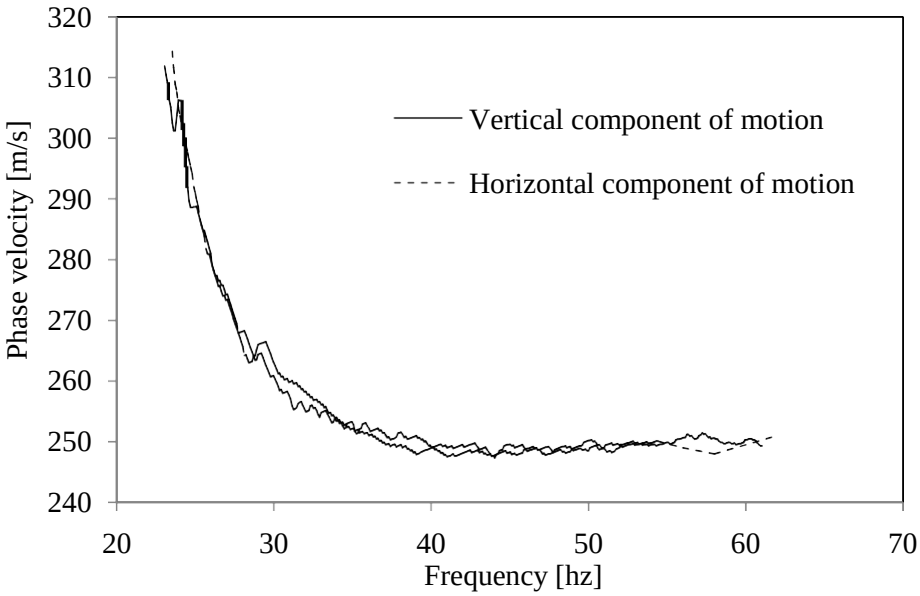

Figure 4.8: Comparison of the Dispersion curves from horizontal and vertical geophones (current study)

The results of MASW tests are influenced by the shot offset distance due to the formation of different wavelengths and the ability of the receiver distances to resolve the wavelengths. Therefore, areliable MASW testing program involves tests at various shot offset distances and receiver spacings to obtain a representative dispersion curve by combining the results with a representative velocity profile. Figure 4.9 presents the effect of the shot distance on the dispersion curve. This effect is visible in the gradual deviation at certain frequencies that are representative of certain depths.

Figure 4.10 presents the velocity profile obtained from dispersion curves of horizontal and vertical component of motion at shot distance of 10 meters. Similarly, Figure 4.11 presents the velocity profiles at a shot distance of five meters. The velocity profiles at respective shot distances agree for the horizontal and vertical component; however, the deviation becomes significant as the depth increases. The increase in disagreement is expected due to a greater decrease in the amplitude of vibration with the depth for the horizontal component of Raleigh Wave propagation[84].

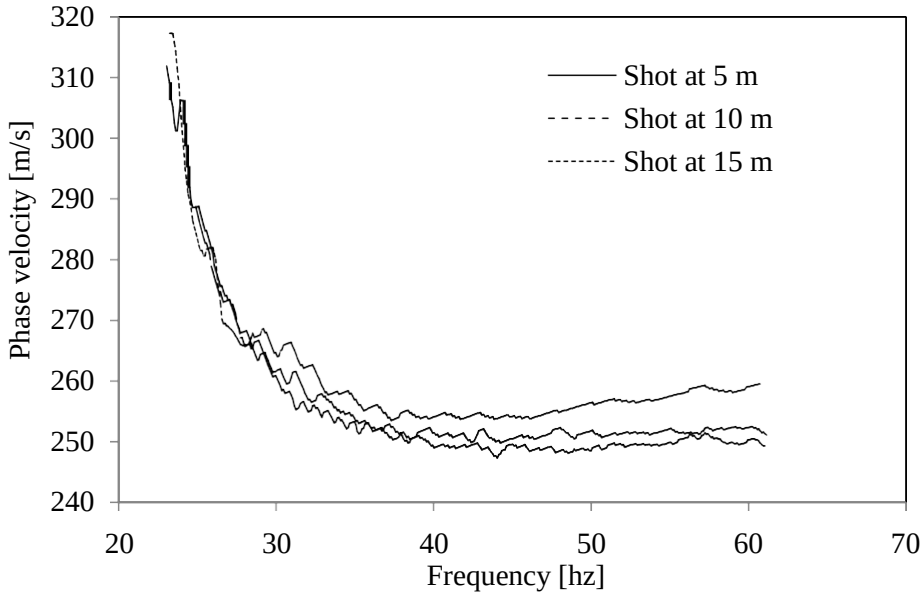

Figure 4.9: Effect of shot offset on dispersion from horizontal geophones.

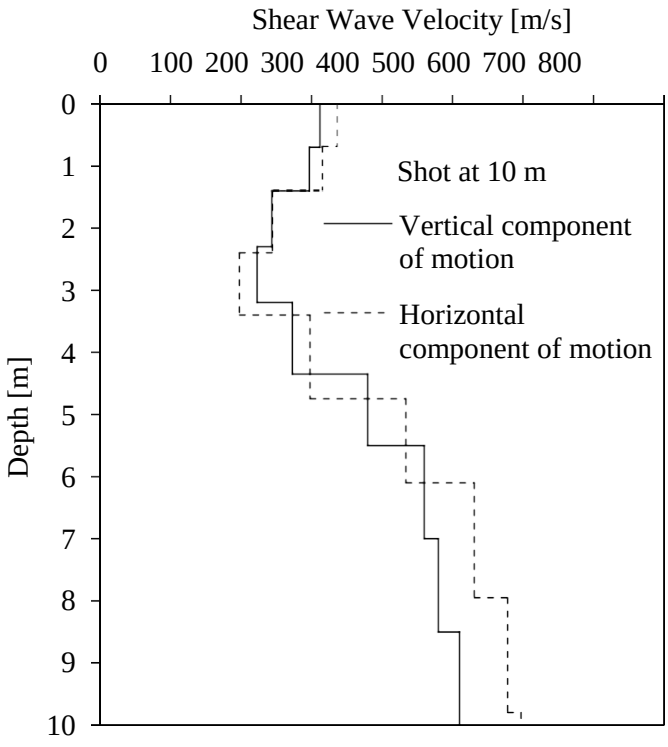

Figure 4.10: Typical velocity profiles from horizontal and vertical geophones at shot offset distance of 10 m.

The effect of shot distance is visible at larger depths due to the combination of limitations to the extent of generated wavelengths and a larger rate of amplitude decay with depth for the horizontal component. The agreement at shallow depths is indicative of particle motion oscillating at the same frequency both in horizontal and vertical directions during an elliptical movement.

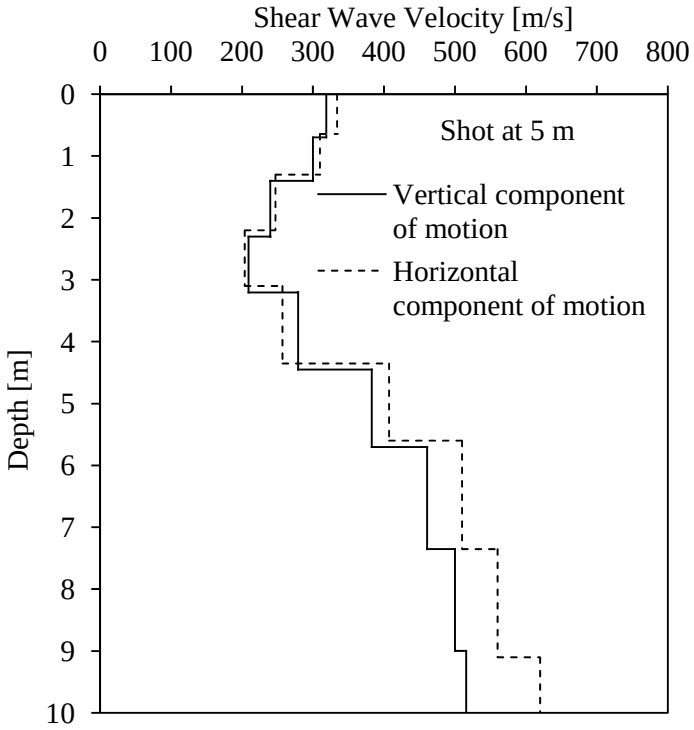

Figure 4.11: Typical velocity profiles from horizontal and vertical geophones at shot offset distance of 5 m.

Chapter5: Conclusions and Recommendations

Correlations between SPT-N values and shear wave velocity are developed for typical soils of Sharjah in the United Arab Emirates. Wave velocities are measured at different locations by conducting MASW field tests. The SPT-N values are obtained from freshly advanced boreholes after approval from the competent authorities. A regression analysis is performed on the data pairs of V_S and N values in order to evaluate the functional form of the model. The results are compared with the models developed during past studies. The main conclusions of this study are presented below.

- The MASW technique is capable of resolving soil layer of velocities lower than the layer overlying and underlying them (inverse velocity). The MASW method is preferred over other surface seismic methods, such as refraction, due to their inability in identifying inverse velocities.
- The effect of shot distance and geophone spacing on inverted velocity profiles is identified, evaluated, and averaged in the inversion process in order to obtain the best possible representation of velocity profiles. The sensitivity of the velocity profiles to these effects is observed at all depths depending upon the combination of shot and geophone spacing and the power spectral range in the frequency-wave number domain.
- The wave lengths produced in the MASW tests were sufficient to penetrate the depths containing N values of interest. N values larger than 50 were neither reported on borehole logs nor considered during the development of dataset of Vs-N pairs.
- During regression analysis, a nonlinear prediction model expressing power function is fitted to the data set. The prediction model has a larger rate of increase than results of the many previous studies on sandy soils. The velocity predictions models of previous studies underestimate the prediction of the presented model at N values larger than 15; however, most recent studies tend to agree with the proposed model.
- The velocities predicted by the present study are in general agreement with many other studies that contain information about measured shear wave velocities and

N values although the objective of those studies were not to develop Vs-N correlations.

- Horizontal geophones are used to measure the horizontal component of the elliptical particle motion during the propagation of the Rayleigh waves. The geophones are capable of not only detecting the horizontal component, but also can be used to measure the dispersion curves.
- The dispersion curves computed from the data measured by horizontal geophones agree with the dispersion curves computed from the data measured by vertical geophones. Likewise, the velocity profiles from both the horizontal and vertical geophones agreed at most depths.
- Variation among the velocity profiles from horizontal and vertical geophones are observed at larger depths due to issues with the generated wave lengths and diminishing amplitude of horizontal motion compared to the vertical motion.
- Horizontal geophones can be used for the computation of dispersion curves and the velocity profiles without complimenting them with vertical geophones; however, high sensitivity geophones are required to measure the particle motions at larger depths. On the other hand, the transmitted energy from the shot impact can be increased to substantiate the particle motion.

5.1Recommendations

The focus of this research was to develop empirical relationships between the SPT-N values and VS for the typical soils found in or around the city of Sharjah in the UAE. The relationships (correlations/prediction equations) are developed from the results of regression analysis of data pairs between N values and V_S. The shear wave velocity is measured by using the MASW method. It is recommended to evaluate the wave velocity by multiple methods simultaneously and perform statistical analysis on the inferred velocity profiles from different methods before developing the V_S-N pairs.

It is also recommended to perform SPT tests simultaneously with the seismic tests and larger N values shall be reported to better predict the trend between V_S and

N values. Similarly other soil properties such as unit weights shall be measured for a better correction of overburden stress on N values.

The seismic tests shall be conducted for other regions of UAE to develop a comprehensive model of V_S predictions as function N values considering the pace of development in all parts of the UAE.

This research also reflects an effort to evaluate the ability of horizontal geophones in calculating the dispersion curves and velocity profiles by measuring the horizontal component of the elliptical particle motion during the propagation of surface waves. It is recommended to perform cross correlation and other signal processing techniques to isolate the pure Rayleigh waves before the computation of dispersion curves. The isolation of Rayleigh waves would eliminate the contamination from reflections and other sources of noise such as traffic and ambient noise at larger wave lengths.

References

[1] ASTM Standard D4015, 2007, “Standard Test Methods for Modulus and Damping of Soils by Resonant-Column Method", ASTM International, West Conshohocken, PA, 2007, www.astm.org.

[2] ASTM Standard D5311, 2013, “Standard Test Method for Load Controlled Cyclic Triaxial Strength of Soil" ASTM International, West Conshohocken, PA, 2013, www.astm.org.

[3] C.Hanumantharao, and G.V. Ramana, “Dynamic soil properties for microzonation of Delhi, India”,*Journal of Earth System Science*, Vol. 117 (S2), pp. 719–730, 2008

[4] U. Dikmen, “Statistical correlations of shear wave velocity and penetration resistance for soils”, *Journal of Geophysics and Engineering*, Vol. 6, pp. 61–72, 2009.

[5] R. Uma Maheswari, A. Boominathan and G.R. Dodagoudar, “Use of Surface waves in statistical correlations of shear wave velocity and penetration resistance of Chennai soils”, *Geotechnical and Geology Engineering*, Vol. 28(2), pp. 119-137, 2010.

[6] G. Tsiambaos and N. Sabatakakis, “Empirical estimation of shear wave velocity from in-situ tests on soil formations in Greece”, *Bulletin of Engineering Geology and the Environment*, Vol. 70, pp. 291–297, 2011.

[7] P. Anbazhagan, A. Kumar, and T.G. Sitharam, “Seismic site classification and correlation between standard penetration test N value and shear wave velocity for Lucknow city”, Indo-Gangetic Basin,*Pure and Applied Geophysics*, 2012.

[8] L. Rayleigh, “Waves propagated along the plane surface of an elastic solid”,*Proceedings of London Mathematical Society*, Vol. 17, pp. 4–11, 1885.

[9] Z. Khan, G. Cascante, H. El Naggar, and L. Carlo, “Measurement of frequency-dependent dynamic properties of soils using the Resonant-Column device”,*Journal of Geotechnical and Geoenvironmental Engineering*, Vol. 134(9),pp. 1319-1326, 2008.

[10] Z. Khan, H. El Naggar, and G. Cascante, “Frequency dependent dynamic properties from resonant column and cyclic triaxial tests”,*Journal of Franklin Institute*, Vol. 348(7), pp. 1363-1376, 2011.

[11] R.D. Woods, “Borehole Methods in Shallow Seismic Exploration: Geophysical Characterization of Sites”, *Volume prepared by ISSMFE, Technical Committee # 10, XIII ICSMFE*, New Delhi, India, Richard Woods, Editor, pp. 91-100, 1994.

[12] R. Whiteley, “Seismic refraction testing-a tutorial”, “Geophysical Characterization of Sites”, Vol. 10, pp. 45-47, 1994.

[13] N. Kobayashi, “A method of determining the underground structure by means ofSH waves”, Zisin, Ser, 2, pp. 19-24, 1959.

[14] ASTM Standard D5777, 2000e1, “Standard Guide for Using the Seismic Refraction Method for Subsurface Investigation," ASTM International, West Conshohocken, PA, 2000, www.astm.org.

[15] D. Motazedian, J.A. Hunter, A. Pugin, and H. Crow, “Development of a V_s(30) (NEHRP) map for the city of Ottawa, Ontario, Canada”,*Canadian Geotechnical Journal*, Vol. 48(3), pp. 458-472, 2011.

[16] S. L. Kramer, “Geotechnical earthquake engineering”, Pearson Education India, 1996.

[17] D. Palmer and K.B. Burke, “The generalized reciprocal method of seismic refraction interpretation”,*Society of Exploration Geophysicists*, 1980.

[18] J.H. Scott, “Seismic refraction modeling by computer”, *Geophysics*, Vol. 38(2), pp. 271-284, 1973.

[19] V. Pereyra, “Ray tracing methods for inverse problems”, Inverse Problems, 16(6), R1-R35, 2000.

[20] N.K. Yacoub, J.H. Scott, and F. McKeown, “Computer ray tracing through complex geological models for ground motion studies”, *Geophysics*, Vol. 35(4), pp. 586-602, 1970.

[21] W. Menke, “Geophysical data analysis: Discrete inverse theory”, Access Online via Elsevier, 1989.

[22] J. Rickettand J. Claerbout, “Passive seismic imaging applied to synthetic data”,*Stanford Exploration Project*, Vol. 92, pp. 83-90, 1996.

[23] I.N. Azwin, R. Saad, and M. Nordiana, “Applying the Seismic Refraction Tomography for Site Characterization”, *APCBEEProcedia*, Dubai, Vol. 5, pp. 227 – 231, 2013.

[24] A. Turesson, “A comparison of methods for the analysis of compressional, shear, and surface wave seismic data, and determination of the shear modulus”, *Journal of Applied Geophysics*, Vol. 61(2), pp. 83-91, 2007.

[25] M. Shahrukh, P. Soupios, N. Papadopoulos, and A. Sarris, “Geophysical investigations at the intron archaeological site, eastern Crete, Greece using seismic refraction and electrical resistivity tomography”,*Journal of Geophysics and Engineering*, Vol. 9(6), pp. 749-760, 2012.

[26] J.R. Sheehan,W.E. Doll, and W.A. Mandell, “An evaluation of methods and available software for seismic refraction tomography analysis”,*Journal of Environmental & Engineering Geophysics*, Vol. 10(1), pp. 21-34, 2005.

[27] D.F. Viana, J. Carvalho, C. Ferreira, J.A. Santos, F. Almeida, E. Pereira, and A. Oliveira, “Characterization of a profile of residual soil from granite combining geological, geophysical and mechanical testing techniques”,*Geotechnical and Geological Engineering*, Vol. 24(5), pp. 1307-1348, 2006.

[28] M.K. Kockar, H. Akgun, and E.M. Rathje, “Evaluation of site conditions for the Ankara basin of Turkey based on seismic site characterization of near-surface geologic materials”,*Soil Dynamics and Earthquake Engineering*, Vol. 30(1-2), pp. 8-20, 2010.

[29] H. Crow, M. Pyne, J. Hunter, S. Pullan, D. Motazedian, and A. Pugin, “Shear wave measurements for earthquake response evaluation in orleans, Ontario”,*Geological Survey of Canada,* Open-File, 5579, 192, 2007.

[30] J. Luetgert, “MacRay: Interactive two-dimensional seismic raytracing for the Macintosh”, *US Geological Survey*, Open File , 92(356), 43, 1992.

[31] E. Cardarelli, M. Cercato, A. Cerreto, and G.D. Filippo, “Electrical resistivity and seismic refraction tomography to detect buried cavities”,*70th European Association of Geoscientists and Engineers Conference and Exhibition - Incorporating SPE EUROPEC*, Vol. 2, pp. 1103-1107, 2008.

[32] I. Koulakov, “LOTOS code for local earthquake tomographic inversion: Benchmarks for testing tomographic algorithms”, *Bulletin of the Seismological Society of America*, Vol. 99(1), pp. 194-214, 2009.

[33] D. Jongmans, “The application of seismic methods for dynamic characterization of soils in earthquake engineering”,*Bulletin of the International Association of Engineering Geology*, Vol. 46(1), pp. 63-69, 1992.

[34] R.A. Williams, W.J. Stephenson, and J.K. Odum, “Comparison of P-and S-wave velocity profiles obtained from surface seismic refraction/reflection and downhole data”, *Tectonophysics*, Vol. 368(1), pp. 71-88, 2003.

[35] W.E. Wightman, F. Jalinoos, P. Sirles, and K. Hanna,“Application of Geophysical Methods to Highway-Related Problems”,*Publication No.FHWA-IF-04-021*,Department of Transportation,Central Federal Lands Highway Division, FHWA, U.S., 2004.

[36] B.B. Redpath, “Seismic Refraction Exploration for Engineering Site Investigations, 1973.

[37] D.I. Doser, R.P. Langford, M.R. Baker, G.M. Kaip, and F. Tate, “Seasonal variations in geophysical surveys of alluvial sediments near the Rio Grande, west Texas”,*Environmental & Engineering Geoscience*, Vol. 9(3), pp. 253-266,2003.

[38] G. Bonnet and M. Meyer, “Seismic refraction tests above water table”, *Journal of Geotechnical Engineering*, Vol. 114(10), pp. 1183-1189, 1988.

[39] D.G. Raptakis, “Pre-loading effect on dynamic soil properties: Seismic methods and their efficiency in geotechnical aspects”,*Soil Dynamics and Earthquake Engineering*, Vol. 34(1), pp. 69-77, 2012.

[40] P. Groves, G. Cascante, D. Dundas, and P.K. Chatterji, “Use of geophysical methods for soil profile evaluation”,*Canadian Geotechnical Journal*, Vol. 48(9), pp. 1364-1377, 2011.

[41] D.R. Hiltunenand B.J. Cramer, “Application of seismic refraction tomography in karst terrain”,*Journal of Geotechnical and Geoenvironmental Engineering*, Vol. 134(7), pp. 938-948, 2008.

[42] R.D. Woods, “Measurement of dynamic soil properties”, Earthquake Engineering and Soil Dynamics-Proceedings of the ASCE Geotechnical Engineering Division Specialty Conference,Pasadena, California, Vol. 11978.

[43] G. Gazetas, “Foundation Vibrations: Foundation Engineering Handbook”, 2nd Edition, Hsai-Yang Fang, pp. 553-593, 1991.

[44] P. Mayne, B. Christopher, and J. DeJong, “Manual on Subsurface Investigations, Geotechnical Site Characterization”, National Highway Institute Publication, 2002.

[45] T. Larkin and P. Taylor, “Comparison of down-hole and laboratory shear wave velocities”,*Canadian Geotechnical Journal*, Vol. 16(1), pp. 152-162, 1979.

[46] R. Luna and H. Jadi, “Determination of dynamic soil properties using geophysical methods”,*Proceedings of the First International Conference on the Application of Geophysical and NDT Methodologies to Transportation Facilities and Infrastructure—Geophysics*, pp. 3-1, 2000.

[47] R. Campanella, “Field methods for dynamic geotechnical testing: Overview of capabilities and needs”,*International Symposium on Dynamic Geotechnical Testing II*, San Francisco, California, USA, 1994.

[48] H. Liu, R.L. Maier, and R.E. Warrick, “An improved air-powered impulsive shear-wave source”,*Bulletin of the Seismological Society of America*, Vol. 86(2), pp. 530-537, 1996.

[49] C. Sun, D. Kim, and C. Chung, “Geologic site conditions and site coefficients for estimating earthquake ground motions in the inland areas of Korea”,*Engineering Geology*, Vol. 81(4), pp. 446-469, 2005.

[50] H. Liu, R.E. Warrick, R.E. Westerlund, J.B. Fletcher, and G.L. Maxwell, “An air-powered impulsive shear-wave source with repeatable signals”,*Bulletin of the seismological society of America*, Vol. 78(1), pp. 355-369, 1988.

[51] E. BangandD. Kim, “Evaluation of shear wave velocity profile using SPT based uphole method”,*Soil Dynamics and Earthquake Engineering*, Vol. 27(8), pp. 741-758, 2007.

[52] K.H. Stokoe II,S.G. Wright, J.A. Bay, and J.M. Roesset, “Characterization of geotechnical sites by SASW method”,*Geophysical characterization of sites*, Volume prepared by ISSMFE, Technical Committee # 10, XIII ICSMFE, New Delhi, India, Richard Woods, Editor, pp. 15-25, 1994.

[53] Z. Khan, M. El-Emam, G. Cascante, and H. El Naggar, “Energy dissipation in engineered sand of large damping ratio”,*Geomechanics and Geoengineering*,an international journal, pp. 1-6, 2012.

[54] C.B. Park, R.D. Miller, andJ. Xia, “Multichannel analysis of surface waves”, *Geophysics*, Vol. 64(3), pp. 800-808, 1999.

[55] S. Nazarianand K.H. Stokoe, “In-situ shear wave velocities from spectral analysis of surface waves”,*Proceedings of the 8th World Conference on Earthquake Engineering*, San Francisco, California, Vol. 3, 31–38, 1984.

[56] K.H. Stokoe II, S.Nazarian, G.J. Rix, I. Sanchez-Salinero, J.C.Sheu, and Y.J.Mok, “In-situ seismic testing of hard-to-sample soils by surface wave method”,*Earthquake Engineering and soil dynamic II* - Recent advances in ground-motion evaluation, Von Thun, J.L (ed), Utah, Geotechnical special publication 20, pp. 264-279, 1988.

[57] M.O.Al-Hunaidi, “Insights on the SASW nondestructive testing method”, *Canadian Journal of Civil Engineering*, Vol.20, pp. 940-950,1993.

[58] J. S. Heisey, K.H. Stokoe II, and A.H. Meyer, “Moduli of pavement systems from spectral analysis of surface waves”,*Transportation Research Record* Vol. 852, pp. 22-31, 1982.

[59] N. Gucunski, “Generation of low frequency Rayleigh waves for the spectral-analysis-of-surface waves method”, *Ph.D. Dissertation*, University of Michigan, 1991.

[60] N. Gucunski, V. Ganji, and M.H. Maher,“Effects of obstacles on Rayleigh wave dispersion obtained from the SASW test”,*Soil Dynamics and Earthquake Engineering*, Vol. 15(4), pp. 223-231, 1996.

[61] K.H. Stokoe II, and S. Nazarian, “Effectiveness of ground improvement from spectral analysis of surface waves”,*Proceedings from the 8th European conference on soil mechanics and foundation engineering*, Improvement of Ground, H.G.Rathmayer, and K.H.O Saari (eds), Helsinki: pp. 91-94, 1983.

[62] G.A. McMechanand M.J. Yedlin, “Analysis of dispersive waves by wave field transformation”,*Geophysics*, Vol. 46, pp. 869-874, 1981.

[63] W. Thomson, “Transmission of elastic waves through a stratified soil medium”,*Journal of Applied Physics*, Vol. 21(2), pp. 89-93, 1950.

[64] N.A. Haskel, “The dispersion of surface waves on multilayered media”, *Bulletin of the Seismological Society of America*, Vol. 54(2), pp. 627-679, 1953.

[65] E. Kauseland J.M. Roesset, “Stiffness matrices for layered soils”,*Bulletin of the Seismological Society of America*, Vol. 71(6), pp. 1743-1761, 1981.

[66] B.L.N. Kennet, “Reflections, rays and reverberations”,*Bulletin of the Seismological Society of America*, Vol. 64(6), pp. 1685-1696, 1974.

[67] F.A. Schwab and L. Knopoff, “Fast surface wave and free mode computations”, Bolt,B.A., Ed., *Methods in computational physics*: Academic Press,pp. 87–180, 1972

[68] W.H. Press, S.A. Teukosky, W.T. Vetterling, and B.P. Flannery, “Numerical recipes”,Cambridge University, 1992.

[69] P.W. Mayne, “Cone Penetration Testing”,*Transportation Research Board*, 2007.

[70] ASTM Standard D3441, 2005e1, “Standard Test Method for Mechanical Cone Penetration Tests of Soil" ASTM International, West Conshohocken, PA, 2005, www.astm.org.

[71] J.D. Rogers, “Subsurface exploration using the standard penetration test and the cone penetrometer test”,*Environmental & Engineering Geoscience*, Vol. 12(2), pp. 161-179, 2006.

[72] P.K. Robertson and R. Campanella, “Guidelines for use and interpretation of the electronic cone penetration test”, University of British Columbia, Department of Civil Engineering, 1984.

[73] ASTM Standard D1586, 2011e1, “Standard Test Method for Standard Penetration Test (SPT) and Split-Barrel Sampling of Soils" ASTM International, West Conshohocken, PA, 2011, www.astm.org.

[74] G.G. Meyerhof, “Penetration tests and bearing capacity of cohesionless soils”,*Journal of the Soil Mechanics and Foundations Division*, ASCE, Vol.82(1), pp. 1-19, 1956.

[75] T. Imai, “P-and S-wave velocities of the ground”,*Procedingsof 9th Int. Conf. on Soil Mechanics and Foundation Engineering*, Japan, Vol. 2, pp. 127-132, 1977.

[76] D. Sykoraand K.I. Stokoe, “Correlations of in situ measurements in sands of shear wave velocity, soil characteristics, and site conditions”*Geotechnical Engineering Report*,The University of Texas at Austin, TX, 1983.

[77] S.H. Lee, “Regression models of shear wave velocities”,*Journal of the Chinese Institute of Engineers*, Vol. 13, pp. 519–532, 1990.

[78] K. Pitilakis, D. Raptakis, K. Lontzetidis, T. Vassilikou, and D. Jongmans, “Geotechnical and geophysical description of euro-seistest, using field, laboratory tests and moderate strong motion recordings”,*Journal of Earthquake Engineering*, Vol. 03(03), pp. 381-409, 1999.

[79] R.D. Andrus, P. Piratheepan, B.S. Ellis, J. Zhang, and C.H. Juang, “Comparing liquefaction evaluation methods using penetration-vs relationships”,*Soil Dynamics and Earthquake Engineering*, Vol. 24, pp.713-721, 2004.

[80] N. Hasançebiand R. Ulusay, “Empirical correlations between shear wave velocity and penetration resistance for ground shaking assessments”, *Bulletin of Engineering Geology and the Environment*, Vol. 66, pp. 203–213, 2007.

[81] J.C. Santamarina andD. Fratta,“Introduction to discrete signals and inverse problems in civil engineering”, *ASCE Press*, Reston, Virginia, 2001.

[82] M. Wathelet, “An improved neighborhood algorithm: parameter conditions and dynamic scaling”, *Geophysical Research Letters*, Vol. 35, L09301, 2008.

[83] S.J. Brandenberg, N. Bellana, and T. Shantz, “Shear wave velocity as function of standard penetration test resistance and vertical effective stress at California bridge sites”,*Soil Dynamics and Earthquake Engineering*, Vol30(10), pp. 1026-1035, 2010.

[84] A. Nasseri-Moghaddam, G. Cascante, C. Phillips, and D.J. Hutchinson, “Effect of underground cavities on Rayleigh waves – Field and numerical experiments”, *Journal of Soil Dynamics and Earthquake Engineering*, Vol. 27, pp. 300-313, 2007.

Appendix A

Selected Frequency-Wave Number (F-K) Plots

Vertical Geophones

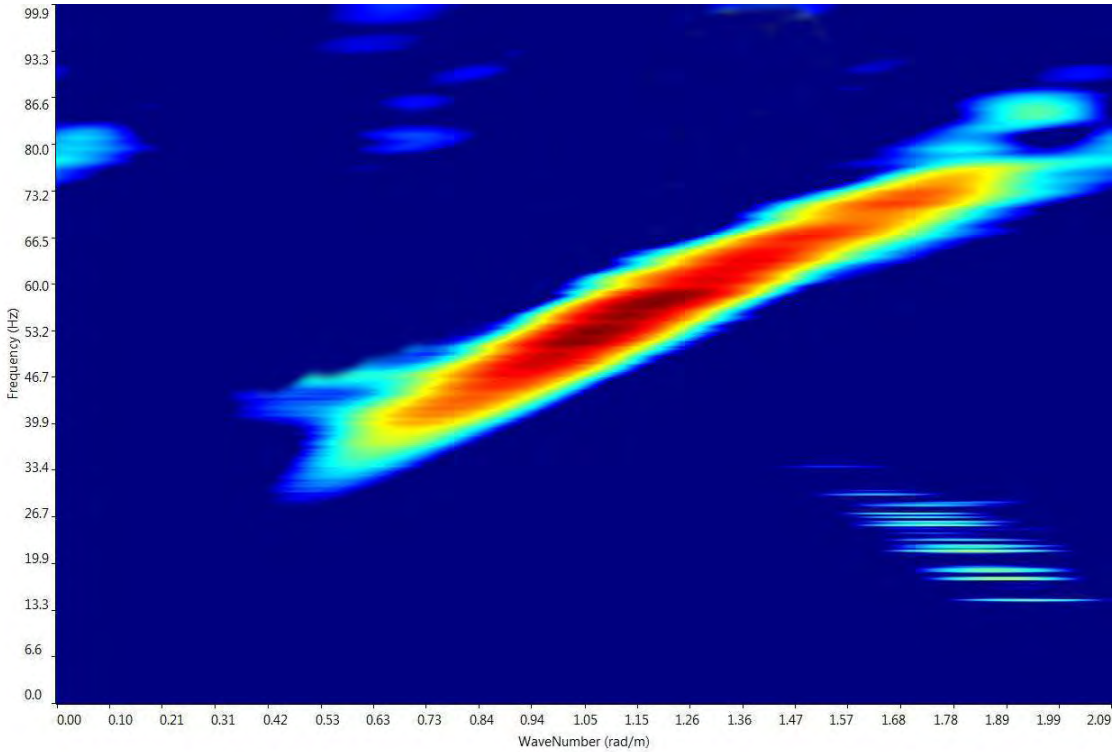

Figure A1: F-K Plot for a shot at Site S1

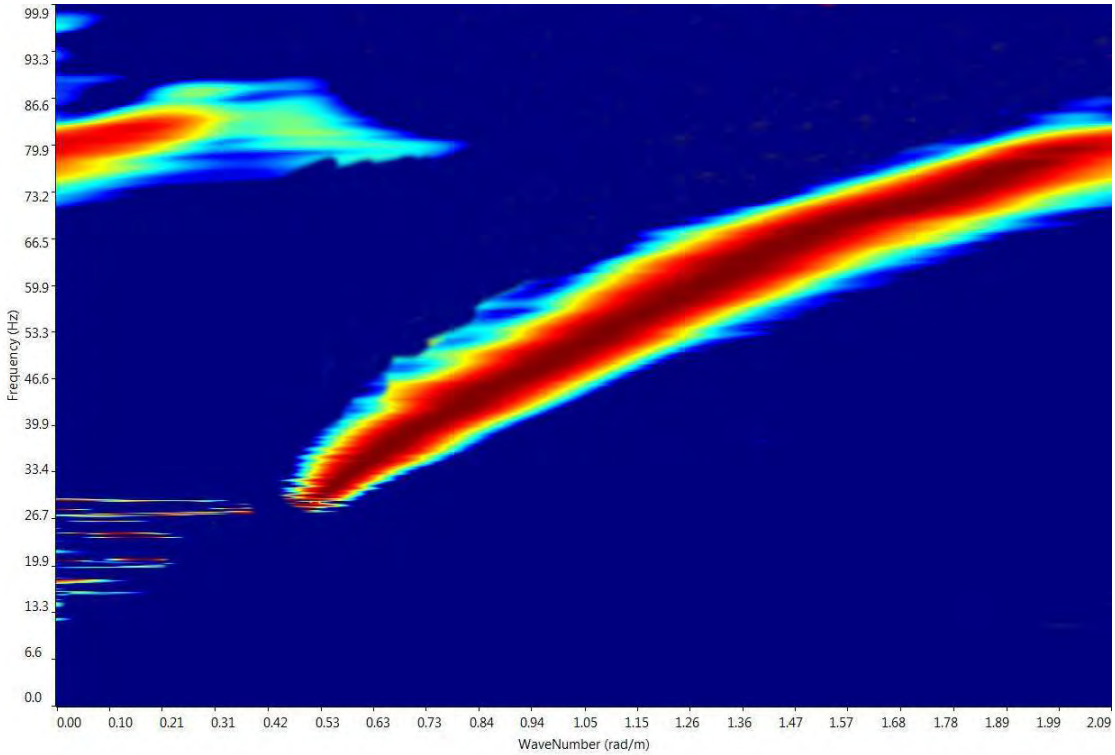

Figure A2: F-K Plot for a shot at Site S2

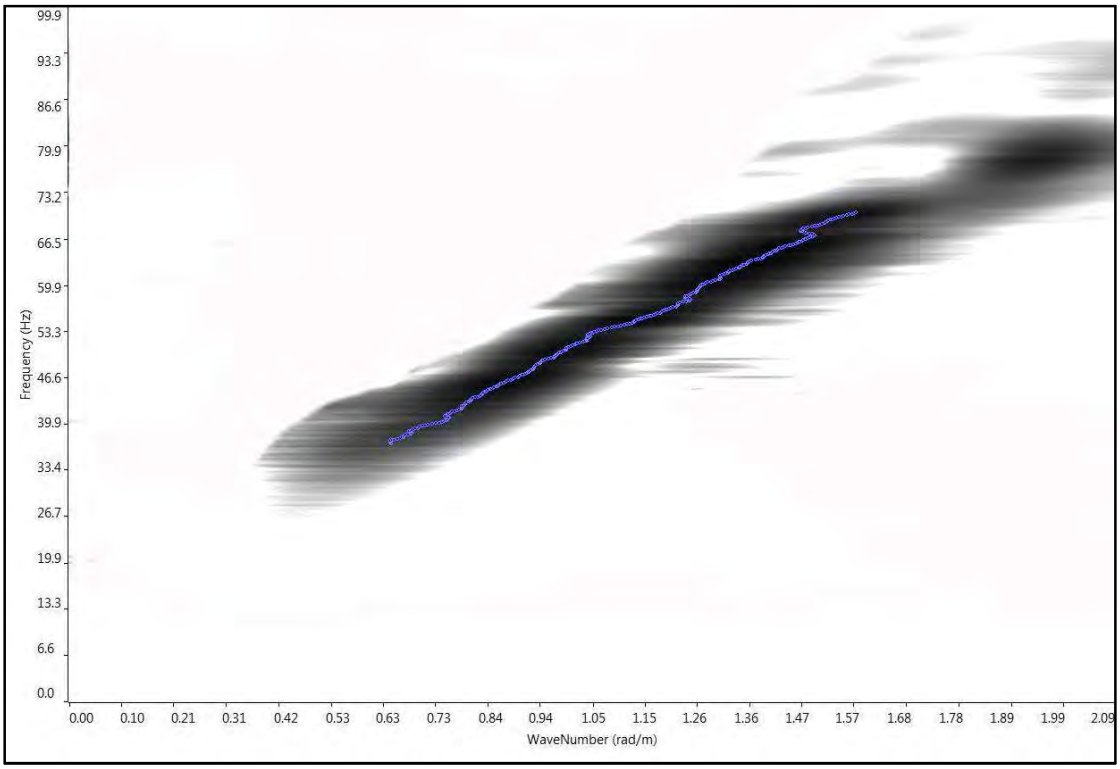

Figure A3: F-K Plot for a shot at Site S3

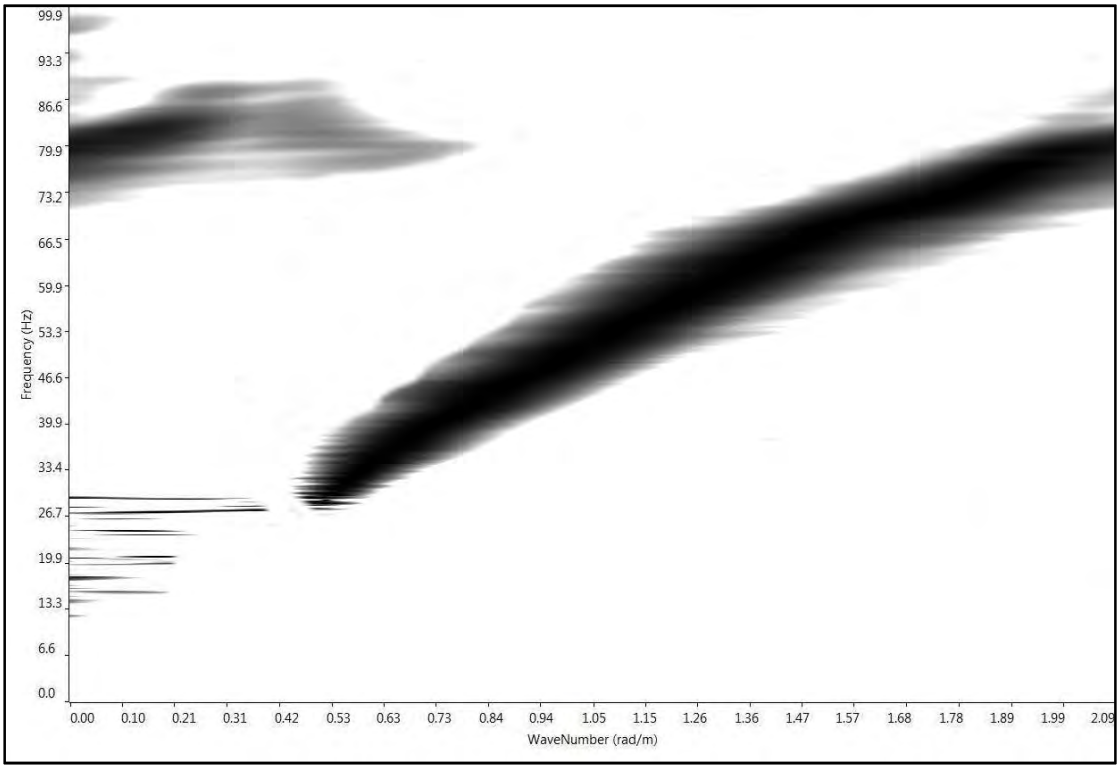

Figure A4: F-K Plot for a shot at Site S4

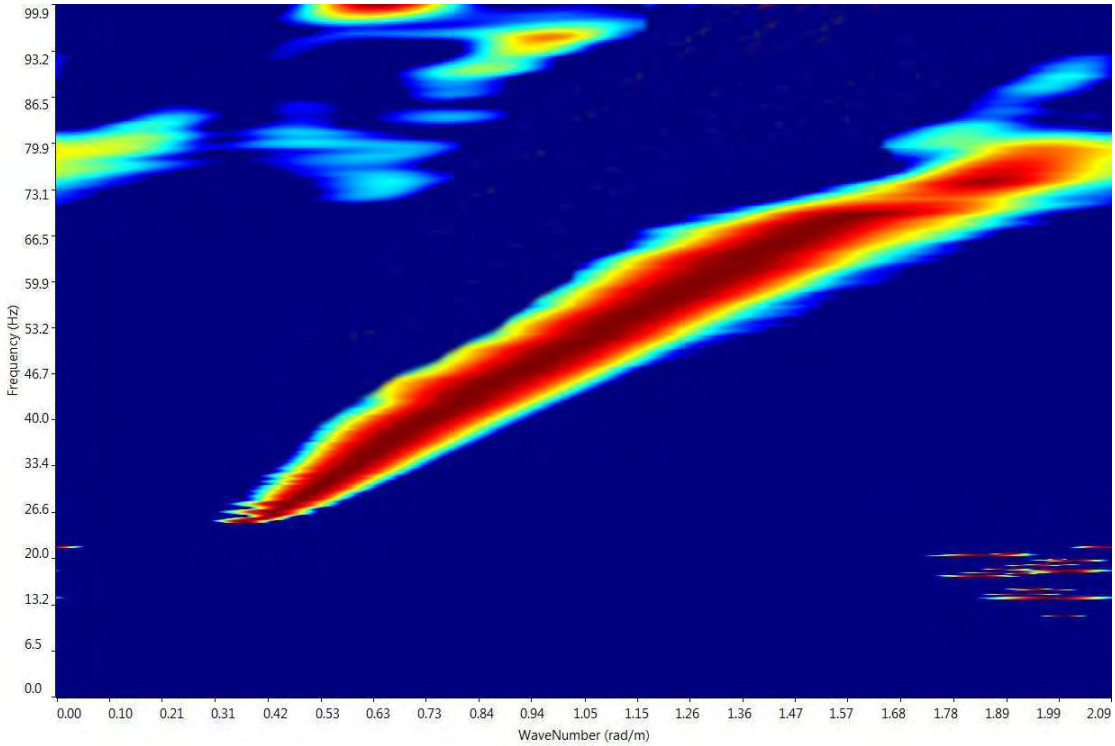

Figure A5: F-K Plot for a shot at Site S5

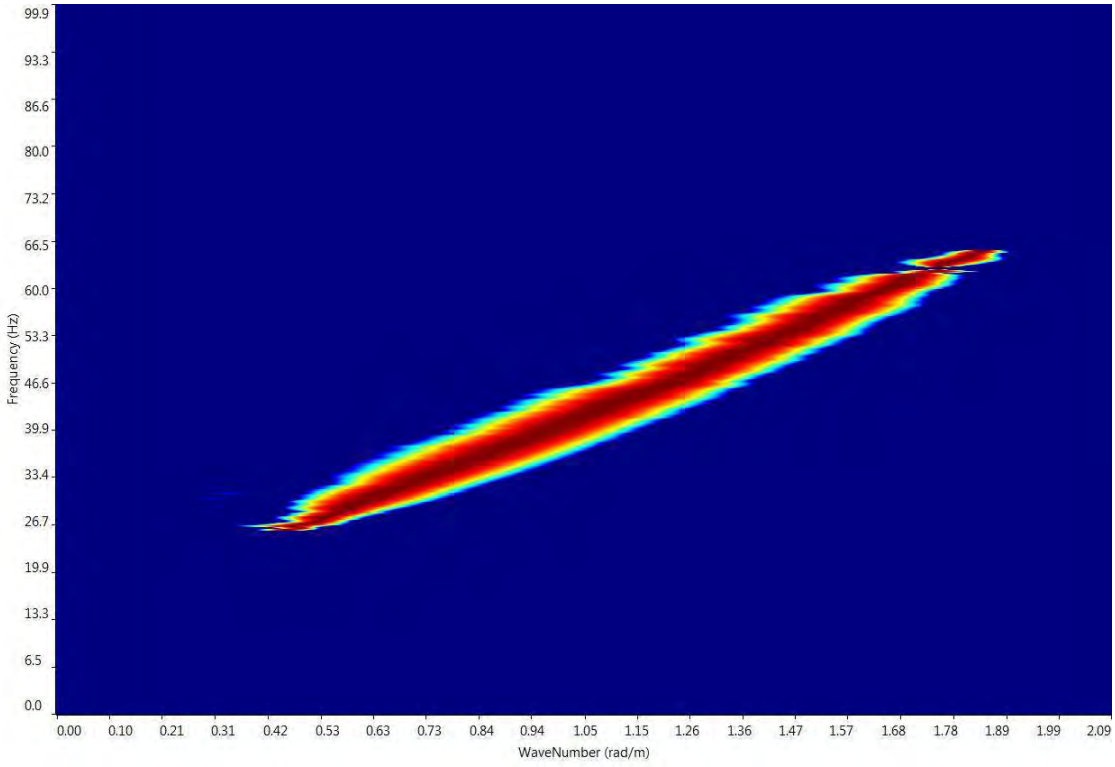

Figure A6: F-K Plot for a shot at Site S6

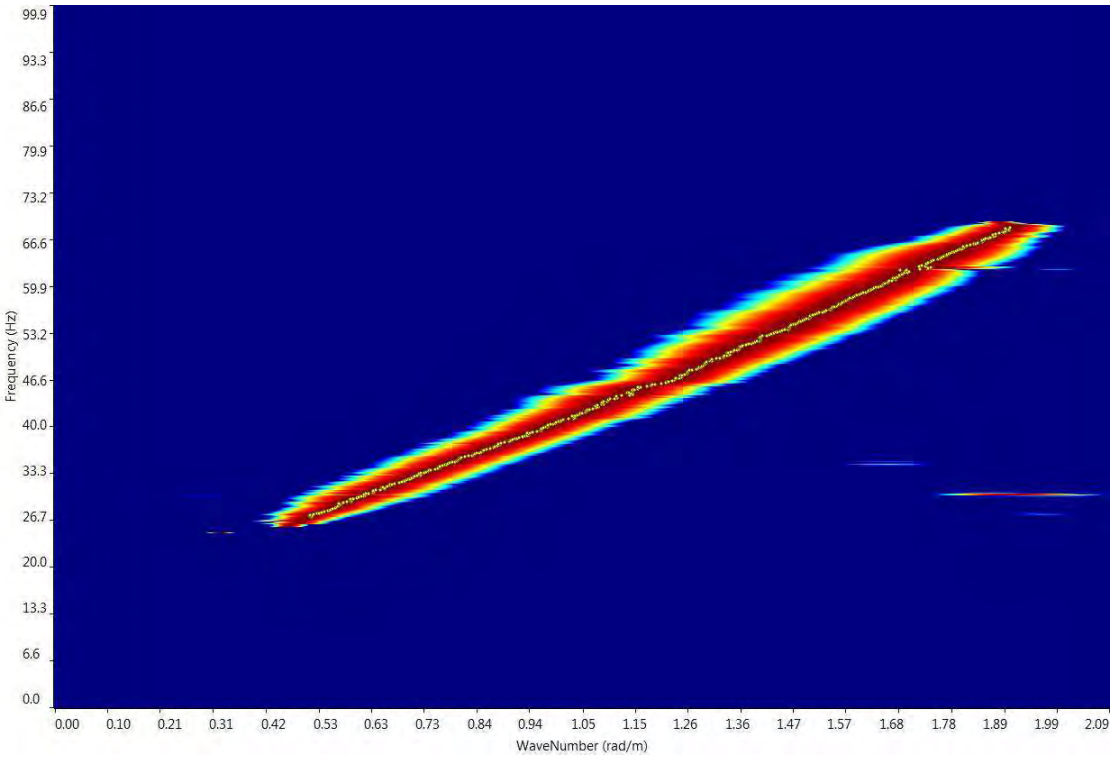

Figure A7: F-K Plot for a shot at Site S7

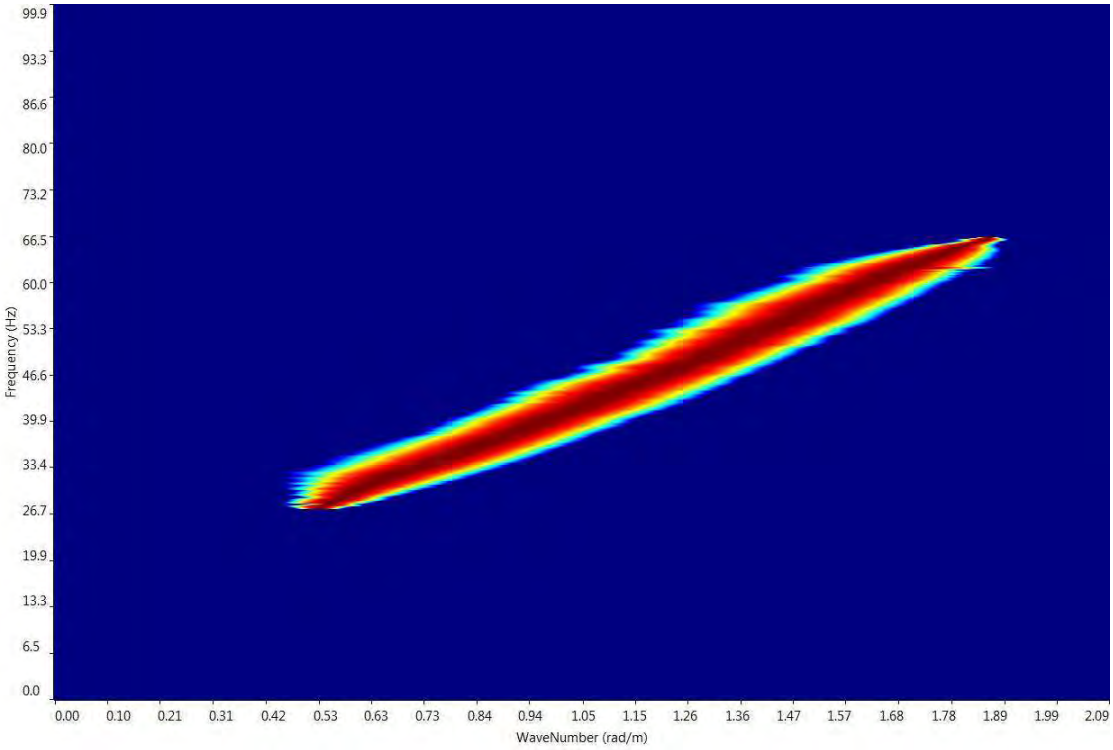

Figure A8: F-K Plot for a shot at Site S8

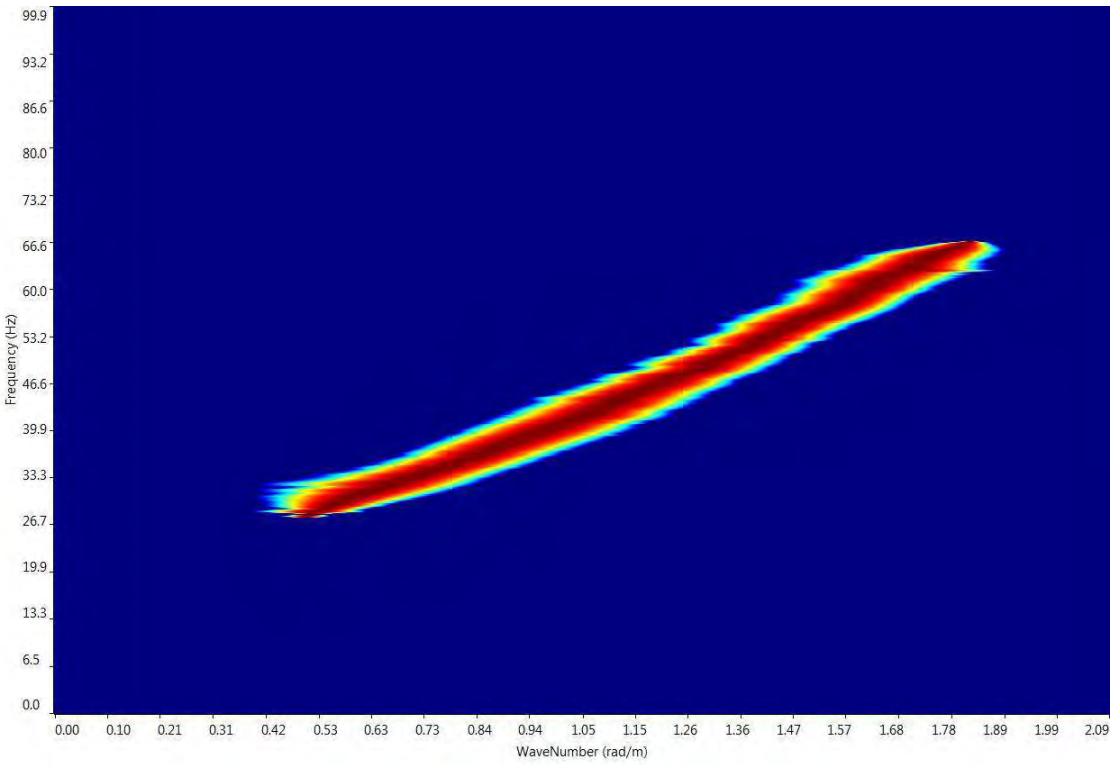

Figure A9: F-K Plot for a shot at Site S9

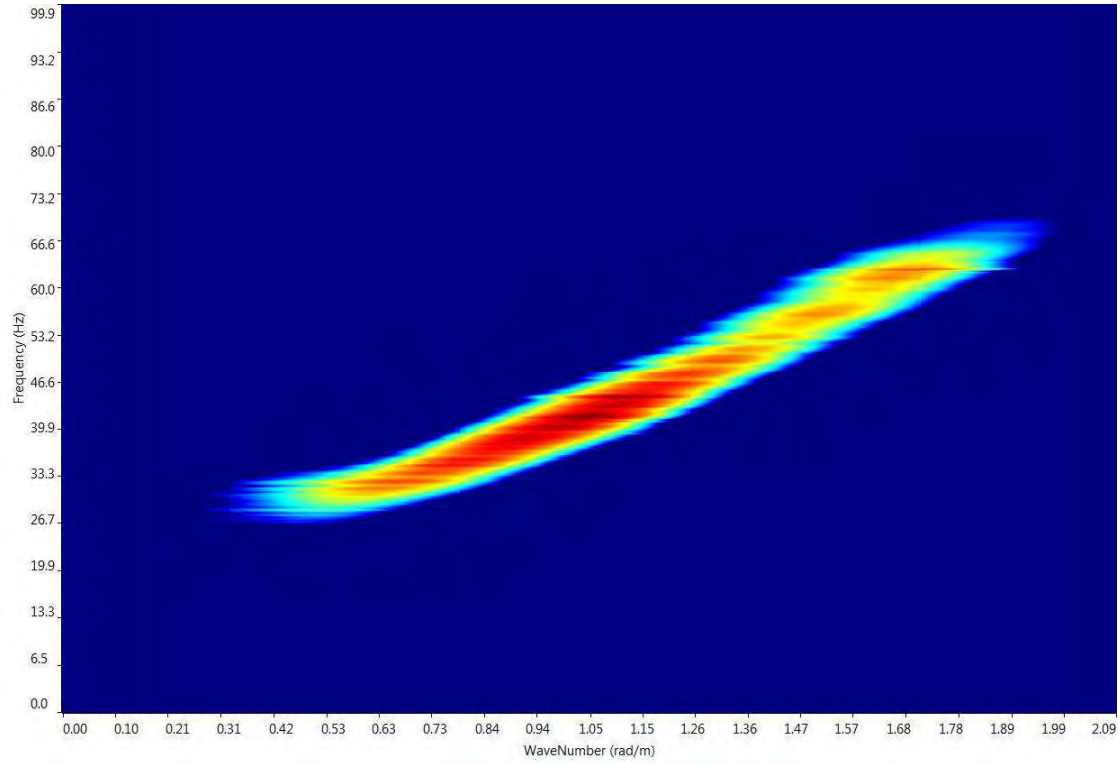

Figure A10: F-K Plot for a shot at Site S10

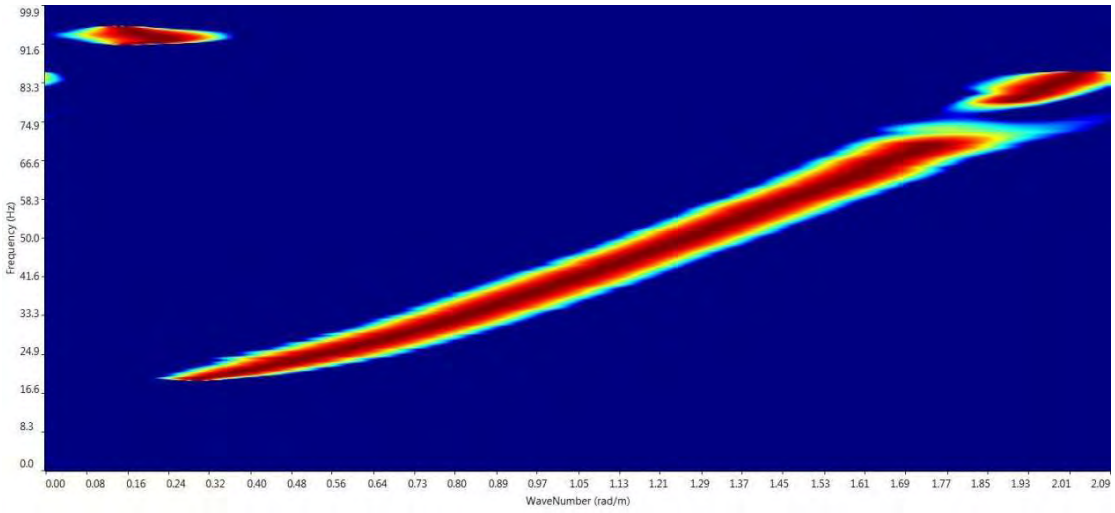

Figure A11: F-K Plot for a shot at Site S12

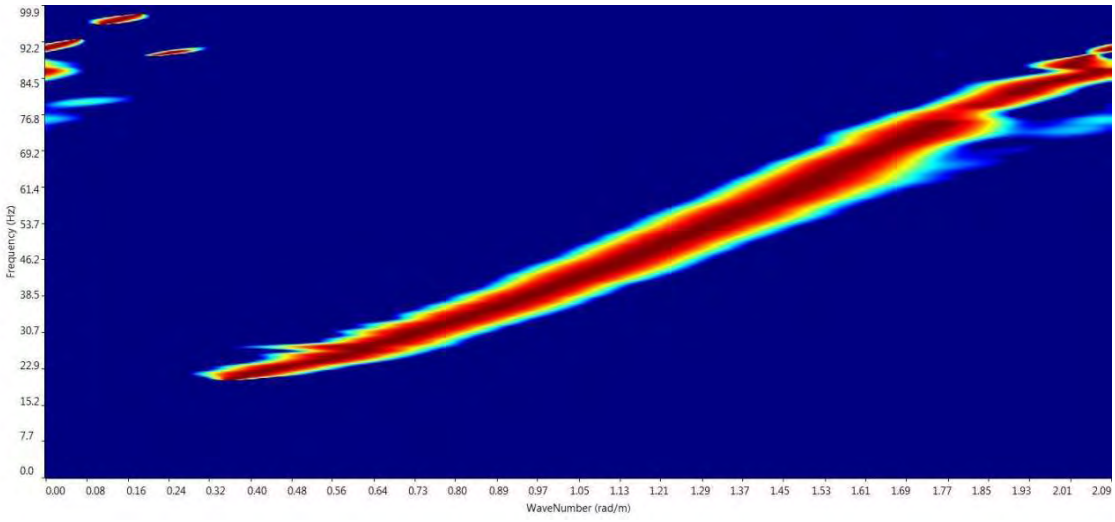

Figure A12: F-K Plot for a shot at Site S13

Vertical and Horizontal Geophones

Vertical

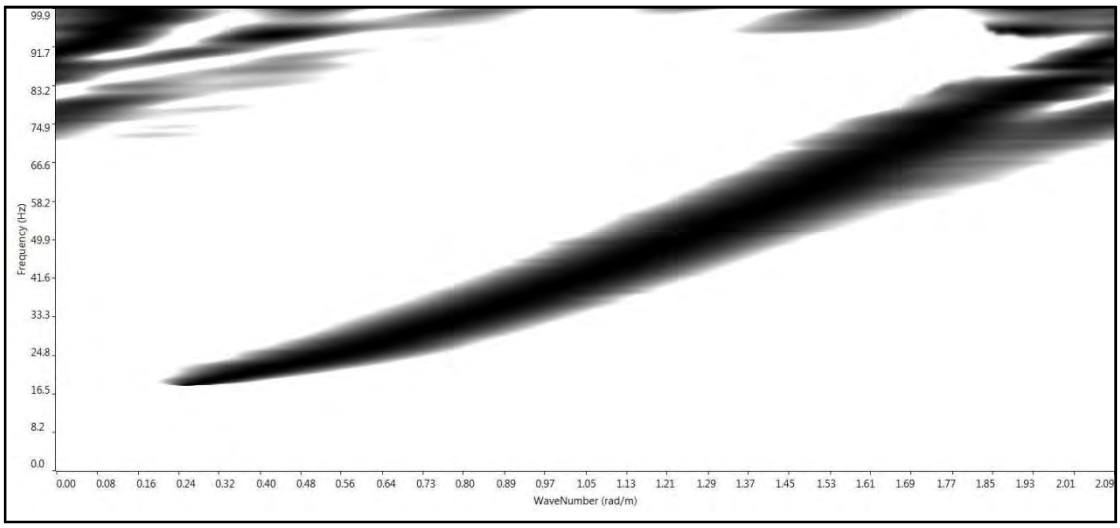

Figure A13: F-K Plot for a shot at Site S11 using vertical geophones (Shot at 5 m)

Horizontal

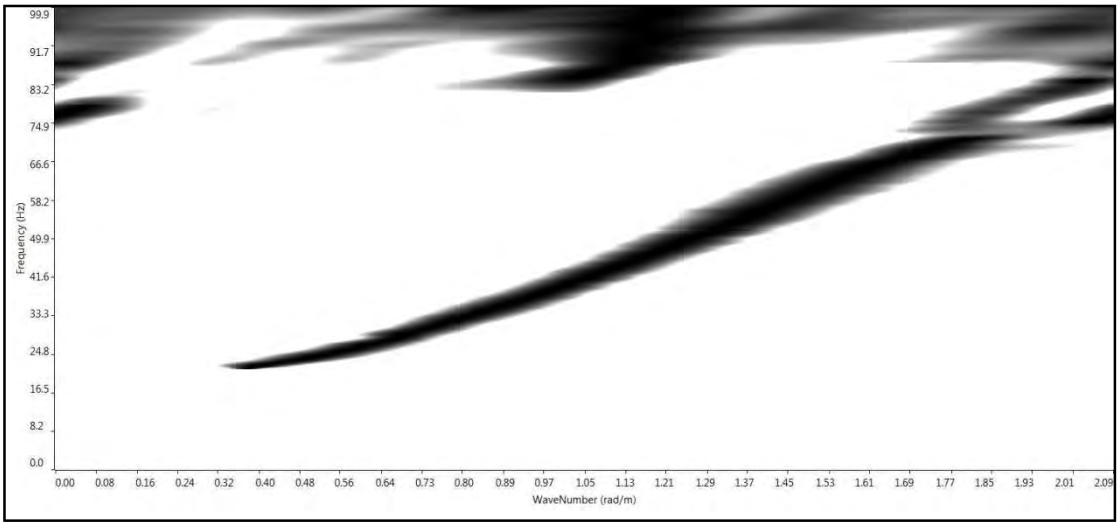

Figure A14: F-K Plot for a shot at Site S11 using horizontal geophones (Shot at 5 m)

Vertical

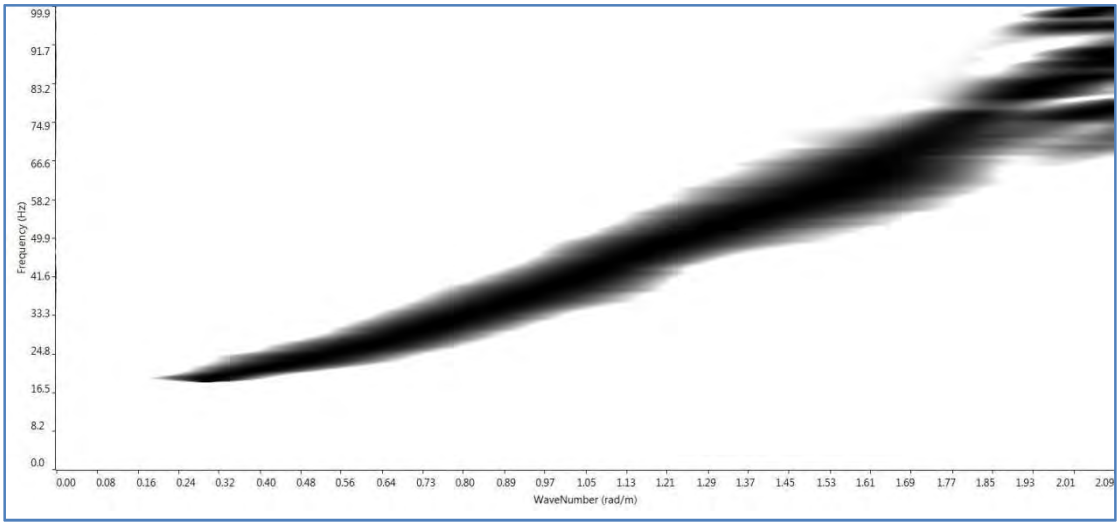

Figure A15: F-K Plot for a shot at Site S11 using vertical geophones (Shot at 10 m)

Horizontal

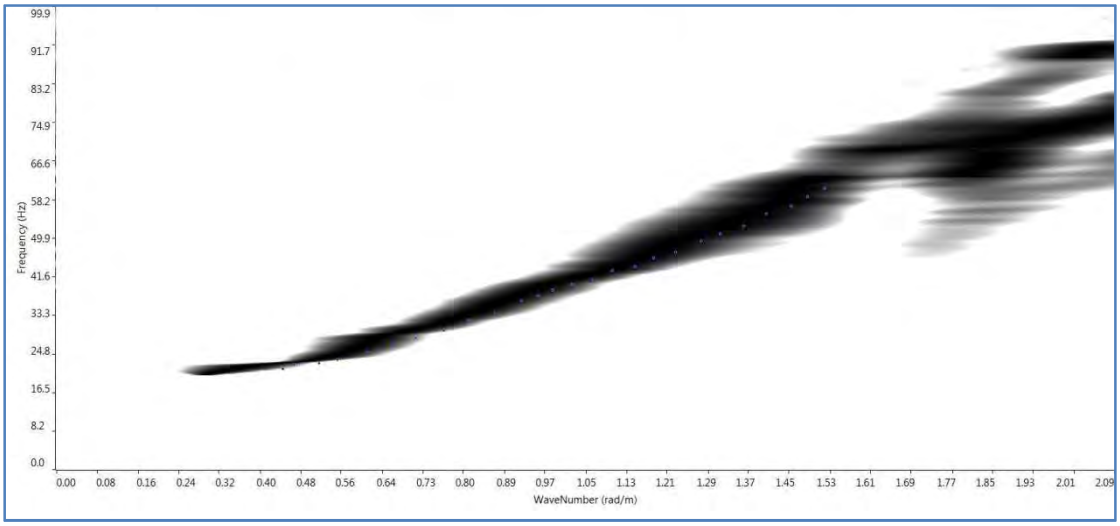

Figure A16: F-K Plot for a shot at Site S11 using vertical geophones (Shot at 10 m)

Appendix B

Selected Dispersion Curves

Vertical Geophones

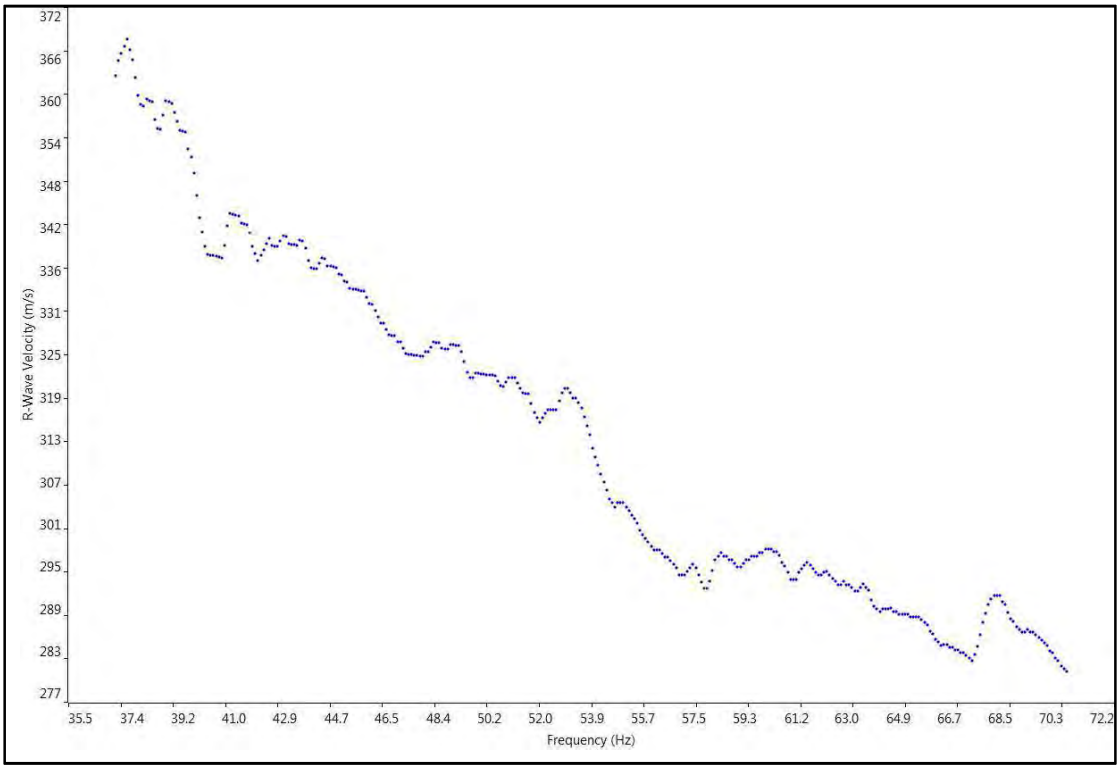

Figure B1: Dispersion curve for a shot at Site S1

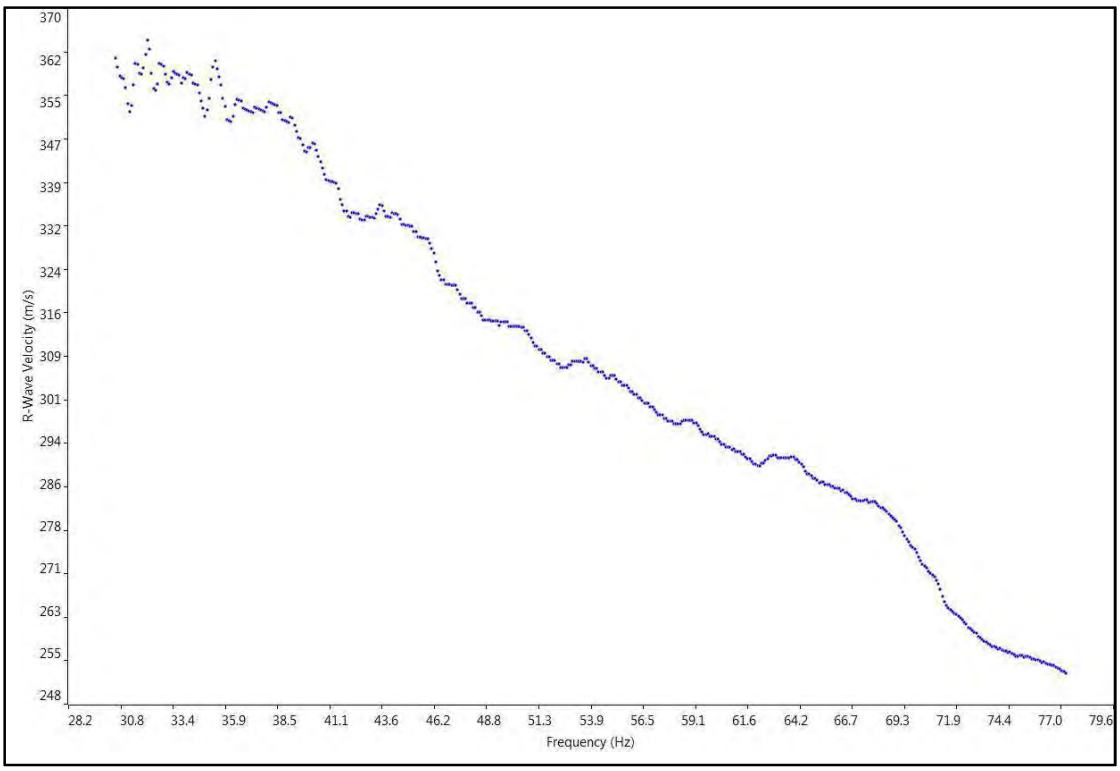

Figure B2: Dispersion curve for a shot at Site S2

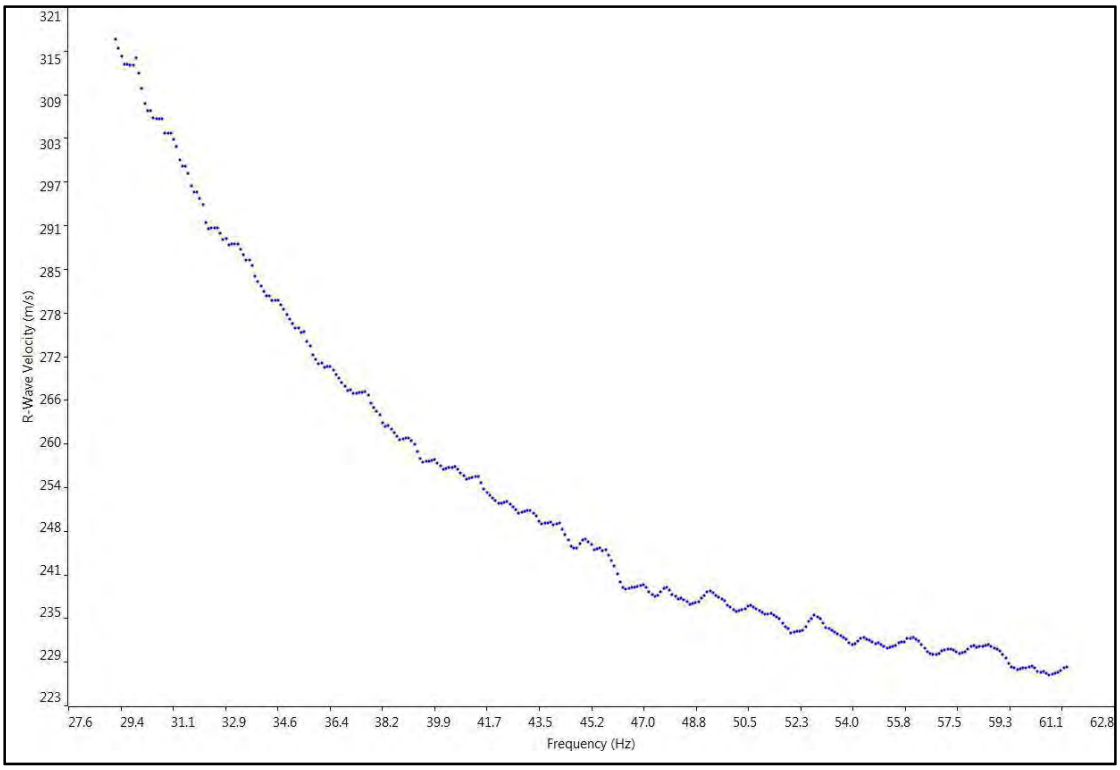

Figure B3: Dispersion curve for a shot at Site S3

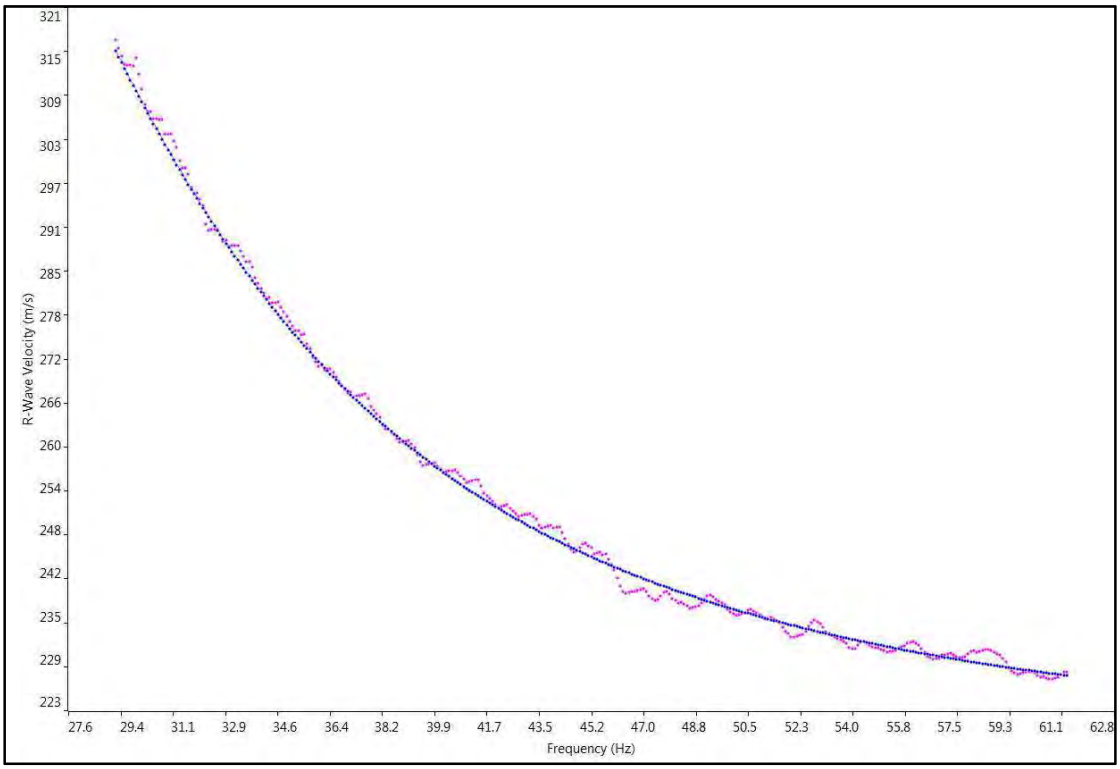

Figure B4: Dispersion curve for a shot at Site S4

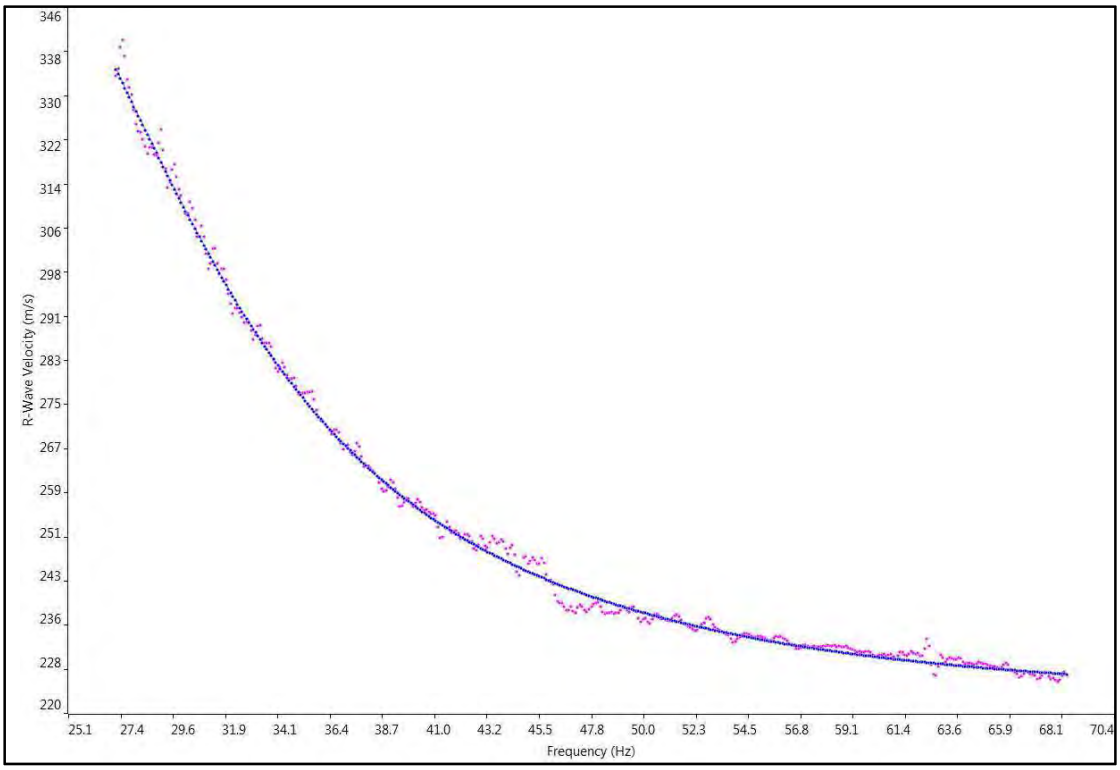

Figure B5: Dispersion curve for a shot at Site S5

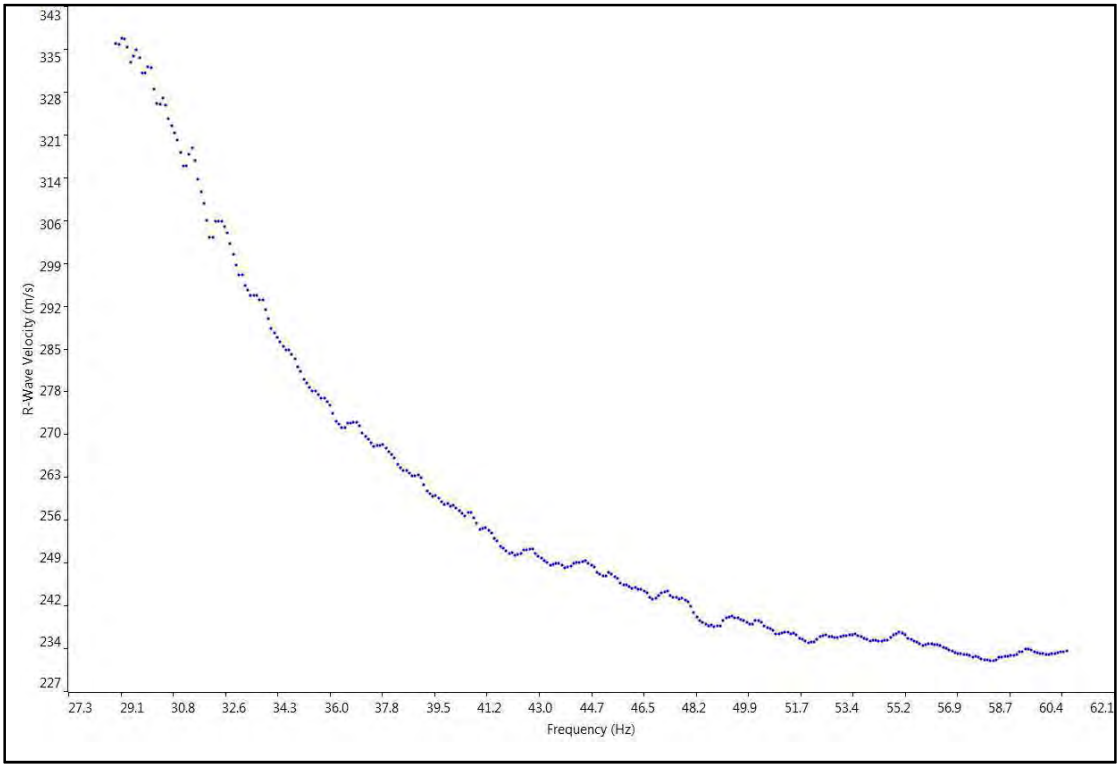

Figure B6: Dispersion curve for a shot at Site S6

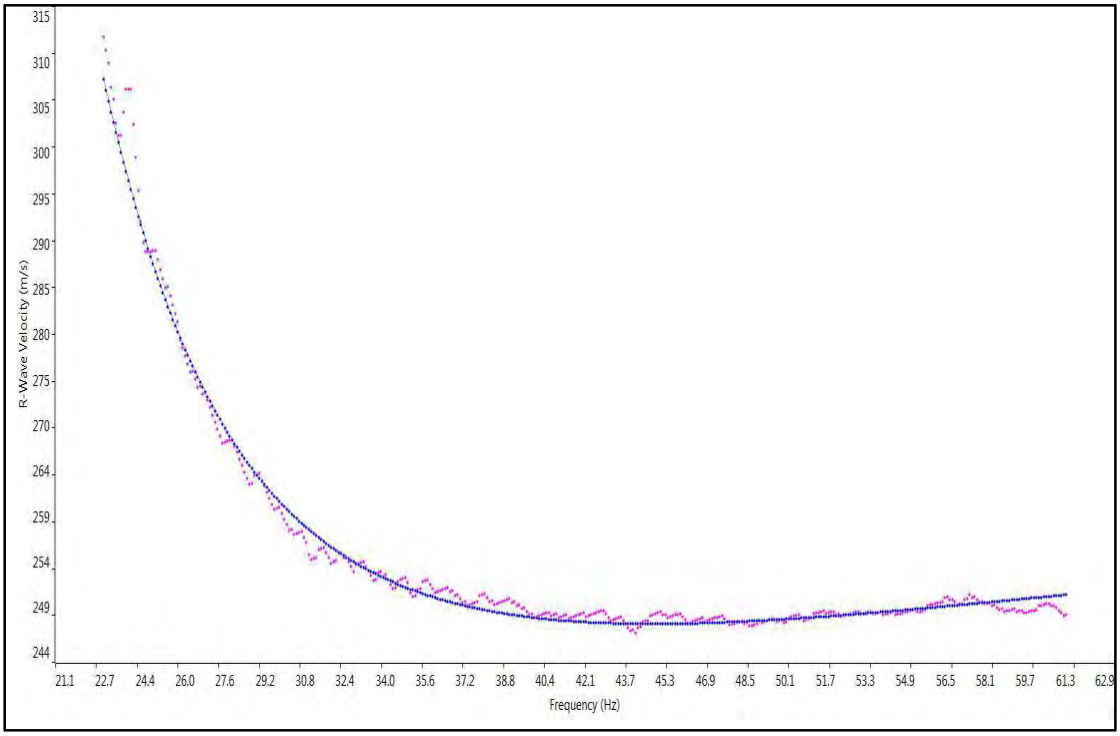

Figure B7: Dispersion curve for a shot at Site S10

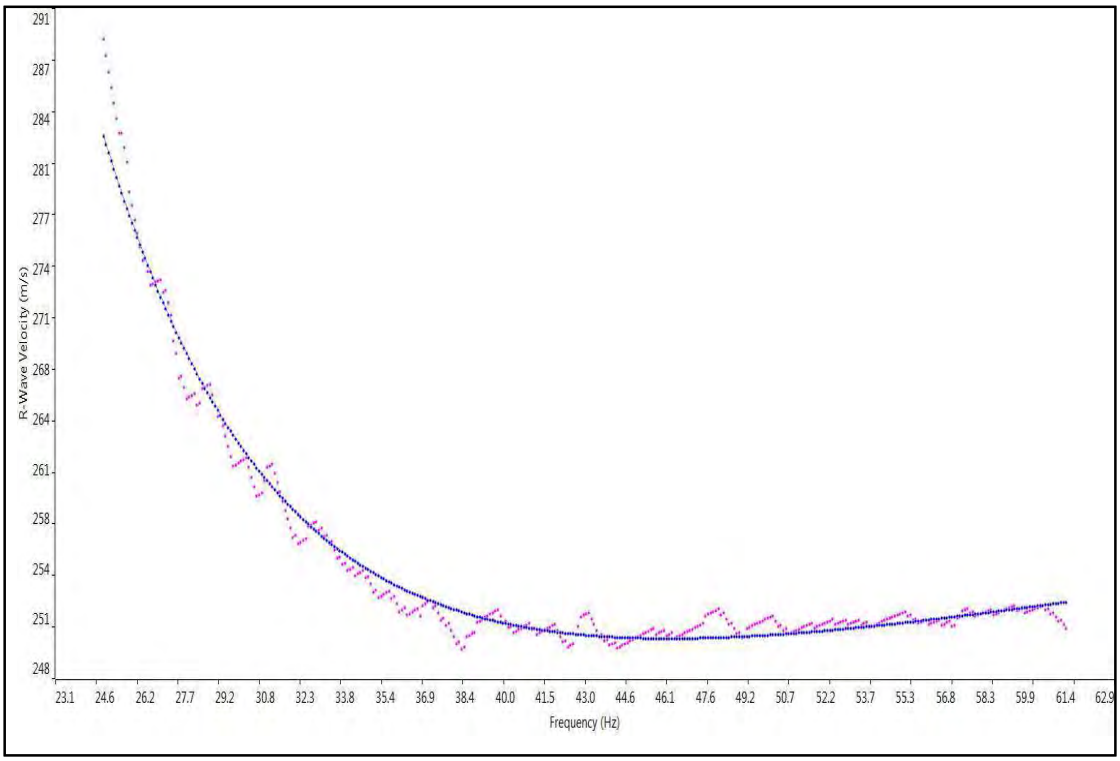

Figure B8: Dispersion curve for a shot at Site S10

Vertical and Horizontal Geophones

Vertical

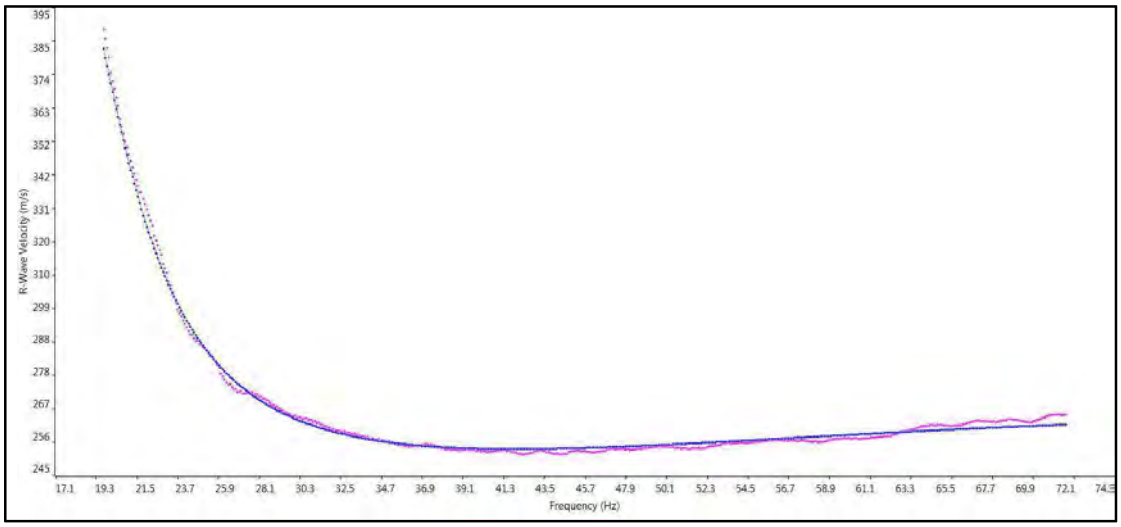

Figure B9: Dispersion curve for shot at Site S11 with vertical geophones (Shot at 5 m)

Horizontal

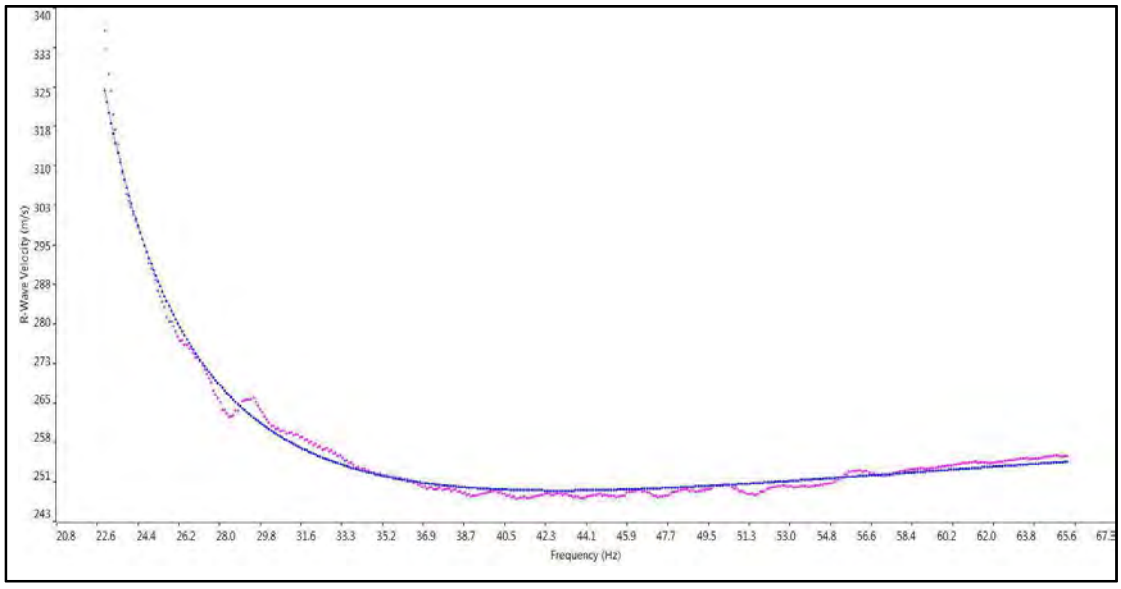

Figure B10: Dispersion curve for shot at Site S11 with horizontal geophones (Shot at 5 m)

Vertical

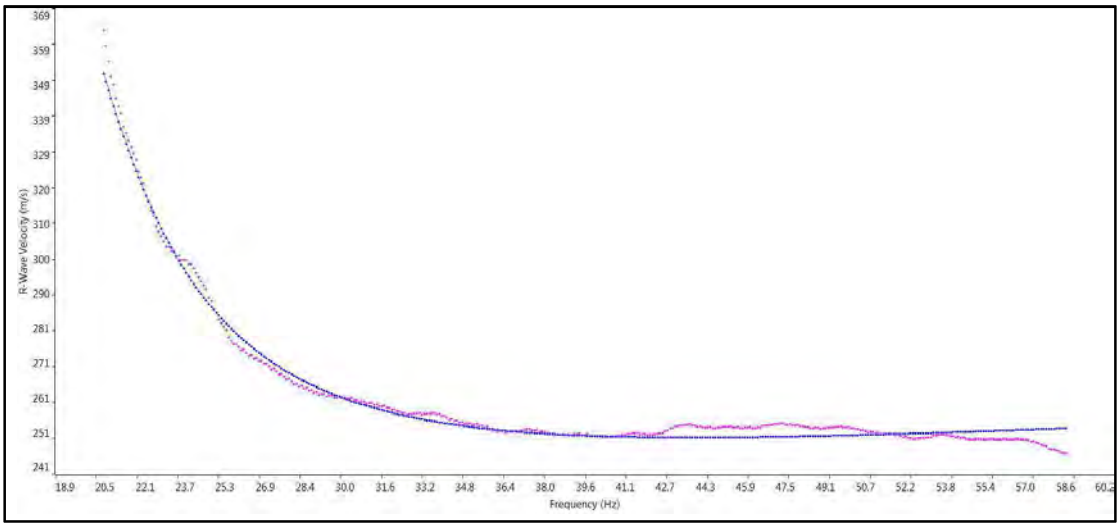

Figure B11: Dispersion curve for a shot at Site S11 using vertical geophones (Shot at 10 m)

Horizontal

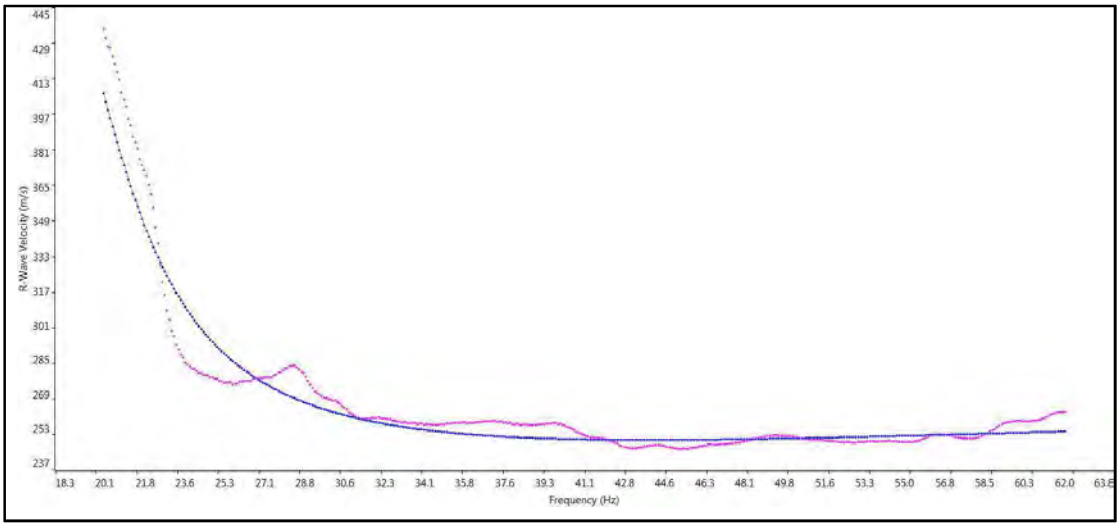

Figure B12: Dispersion curve for a shot at Site S11 using horizontal geophones (Shot at 10 m)

Vertical

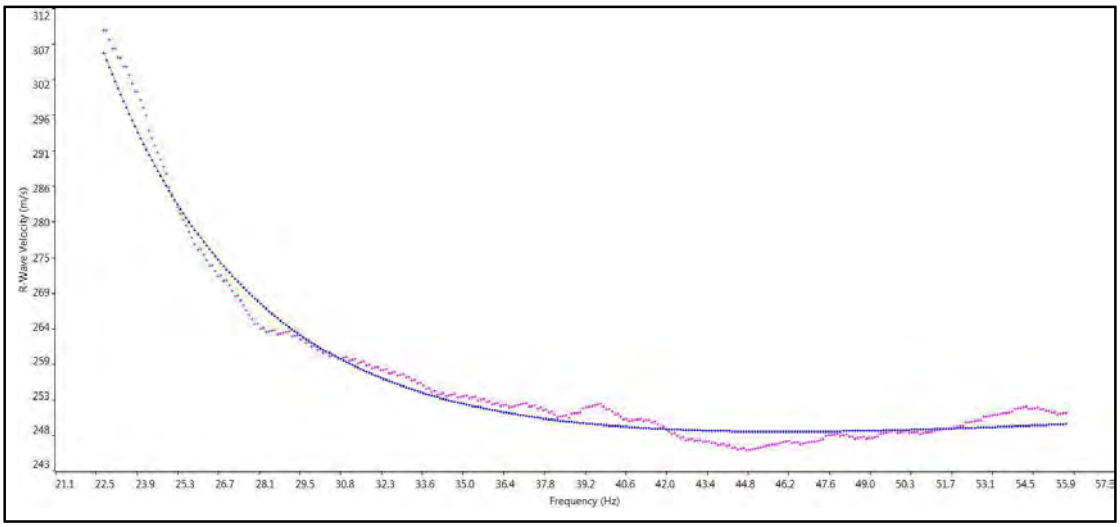

Figure B13: Dispersion curve for a shot at Site S11 using vertical geophones (Shot at 15 m)

Horizontal

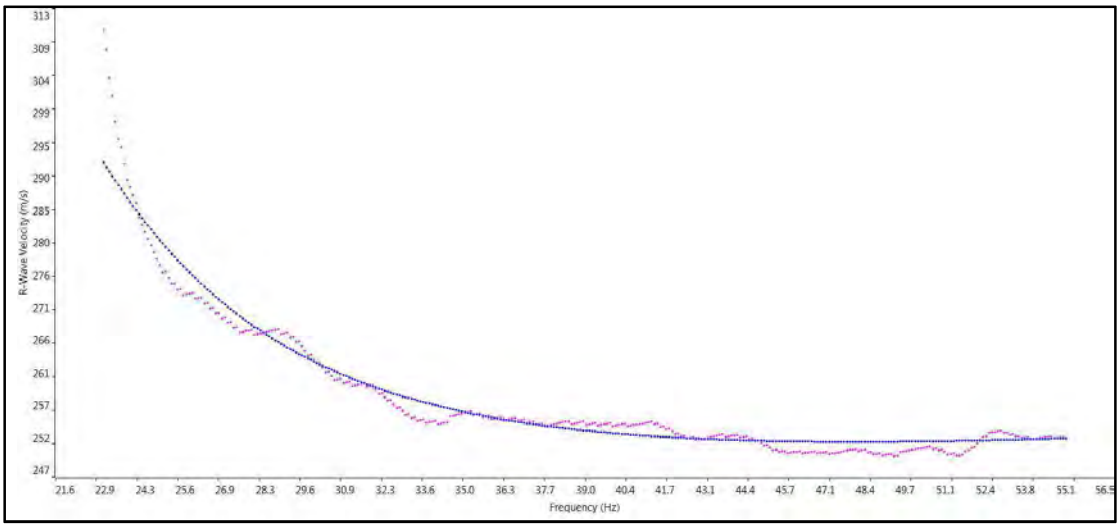

Figure B14: Dispersion curve for a shot at Site S11 using vertical geophones (Shot at 15 m)

Appendix C

Screen Captures of SWAN and GEOPSY

Figure C1:Screen capture from SWAN showing F-K plot and fitting of dispersion curve

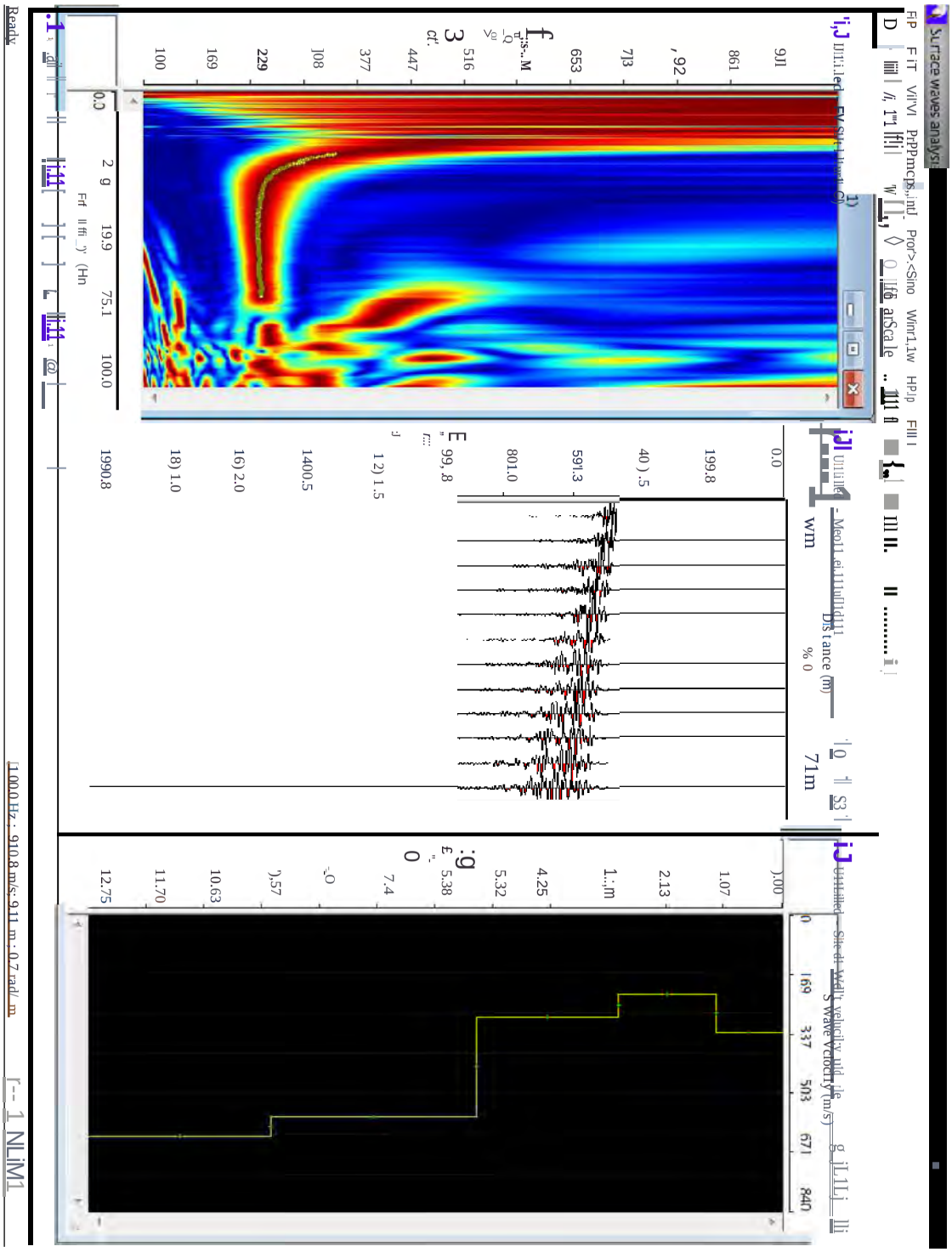

Figure C2: Screen capture from SWAN showing F-K plot, time domain signals, and velocity profile

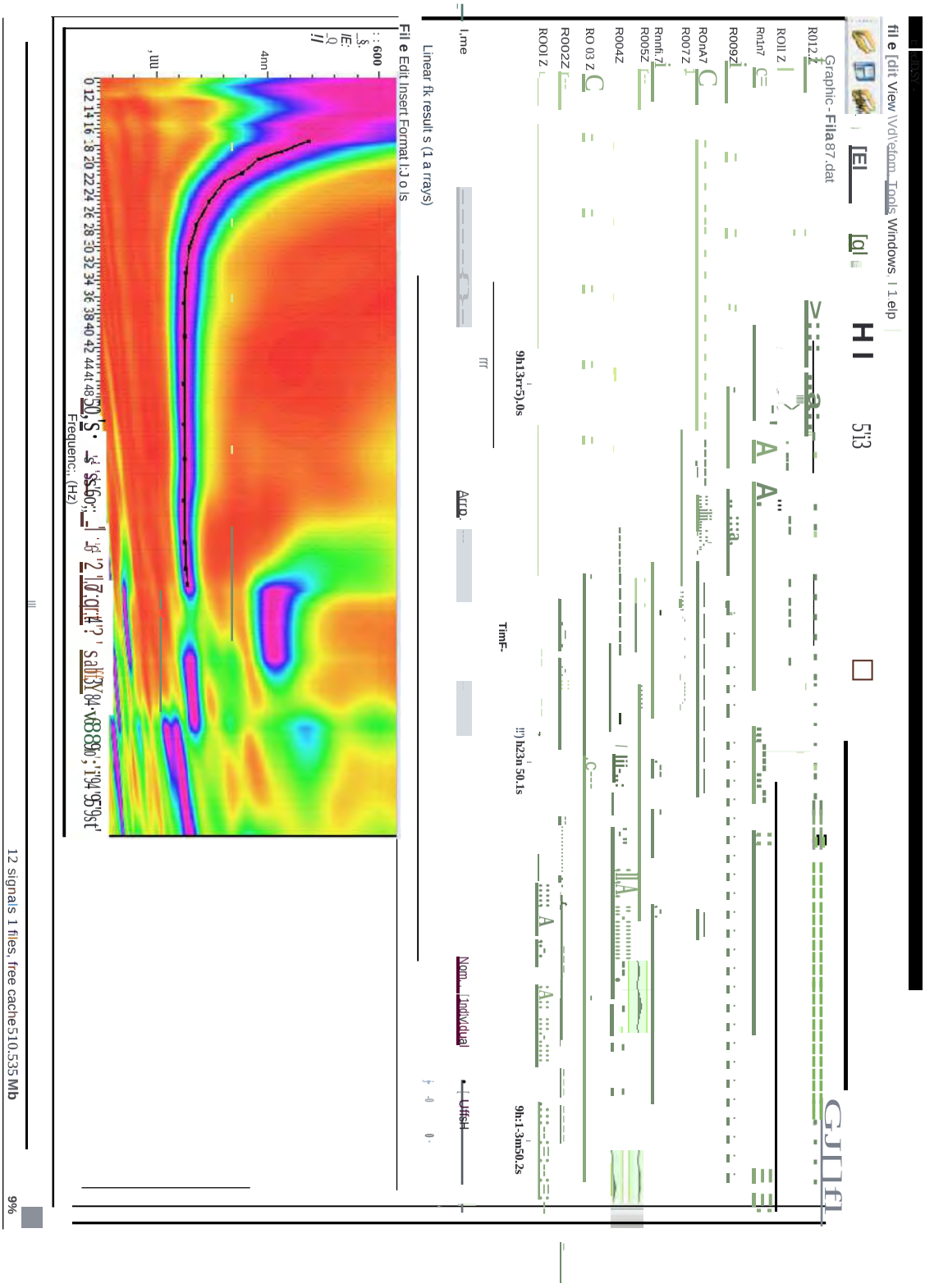

Figure C3: Screen capture from GEOPSY showing F-V plot and time domain signals of Figures C1 and C2

Appendix D

Site Pictures

Figure D1: Spreading the cable on site S12

Figure D2: Connecting geophones to the spread cable on Site S12

Figure D3: Inserting geophones at predetermined locations on Site S10

Figure D4: A view of horizontal and vertical geophone lines on Site S13

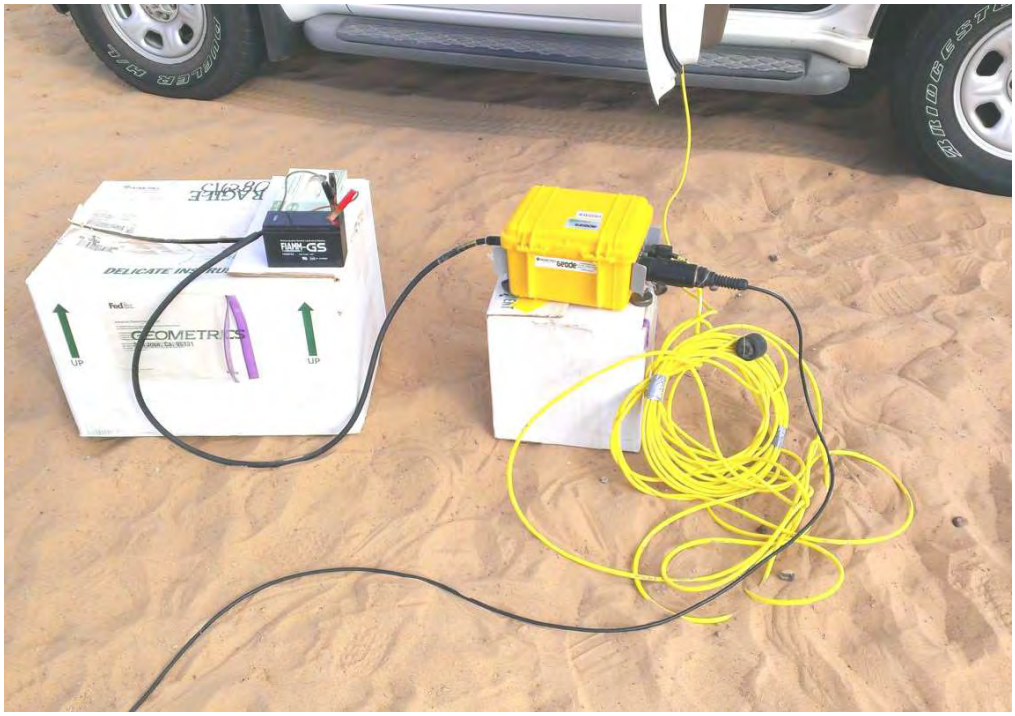

Figure D5: Setting up geode with the power supply and spread cable on Site S14

Appendix E

Borehole Logs

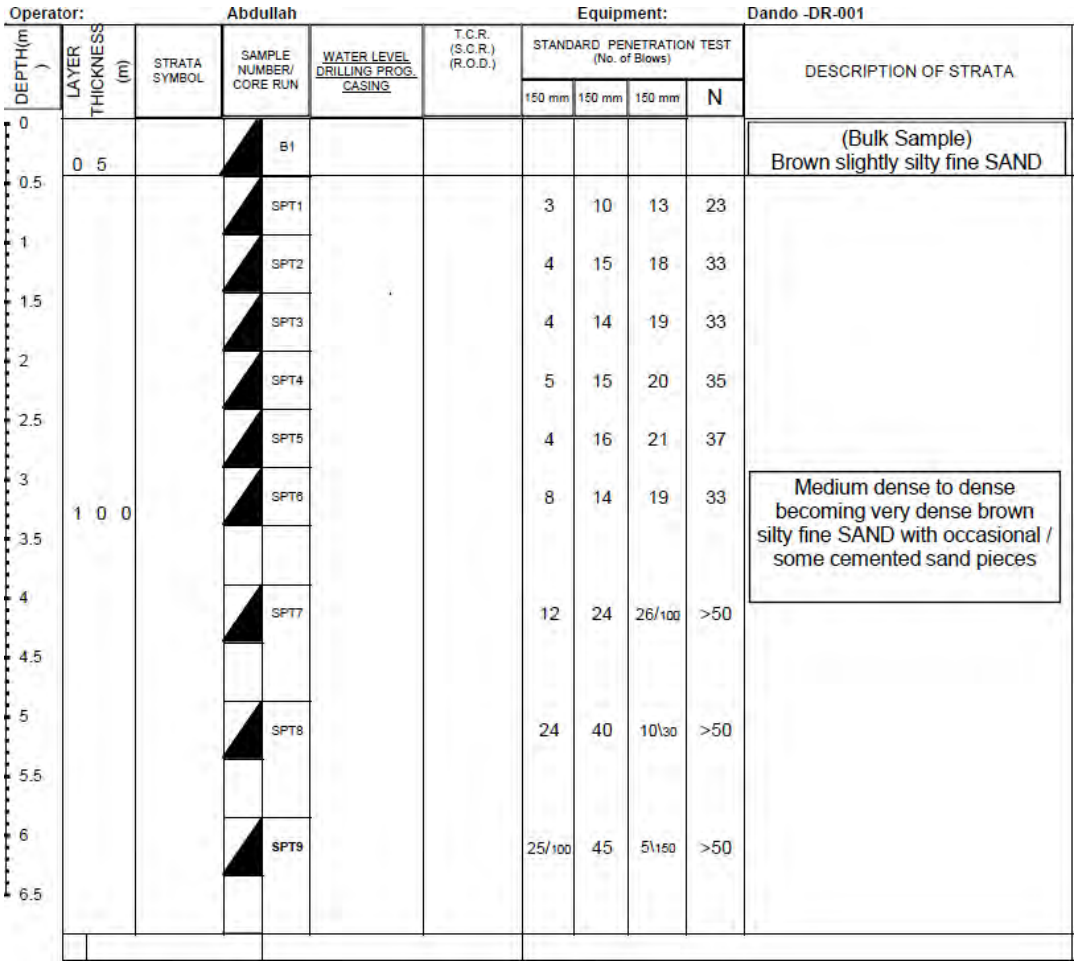

Operator: Abdullah Equipment: Dando -DR-001

DEPTH(m)	LAYER THICKNESS (m)	STRATA SYMBOL	SAMPLE NUMBER/ CORE RUN	WATER LEVEL DRILLING PROG. CASING	T.C.R. (S.C.R.) (R.O.D.)	STANDARD PENETRATION TEST (No. of Blows) 150 mm	150 mm	150 mm	N	DESCRIPTION OF STRATA
0	0 5		B1							(Bulk Sample) Brown slightly silty fine SAND
0.5			SPT1			3	10	13	23	
1			SPT2			4	15	18	33	
1.5			SPT3			4	14	19	33	
2			SPT4			5	15	20	35	
2.5			SPT5			4	16	21	37	
3	1 0 0		SPT6			8	14	19	33	Medium dense to dense becoming very dense brown silty fine SAND with occasional / some cemented sand pieces
3.5										
4			SPT7			12	24	26/100	>50	
4.5										
5			SPT8			24	40	10\30	>50	
5.5										
6			SPT9			25/100	45	5\150	>50	
6.5										

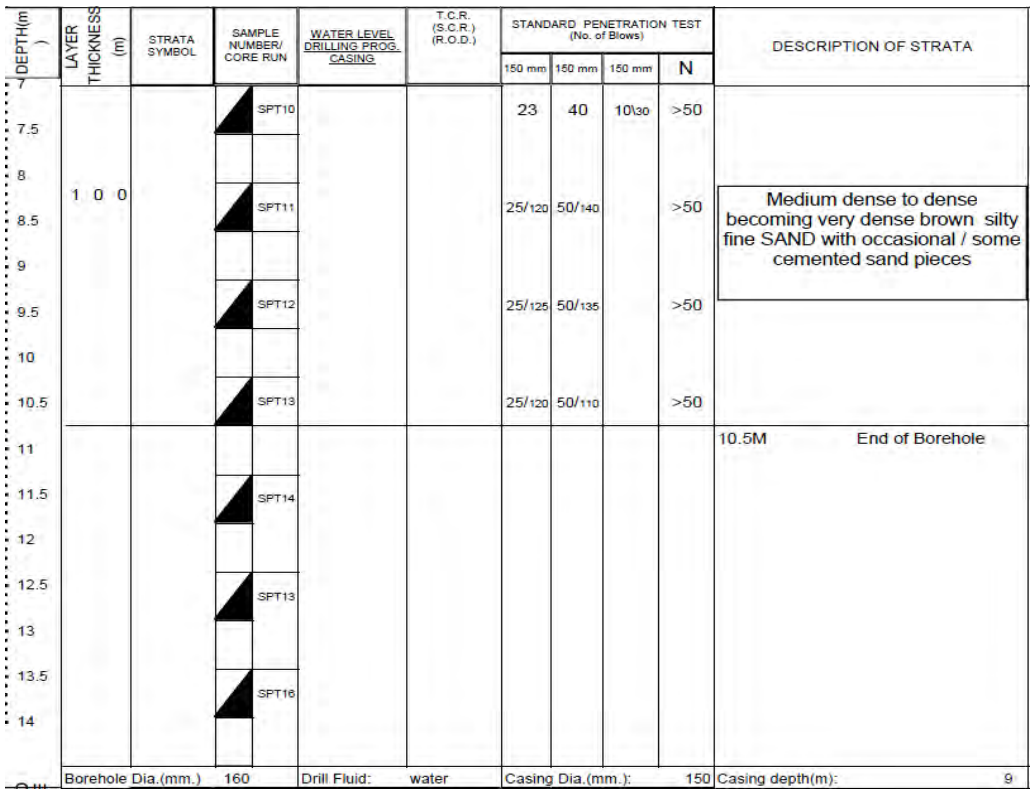

DEPTH(m)	LAYER THICKNESS (m)	STRATA SYMBOL	SAMPLE NUMBER/ CORE RUN	WATER LEVEL DRILLING PROG. CASING	T.C.R. (S.C.R.) (R.O.D.)	STANDARD PENETRATION TEST (No. of Blows) 150 mm	150 mm	150 mm	N	DESCRIPTION OF STRATA
7.5			SPT10			23	40	10\30	>50	
8	1 0 0									
8.5			SPT11			25/120	50/140		>50	Medium dense to dense becoming very dense brown silty fine SAND with occasional / some cemented sand pieces
9										
9.5			SPT12			25/125	50/135		>50	
10										
10.5			SPT13			25/120	50/110		>50	
11										10.5M End of Borehole
11.5			SPT14							
12										
12.5			SPT13							
13										
13.5			SPT16							
14										

Borehole Dia.(mm.) 160 Drill Fluid: water Casing Dia.(mm.): 150 Casing depth(m): 9

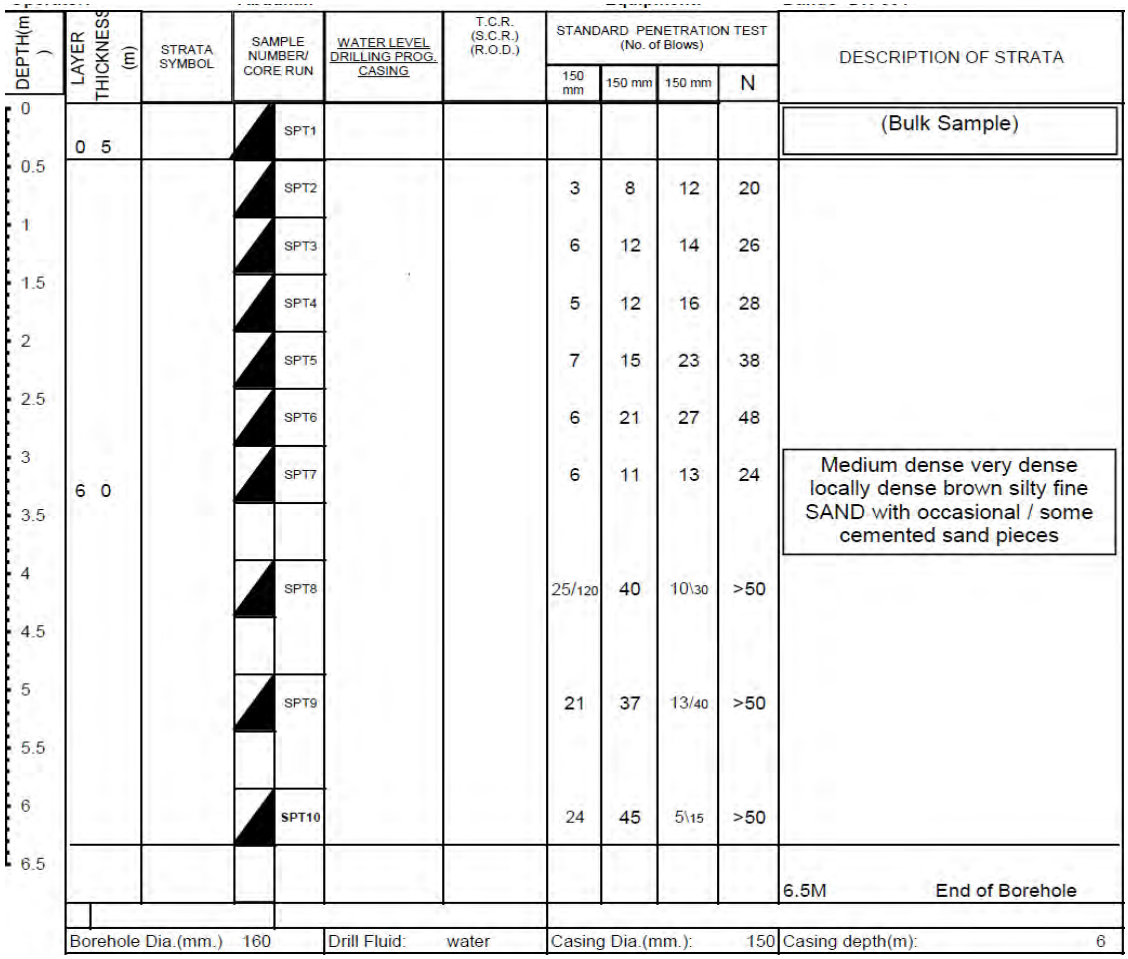

DEPTH(m)	LAYER THICKNESS (m)	STRATA SYMBOL	SAMPLE NUMBER/ CORE RUN	WATER LEVEL DRILLING PROG. CASING	T.C.R. (S.C.R.) (R.O.D.)	STANDARD PENETRATION TEST (No. of Blows) 150 mm	150 mm	150 mm	N	DESCRIPTION OF STRATA
0	0 5		SPT1							(Bulk Sample)
0.5			SPT2			3	8	12	20	
1			SPT3			6	12	14	26	
1.5			SPT4			5	12	16	28	
2			SPT5			7	15	23	38	
2.5			SPT6			6	21	27	48	
3	6 0		SPT7			6	11	13	24	Medium dense very dense locally dense brown silty fine SAND with occasional / some cemented sand pieces
3.5										
4			SPT8			25/120	40	10\30	>50	
4.5										
5			SPT9			21	37	13/40	>50	
5.5										
6			SPT10			24	45	5\15	>50	
6.5										6.5M End of Borehole

Borehole Dia.(mm.) 160 | Drill Fluid: water | Casing Dia.(mm.): 150 | Casing depth(m): 6

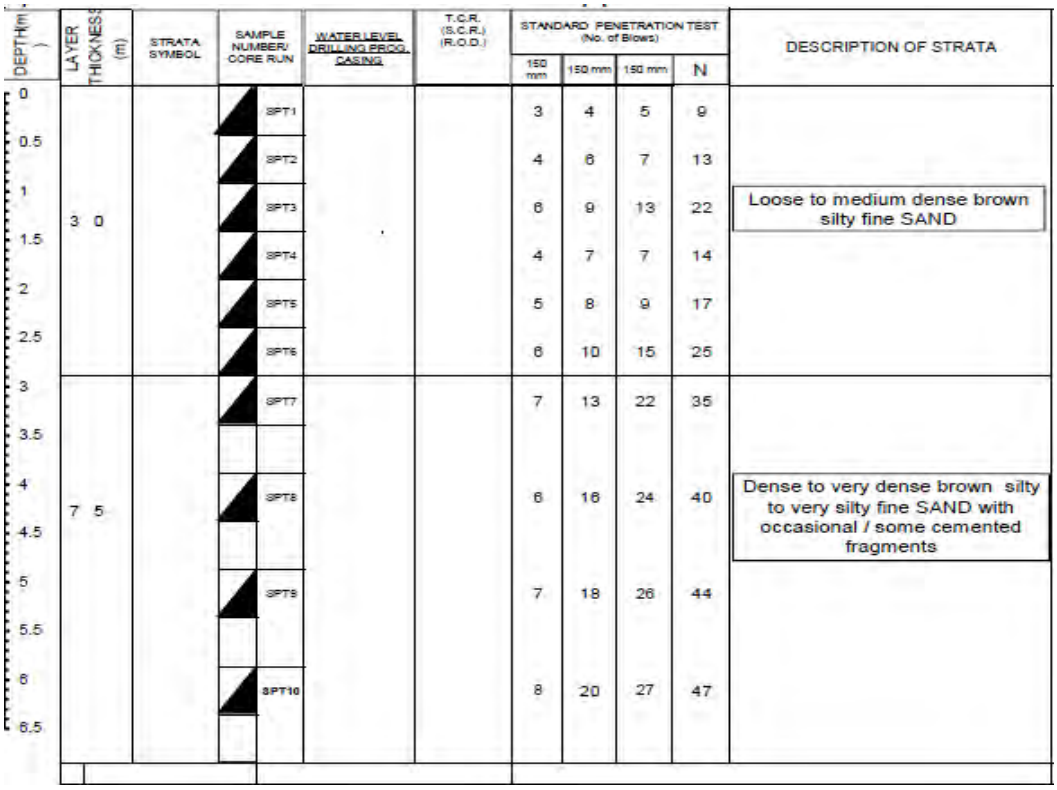

DEPTH(m)	LAYER THICKNESS (m)	STRATA SYMBOL	SAMPLE NUMBER/ CORE RUN	WATER LEVEL DRILLING PROG. CASING	T.C.R. (S.C.R.) (R.O.D.)	STANDARD PENETRATION TEST (No. of Blows) 150 mm	150 mm	150 mm	N	DESCRIPTION OF STRATA
0			SPT1			3	4	5	9	
0.5			SPT2			4	6	7	13	
1	3 0		SPT3			6	9	13	22	Loose to medium dense brown silty fine SAND
1.5			SPT4			4	7	7	14	
2			SPT5			5	8	9	17	
2.5			SPT6			6	10	15	25	
3			SPT7			7	13	22	35	
3.5										
4	7 5		SPT8			6	16	24	40	Dense to very dense brown silty to very silty fine SAND with occasional / some cemented fragments
4.5										
5			SPT9			7	18	26	44	
5.5										
6			SPT10			8	20	27	47	
6.5										

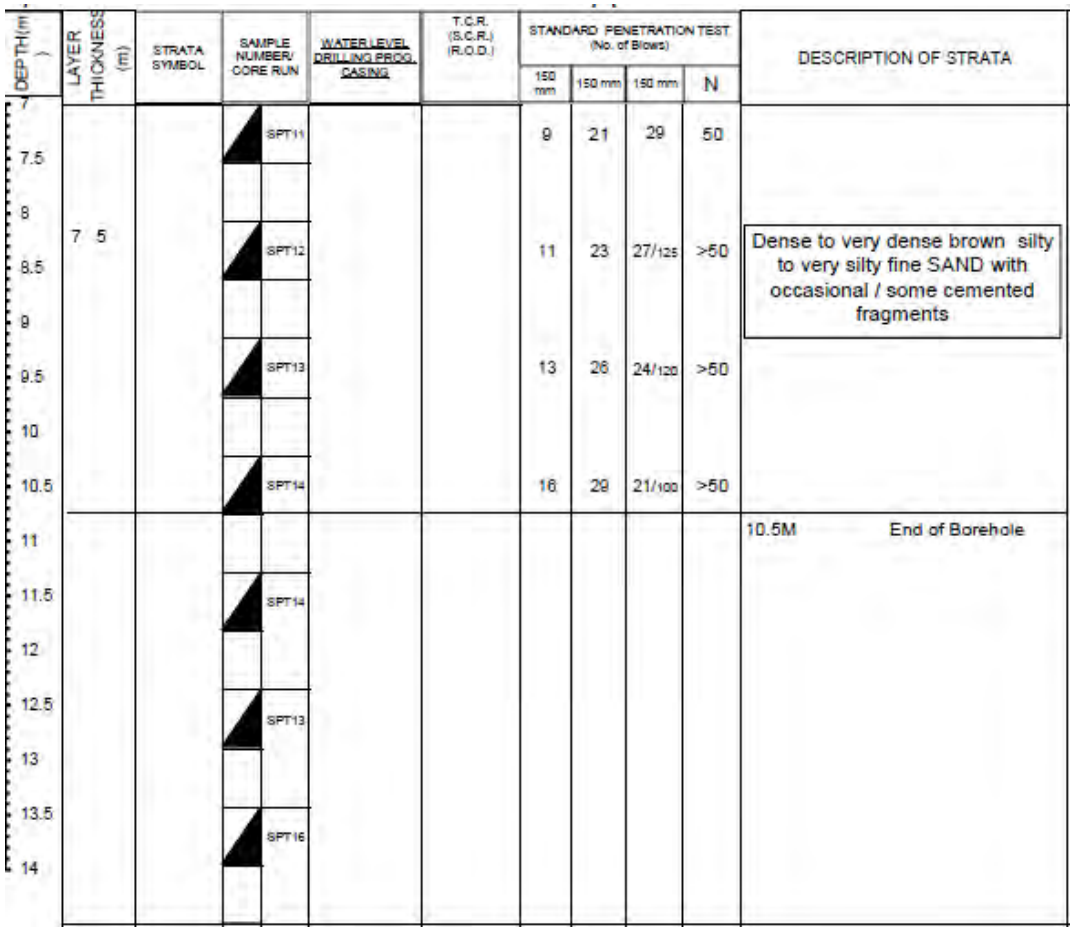
DEPTH(m)
LAYER THICKNESS (m)
STRATA SYMBOL
SAMPLE NUMBER/ CORE RUN
WATER LEVEL DRILLING PROG. CASING
T.C.R. (S.C.R.) (R.O.D.)
STANDARD PENETRATION TEST (No. of Blows)
150 mm
150 mm
150 mm
N
DESCRIPTION OF STRATA
7
7.5
8
8.5
9
9.5
10
10.5
11
11.5
12
12.5
13
13.5
14
7 5
SPT11
SPT12
SPT13
SPT14
SPT14
SPT13
SPT16
9 21 29 50
11 23 27/125 >50
13 26 24/120 >50
16 29 21/100 >50
Dense to very dense brown silty to very silty fine SAND with occasional / some cemented fragments
10.5M End of Borehole

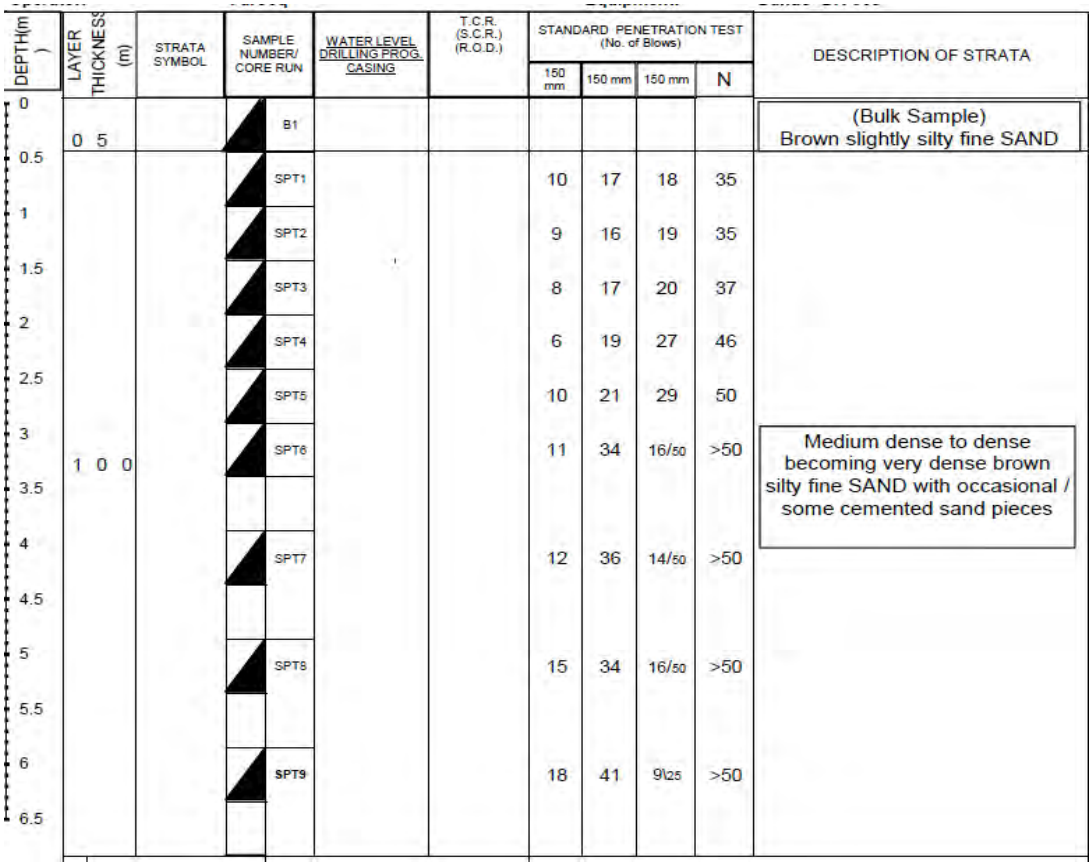
DEPTH(m)
LAYER THICKNESS (m)
STRATA SYMBOL
SAMPLE NUMBER/ CORE RUN
WATER LEVEL DRILLING PROG. CASING
T.C.R. (S.C.R.) (R.O.D.)
STANDARD PENETRATION TEST (No. of Blows)
150 mm
150 mm
150 mm
N
DESCRIPTION OF STRATA
0
0.5
1
1.5
2
2.5
3
3.5
4
4.5
5
5.5
6
6.5
0 5
1 0 0
B1
SPT1
SPT2
SPT3
SPT4
SPT5
SPT6
SPT7
SPT8
SPT9
10 17 18 35
9 16 19 35
8 17 20 37
6 19 27 46
10 21 29 50
11 34 16/50 >50
12 36 14/50 >50
15 34 16/50 >50
18 41 9\25 >50
(Bulk Sample)
Brown slightly silty fine SAND
Medium dense to dense becoming very dense brown silty fine SAND with occasional / some cemented sand pieces

DEPTH(m)	LAYER THICKNESS (m)	STRATA SYMBOL	SAMPLE NUMBER/ CORE RUN	WATER LEVEL DRILLING PROG. CASING	T.C.R. (S.C.R.) (R.O.D.)	STANDARD PENETRATION TEST (No. of Blows) 150 mm	150 mm	150 mm	N	DESCRIPTION OF STRATA
7										
7.5			SPT10			15	31	19/65	>50	
8	1 0 0									Medium dense to dense becoming very dense brown silty fine SAND with occasional / some cemented sand pieces
8.5			SPT11			25/120	50/140		>50	
9										
9.5			SPT12			25/125	50/135		>50	
10										
10.5			SPT13			25/120	50/110		>50	
11										10.5M End of Borehole
11.5			SPT14							
12										
12.5			SPT13							
13										
13.5			SPT16							
14										

DEPTH(m)	LAYER THICKNESS (m)	STRATA SYMBOL	SAMPLE NUMBER/ CORE RUN	WATER LEVEL DRILLING PROG. CASING	T.C.R. (S.C.R.) (R.O.D.)	STANDARD PENETRATION TEST (No. of Blows) 150 mm	150 mm	150 mm	N	DESCRIPTION OF STRATA
0										
0.5	0 5		B1							(Bulk Sample) Brown slightly silty fine SAND.
1			SPT1			3	5	7	12	
1.5			SPT2			6	11	12	23	
2			SPT3			5	13	14	27	
2.5	4 5		SPT4			7	13	21	34	Medium dense to dense brown slightly silty fine SAND with occasional gravel
3			SPT5			5	19	24	43	
3.5			SPT6			8	22	26	48	
4			SPT7			8	23	26	49	
4.5										
5			SPT8			10	28	22/130	>50	
5.5	5 3									Very dense brown silty fine SAND with locally occasional cemented fragments
6			SPT9			15	30	20/120	>50	
6.5										

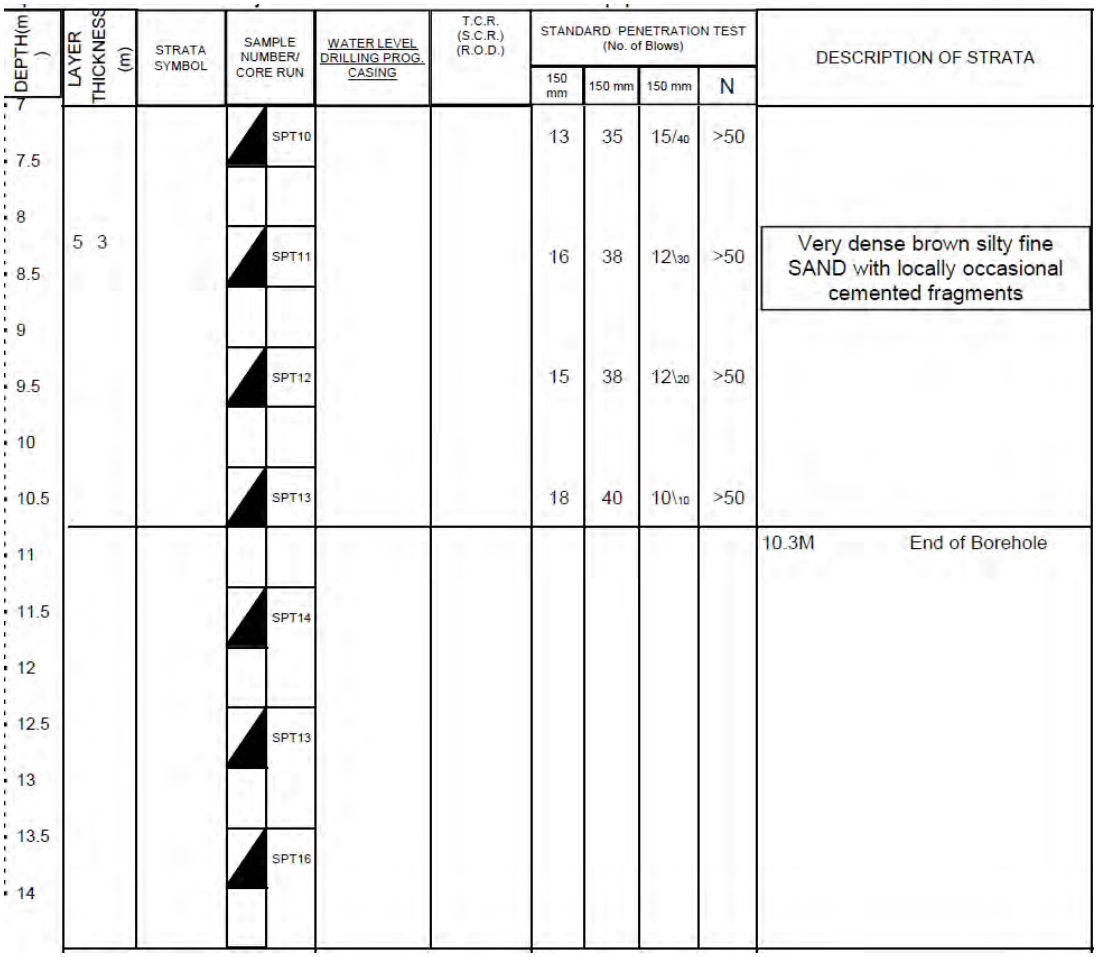
DEPTH(m)
LAYER THICKNESS (m)
STRATA SYMBOL
SAMPLE NUMBER/ CORE RUN
WATER LEVEL DRILLING PROG. CASING
T.C.R. (S.C.R.) (R.O.D.)
STANDARD PENETRATION TEST (No. of Blows)
150 mm
150 mm
150 mm
N
DESCRIPTION OF STRATA
7
7.5
8
8.5
9
9.5
10
10.5
11
11.5
12
12.5
13
13.5
14
5 3
SPT10
SPT11
SPT12
SPT13
SPT14
SPT13
SPT16
13 35 15/40 >50
16 38 12\30 >50
15 38 12\20 >50
18 40 10\10 >50
Very dense brown silty fine SAND with locally occasional cemented fragments
10.3M End of Borehole

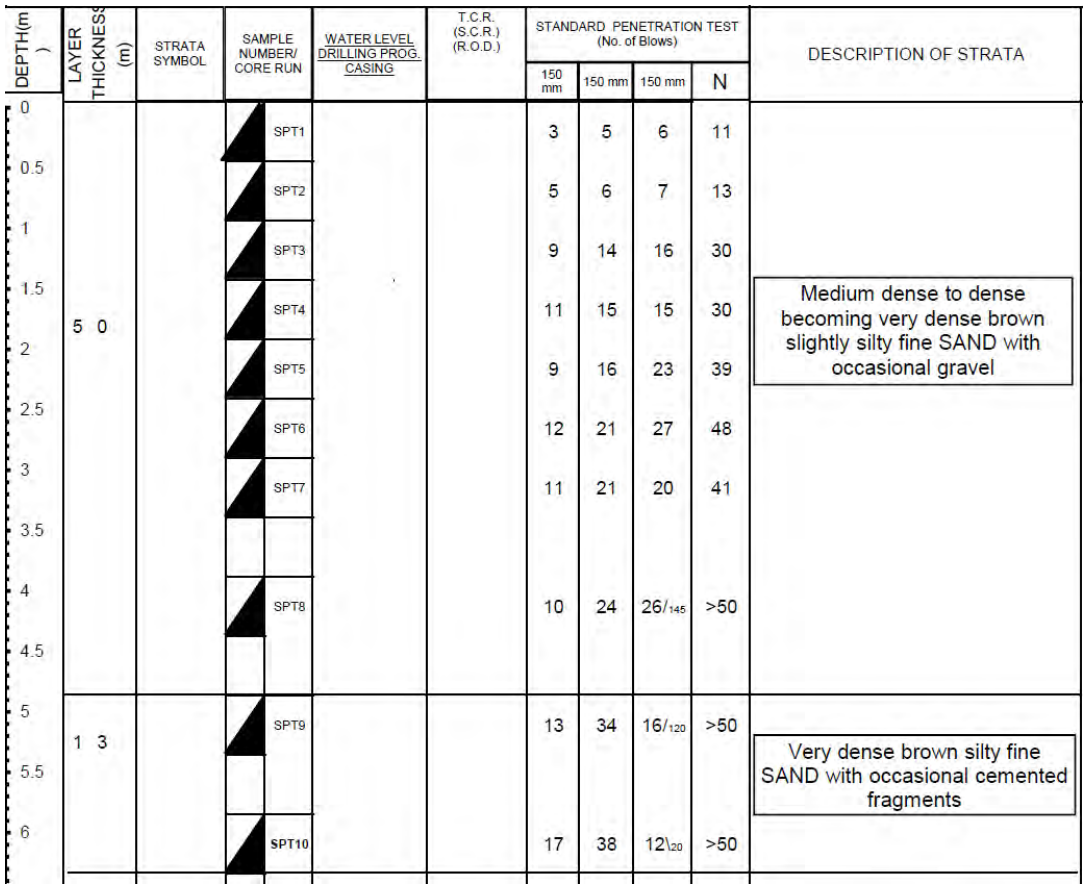
DEPTH(m)
LAYER THICKNESS (m)
STRATA SYMBOL
SAMPLE NUMBER/ CORE RUN
WATER LEVEL DRILLING PROG. CASING
T.C.R. (S.C.R.) (R.O.D.)
STANDARD PENETRATION TEST (No. of Blows)
150 mm
150 mm
150 mm
N
DESCRIPTION OF STRATA
0
0.5
1
1.5
2
2.5
3
3.5
4
4.5
5
5.5
6
5 0
1 3
SPT1
SPT2
SPT3
SPT4
SPT5
SPT6
SPT7
SPT8
SPT9
SPT10
3 5 6 11
5 6 7 13
9 14 16 30
11 15 15 30
9 16 23 39
12 21 27 48
11 21 20 41
10 24 26/145 >50
13 34 16/120 >50
17 38 12\20 >50
Medium dense to dense becoming very dense brown slightly silty fine SAND with occasional gravel
Very dense brown silty fine SAND with occasional cemented fragments

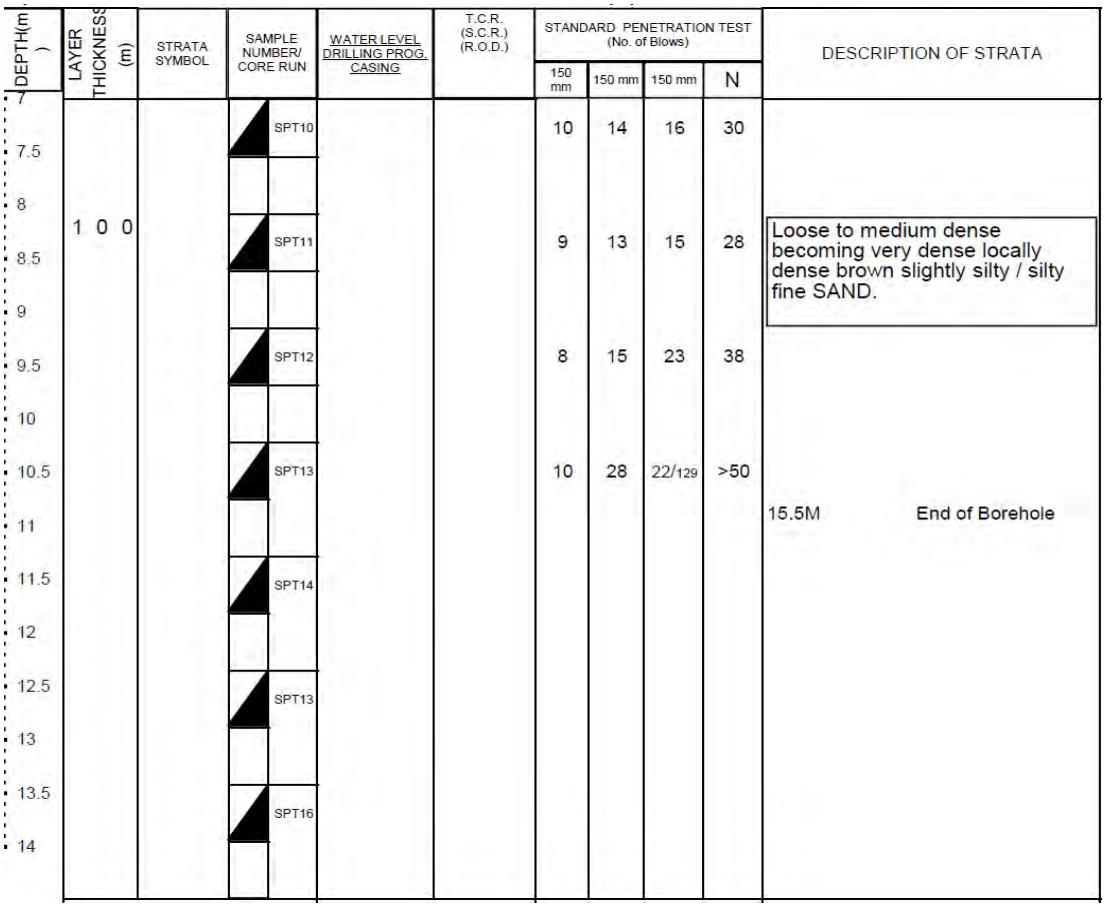

DEPTH(m)	LAYER THICKNESS (m)	STRATA SYMBOL	SAMPLE NUMBER/ CORE RUN	WATER LEVEL DRILLING PROG. CASING	T.C.R. (S.C.R.) (R.O.D.)	STANDARD PENETRATION TEST (No. of Blows) 150 mm	150 mm	150 mm	N	DESCRIPTION OF STRATA
7										
7.5			SPT10			10	14	16	30	
8	1 0 0		SPT11			9	13	15	28	Loose to medium dense becoming very dense locally dense brown slightly silty / silty fine SAND.
8.5										
9			SPT12			8	15	23	38	
9.5										
10			SPT13			10	28	22/129	>50	
10.5										
11										15.5M End of Borehole
11.5			SPT14							
12										
12.5			SPT13							
13										
13.5			SPT16							
14										

DEPTH(m)	LAYER THICKNESS (m)	STRATA SYMBOL	SAMPLE NUMBER/ CORE RUN	WATER LEVEL DRILLING PROG. CASING	T.C.R. (S.C.R.) (R.O.D.)	STANDARD PENETRATION TEST (No. of Blows) 150 mm	150 mm	150 mm	N	DESCRIPTION OF STRATA
0										
0.5	1 0		B1							Brown slightly silty fine SAND (Bulk)
1			B2							
1.5			SPT1			4	7	10	17	
2			SPT2			5	10	12	22	
2.5			SPT3			5	12	15	27	
3			SPT4			3	7	9	16	
3.5	4 0		SPT5			2	4	6	10	Medium dense to dense brown slightly silty fine SAND
4										
4.5			SPT6			7	17	16	33	
5										
5.5	5 5		SPT7			2	4	5	9	Loose to medium dense becoming very dense locally dense brown silty fine SAND with some cemented sand pieces
6			SPT8			7	8	21	29	
6.5										

Vita

Niamatullah Haji Bismillah was born in 1985, Kabul, Afghanistan. Hedid his high school from Pakistan Education Academy Dubai, UAE, in 2005. He received a Bachelor's degree in Civil Engineering from American University of Sharjah (AUS) in 2009, cum laude.

Mr. Niamatullah started Mastersdegree in Civil Engineering at AUS along with being Graduate Teaching Assistant (GTA) in the same university. Within four years after graduation, Mr. Niamatullah reached to the position of Project Engineer in a construction company in Dubai, UAE. Mr. Niamatullah is a member of Society of Engineers UAE.